International Journal of Biological Macromolecules 330 (2025) 147986

Contents lists available at ScienceDirect

International Journal of Biological Macromolecules

journal homepage: www.elsevier.com/locate/ijbiomac

Review

A review of LDH–cellulose hybrid adsorbents for organic and inorganic pollutant removal from wastewater

Noureddine El Messaoudi [a,*], Youssef Miyah [b,c], Jordana Georgin [d], Dison S.P. Franco [d], B.V.N. Sewwandi [e], Neha Singh [f], Salah Knani [g]

[a] Department of Chemistry, College of Science, Imam Mohammad Ibn Saud Islamic University (IMSIU), Riyadh, 11623, Saudi Arabia
[b] Laboratory of Materials, Processes, Catalysis, and Environment, Higher School of Technology, Sidi Mohamed Ben Abdellah University, Fez, Morocco
[c] Ministry of Health and Social Protection, Higher Institute of Nursing Professions and Health Techniques, Fez, Morocco
[d] Department of Civil and Environmental, Universidad de la Costa, CUC, Calle 58 #55-66, Barranquilla, Atlántico, Colombia
[e] Centre for Water Quality Research, National Institute of Fundamental Studies, Kandy, Sri Lanka
[f] Amity School of Earth and Environmental Science, Amity University, Punjab, India
[g] Center for Scientific Research and Entrepreneurship, Northern Border University, Arar, 73213, Saudi Arabia

ARTICLE INFO

Keywords:
LDH–biopolymer composites
Aqueous effluent remediation
Hybrid material regeneration strategies

ABSTRACT

This review reported the recent advances in the synthesis of LDH–cellulose hybrid adsorbents for wastewater treatment. Particular emphasis is placed on the different forms of cellulose employed: microfibrillated cellulose, cellulose nanofibrils, cellulose nanocrystals, and bacterial cellulose, which provide rich functional groups, high specific surface area, biodegradability, and structural flexibility. LDHs, including widely studied Mg—Al, Zn—Al, Ni—Fe, and Ca—Al layered double hydroxides with variable interlayer anions, have excellent anion exchange capacity, tunable chemical composition, and good binding ability with a wide range of pollutants, while cellulose can offer rich functional groups, high specific surface area, biodegradability, and structural flexibility. Assembling these two building blocks creates an LDH–cellulose composite with adsorption properties, mechanical properties, and ecological safety. Unlike previous reviews, this work integrates a comprehensive analysis of LDH–cellulose hybrid adsorbents by simultaneously addressing synthesis strategies, structural-property relationships, adsorption mechanisms, regeneration and challenges, and future perspectives. The review categorizes the main synthesis strategies, i.e., in situ co-precipitation, impregnation, and hydrothermal processes, indicating how the synthesis routes influence the particle morphology, pollutant dispersion, and pollutant removal capacity. It critically investigates the adsorption processes, i.e., ion exchange, electrostatic interaction, hydrogen bonding, and surface complexation. Finally, the review presents existing limitations like regeneration issues, cost-effectiveness, and applicability in real wastewater systems, and proposes avenues for future research. Briefly put, the article brings to the fore the application of LDH–cellulose composites, engineered from specific cellulose derivatives and LDH compositions, as forward-looking and enhanced-efficiency materials for high-end wastewater treatment.

1. Introduction

Global water pollution is on the rise via industrialization, urbanization, agricultural runoff, and effluent discharge without treatment [1,2]. A vast diversity of dyes, heavy metals, pharmaceuticals, pesticides, and other recalcitrant contaminants pose threats to human health, aquatic organisms, and environmental sustainability [3–6]. Conventional treatment technologies such as coagulation, sedimentation, filtration, and biological treatments were mainly designed for bulk organics and pathogens and are generally incapable of eliminating trace-level or recalcitrant pollutants [7,8]. These technologies are power-intensive, release toxic sludge, require strict monitoring, and in the majority of instances are old or inadequately maintained [9,10]. The disparity captures the urgent need for ground-breaking, low-cost, and low-environmental-impact technologies to treat emerging contaminants, facilitate sustainable water reuse, and provide for long-term water security [11,12].

Heavy metal levels in the majority of industrial and municipal

* Corresponding author.
E-mail addresses: NElmessaoudi@imamu.edu.sa, noureddine.elmessaoudi@edu.uiz.ac.ma (N. El Messaoudi).

https://doi.org/10.1016/j.ijbiomac.2025.147986
Received 3 August 2025; Received in revised form 15 September 2025; Accepted 27 September 2025
Available online 6 October 2025

wastewaters consistently range from 5- to 100-fold higher than guideline values: for instance, manganese was analyzed at ~19.10 mg L^{-1} wastewater samples, far in excess of the WHO standard of 0.2 mg L^{-1} [13,14]. Similarly, in Bangladesh's Shitalakkhya-Dhaleshwari river basin, up to 0.14 mg L^{-1} of lead and up to ~12 mg L^{-1} of chromium were identified; again above human and environmental safety thresholds [15]. Conventional wastewater treatment plants also frequently fail to reduce such trace or recalcitrant contaminants to safe levels, and there remain permanently high loads downstream [16]. These magnitudes present a clear gap: there are pollutants at toxic magnitudes, the treatments in use cannot decrease concentrations to a satisfactory level, and thus, there is a need for high-capacity, stable adsorbents at an urgent scale to fill the gap.

LDHs and cellulose are two highly compatible materials whose interaction gives synergistic characteristics of a much more efficient removal of pollutants from wastewater [17–23]. LDHs, or anionic clays, possess a characteristic lamellar structure with positively charged brucite-like layers intercalated with exchangeable anions and water molecules [24–26]. They can be readily altered through the chemical structure by tuning the divalent and trivalent metal cations between the layers to allow for selective adsorption of various anionic contaminants such as nitrates, phosphates, dyes, and heavy metals through anion exchange, surface complexation, and electrostatic interaction [27,28]. LDHs have a high surface area, are thermally stable [29], and are regenerable [30], and hence suit repeated application in treatment processes [31]. Their tendency to agglomerate and lack of structural stability in certain environmental conditions, however, serve to take away from performance [32].

Cellulose, the world's largest biopolymer, is renewable, biodegradable, hydrogen-rich, and has many sites for chemical modification and functionalization [33–35]. Cellulose serves as a rigid matrix when it is incorporated with LDHs, where it inhibits the agglomeration of LDH particles [36] and stabilizes them while contributing mechanical strength [37,38]. The porosity of cellulose facilitates mass transfer, which provides enhanced accessibility of pollutants to active sites [39,40]. Besides, carboxyl and hydroxyl groups are present on the cellulose surface, which can synergistically interact with LDH components to endow the composite with improved adsorption capacity and stability [41]. Hybridization yields a material that, besides being green, also exhibits improved hydrophilicity, recyclability, and adsorption kinetics. Functionalized cellulose also creates an added synergy by incorporating some ligands or groups for a target impurity to create an ultraselective and efficient adsorption platform [42].

In addition, the biocompatibility and low ecofootprint of cellulose balance environmental drawbacks sometimes associated with synthetic adsorbents, while the chemical flexibility of LDHs is adequate for treating the complex mixtures of contaminants [43,44]. All these enable a simultaneous elimination of organic and inorganic contaminants, e.g., dyes and heavy metals, from vast varieties of wastewater streams. The resulting LDH–cellulose composites thus constitute an effective, eco-friendly, and multi-contaminant water-treatment system [45]. Their synergy not only fills in the shortfall of each material but is also a notable advance in future-generation adsorptive material design for the application of solving global environmental problems.

The novelty of this review lies in the fact that it gives a comprehensive and forward-looking summary of LDH–cellulose composites as a hybrid adsorbent class in themselves and not as separate LDH or cellulose entities. Whereas the majority of reviews thus far encapsulate either LDHs or cellulose derivatives separately, this review takes a bold step in bringing together proficiency at the intersection of the two with emphasis on how the two entities cooperate to achieve maximum adsorption capacity, stability, and ecocompatibility. It structures the literature in a different way by connecting synthesis route, composite structure, and pollutant type to underlying mechanisms of adsorption, with well-defined structure–function relationships and practical design guidelines. The review also departs from performance-only surveys in a vacuum by critically assessing real-world concerns like LDH leaching, regeneration efficiency, and scale-up viability, placing the materials in the context of industrial wastewater treatment and not just laboratory environments. Furthermore, it prescribes clear future directions; selective surface functionalization, hierarchical structures for fast mass transfer, and integration with membrane or catalytic systems, while maintaining a sustainability and techno-economic perspective. This synergy of mechanistic understanding, operational significance, and roadmap vision distinguishes it from previous reviews and makes it a guidebook for the future.

This review aims to critically discuss the recent advances in the preparation, fabrication, and use of LDH–cellulose hybrid materials for environmental remediation. Synergism in enabling adsorption capacity, structural stability, and eco-friendliness will be discussed to illuminate the role of layered double hydroxides and cellulose. It strives to categorize and compare various synthesis approaches, i.e., in situ co-precipitation, impregnation, and hydrothermal syntheses, and investigate their effect on the physicochemical properties of the composites. The book also expounds on the prevailing adsorption mechanisms involved in the elimination of organic dyes and inorganic heavy metal ions, i.e., ion exchange, electrostatic interaction, hydrogen bonding, and surface complexation. The second underlying basic objective is to compare the performance of composites at different operating conditions, i.e., pH, temperature, and ionic strength, through case studies. The article also addresses existing deficiencies regarding regeneration, scalability, and implementation in actual wastewater systems. Lastly, the research attempts to set a general platform for future research and facilitate the creation of sustainable high-performance materials for prospective wastewater treatment systems.

2. Structural and chemical features of LDHs and cellulose

Polymeric matrices are often reinforced with inorganic fillers to improve their properties and expand their applications [46]. Traditional fillers like calcium carbonate, silicates, fibers, and carbon materials require high loadings that increase composite weight and limit applications. Nanoparticles, however, can enhance polymer properties at low concentrations, preserving low density. Consequently, layered inorganic fillers have gained attention for developing lightweight polymer nanocomposites with improved performance [47]. Double hydroxide nanocomposites are a key class of inorganic polymer nanocomposites, valued for their flame retardancy, improved thermal stability, and enhanced overall physical properties [48,49]. Due to increased environmental concerns that restrict the use of halogenated chemicals, LDHs have become a possible substitute for halogenated flame retardants [50–53]. Hydrothermal synthesis, urea hydrolysis, ion exchange, and coprecipitation are common synthesis strategies for LDHs and are well-established in the scientific literature [54,55].

From a chemical perspective, the following formula can be used to represent the structure of LDH: $[M^{II}_{1-x}M^{III}_{x}(OH)_2]_{intra}$ $[A^{m-}_{x/m}\cdot nH_2O]_{inter}$. The intralayer crystal domain and the interlayer spaces are denoted by the formula's terms intra and inter, respectively. Charge-compensating interlayer anions with optional solvation in water are dotted throughout the positively charged, edge-shared, octahedral coordinated metal hydroxide crystal formations that make up LDH layers. Defining an anion as having a valence of 'm' and outlining the cationic species as $M^{III}(M^{3+})$ (trivalent cation) and $M^{II}(M^{2+})$ (divalent cation), it's evident that LDHs possess a high charge density within their interlayer space and exhibit a barrier effect against hydroxides, making their exfoliation significantly difficult, unlike layered silicates [47]. Due to the hydrophobicity of polymers, their intercalation in LDH layers is limited; incorporating anionic elements and modifying the clay with surfactants or additives such as cellulose is an effective strategy to form stable and functional polymer/LDH nanocomposites [56].

The discovery of minerals containing LDHs in Sweden in 1842 marked the beginning of the existence of LDHs [57]. LDHs were first

synthesized in laboratories in 1942 by the interaction of bases with diluted metal solutions [58]. Hydrotalcite-like compounds were the name given to LDHs because of their structural resemblance to hydrotalcites [59]. Hydrotalcites are substances that are found as iron and magnesium (pyroaurite) or aluminum and magnesium hydroxycarbonates. In nature, these hydroxycarbonates appear as twisted, foliated plates [60]. The use of hydrotalcites as catalyst precursors in the 1970s sparked significant interest in LDH research [60]. Early X-ray diffraction studies revealed that LDHs possess a layered structure with two cations per layer and interlayers filled with water and carbonate ions. However, the structural details were initially debated, as some researchers considered aspects of their configuration still unclear [61]. It is feasible for LDHs to be produced in a lab or by naturally occurring mechanisms. Natural processes that produce LDHs in the environment include the weathering of basaltic rocks and the precipitation of saline water. Similar to naturally occurring hydrotalcites, which have the formula $[Mg_6Al_2\ (OH)_{16}]CO_3{\cdot}4H_2O$ and a generic formula, $M(II)_{1-x}M(III)_x(OH)_{2\times}/nYH_2O$, LDHs share a similar structure. Here, the metals M (III) and M(II) are trivalent and divalent, respectively, while the interlayer anions Yn^- and $0.2 < x < 0.33$ are interchangeable [62–64]. LDHs that are synthesized have a semicrystalline or hexagonal amorphous structure and are extremely hydrophilic. The chemical $Mg(OH)_2$, brucite, serves as the foundation for the structure of LDH layers. The brucite-like layers in Fig. 1 schematically depict the LDH framework, where trivalent cations (M^{3+}) partially replace divalent cations (M^{2+}) to produce a net positive charge within the hydroxide sheets. The addition of interlayer anions (such as CO_3^{2-}, NO_3^-, and SO_4^{2-}) and water molecules, which are situated in between the stacked layers, balances this positive charge [60]. The figure illustrates the presence of exchangeable anions and water species in the interlayer area, as well as the alternating arrangement of octahedrally coordinated cations (M^{2+} and M^{3+}) in the hydroxide lattice. These structural characteristics provide LDHs their strong hydrophilicity, variable chemical composition, and high anion-exchange capacity, all of which support their adaptability in catalytic and environmental applications [60].

Following exfoliation in various solvents, LDH transforms into nanosheets. The exfoliation and delamination processes of LDHs that result in the creation of nanosheets are schematically depicted in Fig. 2. The intercalated anions and water molecules, which can be swapped out for either organic or inorganic anions, first divide the stacked brucite-like layers [65]. The electrostatic interactions between the positively charged metal hydroxide layers and the compensatory anions are weakened as the interlayer distance increases due to intercalation with appropriate guest species [66]. Individual LDH nanosheets are formed through further exfoliation in suitable solvents. These ultrathin structures provide a greater surface area, better dispersibility, and improved accessibility of active sites while maintaining the inherent chemical diversity of the parent LDH [66]. Because the layered arrangement can be customized via controlled intercalation and exfoliation techniques, these characteristics make LDH-derived nanosheets very appealing for catalytic, adsorption, and energy storage applications [62,67–69]. In general, LDHs are chosen over layered materials like clays. This is due to the possibility of creating LDHs with a broad variety of metal ion compositions and combinations throughout the synthesis process. The high charge density of LDHs is another reason for their choice over clay. The ratio of trivalent to divalent metal cations determines the charge density of LDHs. The charge density rises with a low trivalent/divalent ratio [60]. The physical and chemical characteristics of LDHs are distinct and closely resemble those of clays. Properties including anion mobility, anion exchangeability, and surface basicity are induced by the positively charged layered structure of LDHs. Between the layers of LDHs lie labile anions and water. Consequently, either organic or inorganic anions can be employed to replace these interlayer anions through exchange processes [70]. Mixed metal oxides with characteristics like surface basicity and wide surface area are produced during the calcination of LDHs. The resulting metal oxides also combine to form a uniform mixture with tiny crystallite sizes at high temperatures [60]. High catalytic activity is also shown by LDHs and metal oxides produced after calcination.

LDHs are special in that they have a memory effect or structural reconstruction property. One property that is brought about by calcining the LDHs and treating metal oxides with a particular anionic solution is structural reconstruction [71]. Cations and anions can be readily adsorbed by these materials [72,73]. The chemical makeup of the interlayer gaps in LDHs often controls their magnetic characteristics. Intercalation with organic anions of varying chain lengths can alter the chemical environment in these areas. Consequently, hybrid materials with adjustable magnetic characteristics are produced [74]. When LDHs are intercalated with long-chain surfactants, such as dodecyl sulfates, hybrid materials are created that swell in organic solvents. The creation of monolayers for usage in nanocomposite and nanohybrid synthesis

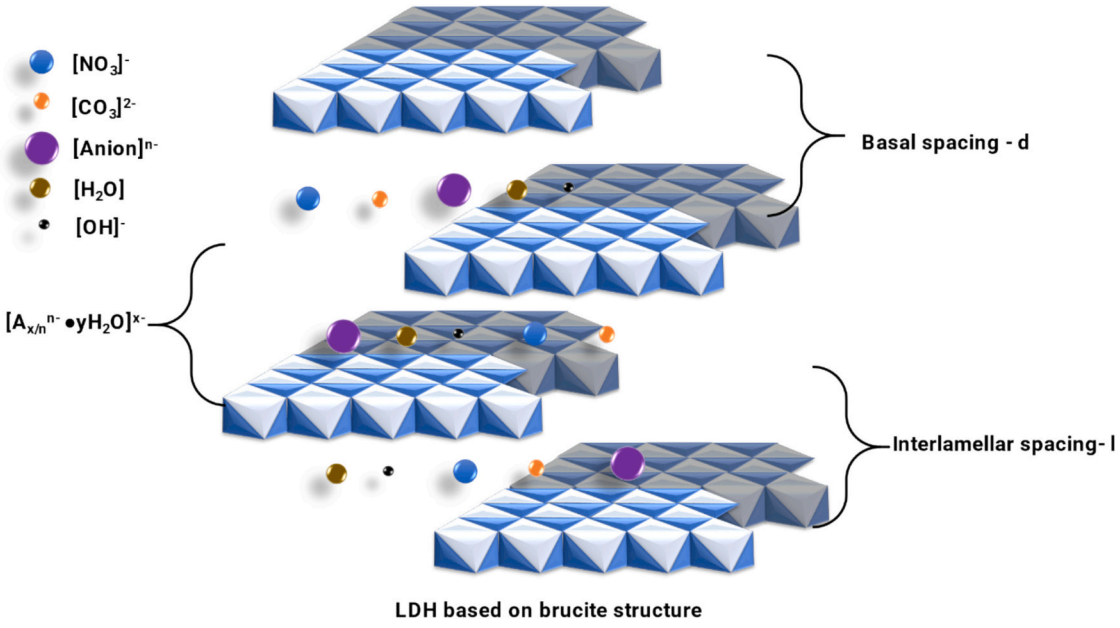

Fig. 1. LDHs' general chemical makeup.

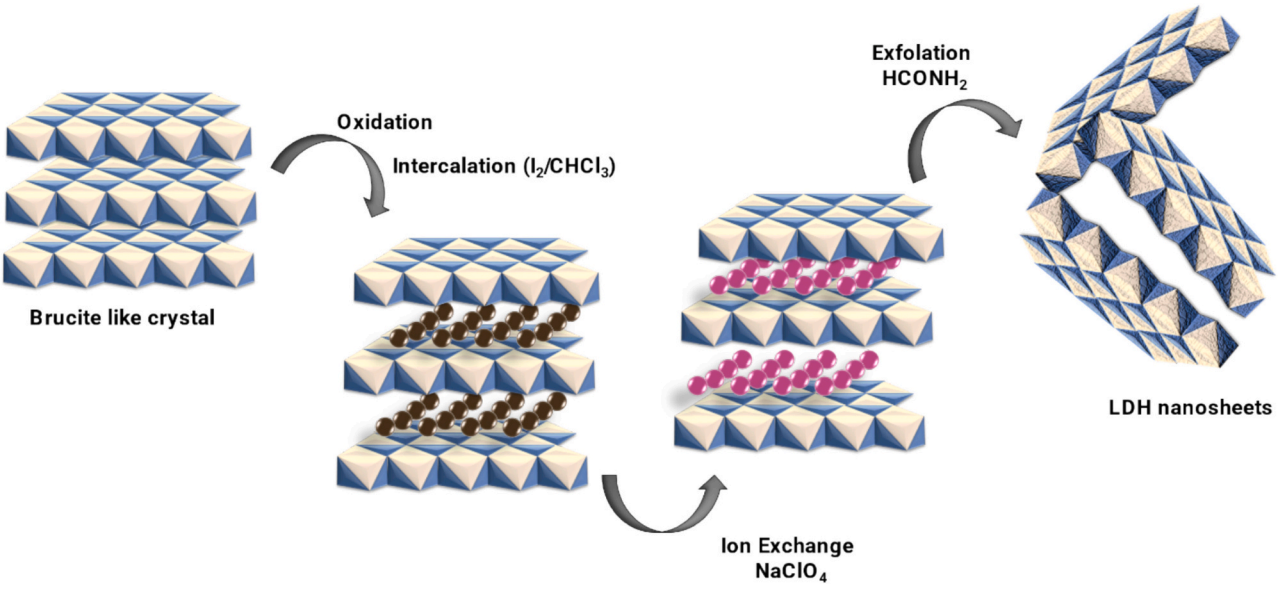

Fig. 2. Fe—Co LDH nanosheet exfoliation and topochemical production.

frequently takes advantage of this swelling property [75]. Anion exchange often modifies the chemical environment between LDH layers, and it preferentially occurs in the following order: $NO_3^- < Br^- < Cl^- < F^- < OH^- < SO_4^{2-} < CO_3^{2-}$.

In this case, the CO_3^{2-} anion can easily take the place of the NO_3^- anion. As a result, NO_3^- is preferred over CO_3^{2-} when creating an interaction precursor. This is because the interaction needs to take place in a way that does not change the host's structure when the guest molecule is introduced. The guest molecule takes the place of the current ion during this contact. Weakly coupled anions to the hydroxide layers are typically the most susceptible to being replaced by other ions [76–78]. LDHs are synthesized using a variety of techniques. The uses of the final product and the necessary properties determine the kind of approach that is taken. Hydrothermal synthesis, coprecipitation, sol-gel, urea hydrolysis, rehydration, and ion exchange are the most often employed processes. Other often-used techniques include the surface synthesis method, the autoxidation approach, and the template synthesis method. One of the most popular techniques is coprecipitation, which involves combining aqueous solutions of M(III), M(II), and intercalary anions to produce the structure of LDH. This technique allows for the synthesis of LDHs with a broad variety of cations and anions. To manufacture LDHs from organic anions, the coprecipitation approach is the only method utilized [61]. Coprecipitation at lower supersaturation, coprecipitation by filtering, and coprecipitation at higher supersaturation are the three subtypes of the coprecipitation method.

To control the particle size distribution, the hydrothermal synthetic technique is typically used. There are two synthesis routes used in the hydrothermal synthesis process. The first involves preparing the materials in a pressurized autoclave at temperatures higher than 373 K. In this case, Al_2O_3 and MgO precursors or combinations created by the breakdown of nitrate precursor molecules are used to develop LDHs [60]. LDHs are synthesized at low temperatures and undergo an aging process in the alternative synthesis method. The LDH precipitate is refluxed for 18 h at a particular temperature during the aging process. Urea is utilized as a precipitating agent in the manufacture of LDHs at particular temperatures in the urea hydrolysis process. The rate of breakdown and the temperature of synthesis determine the degree of crystallinity of LDHs. The sluggish nucleation and low urea breakdown rates at low temperatures result in the formation of big particles [79,80]. LDHs with a high charge density are only synthesized via the urea hydrolysis technique [79].

The sol-gel process creates LDHs by hydrolyzing and partially condensing a metal precursor to create a sol, which is then followed by the gel's creation. Here, the characteristics of the final LDHs are determined by the rates of hydrolysis and the condensation of the metal precursors [81]. Numerous reaction parameters, including the concentration and type of the precursor, pH, solvent utilized, and synthesis temperature, can also affect the rates of hydrolysis and condensation of metal precursors. LDHs created using the sol-gel approach have a greater surface area than those created using the coprecipitation method [82–84]. Nevertheless, characteristics like basicity and the molar ratios of trivalent and divalent metal ions of LDHs produced by the sol-gel approach remain unclear [83–85]. To obtain the guest compound LDH, the ion exchange technique exchanges interlayer anions with additional guest anions that are injected into the LDH structure. Ion exchange in LDHs is influenced by a several variables, including pH, the exchange medium, affinity for guest anions, and the chemical makeup of brucite layers. The rehydration process involves rehydrating mixed metal oxides that are produced when LDHs are calcined at high temperatures (500–800 °C) to generate an LDH structure with the help of required anions [86–88].

2.1. Cellulose and synergy in composite formation

Biopolymers, both natural (e.g., cellulose, starch, lignin, DNA) and synthetic (e.g., carboxymethyl cellulose, polylactic acid, chitosan), are sustainable, biodegradable, and environmentally friendly [89,90]. They break down into harmless molecules without damaging ecosystems. Their biocompatibility and degradability make them valuable in diverse applications, including medicine, drug delivery, sensors, gene therapy, packaging, and catalysts [91].

LDH-based bionanocomposites combine the ion-exchange capacity, large surface area, flame retardancy, and low toxicity of LDHs with the biodegradability, biocompatibility, and mechanical strength of biopolymers [44]. In particular, LDH/cellulose composites synergistically integrate different forms of cellulose with LDHs, creating environmentally friendly materials with diverse functions [92]. These composites are increasingly used in biomedical devices, packaging, and environmental remediation, with cellulose sourced from plants such as hemp, cotton, jute, and flax [93]. These plants are the primary sources of nanocellulose, which is produced through enzymatic, mechanical, or chemical processes [94]. Nanocellulose, including cellulose nanofibrils and nanocrystals, features high aspect ratios and dimensions below 100 nm [94]. Cellulose nanofibrils, produced by mechanical fibrillation, are

long and flexible, while cellulose nanocrystals, formed via acid hydrolysis, are rod-like and highly crystalline. Both have high surface areas and strong mechanical properties. Bacterial cellulose, synthesized by bacteria such as *Komagataeibacter xylinus*, is highly pure, ultrafine, crystalline, and retains water efficiently, making it ideal for biocompatible applications. The abundant surface hydroxyl groups in all cellulose forms enhance reactivity and compatibility with LDHs and other polymers [95].

The processes include enzymatic functionalization, esterification, and oxidation [96]. TEMPO-mediated oxidation converts cellulose hydroxyl groups to carboxyl groups, increasing negative charge density and enhancing interactions with positively charged LDHs [93]. Esterification introduces ester groups to cellulose, altering its hydrophilicity and thermal properties, while enzymatic functionalization sustainably adds functional groups and modifies crystallinity and porosity. Both approaches enhance stability, dispersion, and interfacial bonding with LDHs in composites [96]. Cellulose–LDH bionanocomposites exhibit synergistic effects, with nanocellulose fibers significantly enhancing mechanical strength, including Young's modulus and tensile strength. Cellulose nanocrystals reach values comparable to magnesium alloys and carbon steel. Bacterial cellulose and nanocellulose also form clear, uniform films with excellent gas and moisture barrier properties, making them ideal for packaging [95]. Nanocellulose films are lightweight yet strong, with stiffness around 20 GPa, strength above 200 MPa, and a weight-to-strength ratio eight times higher than stainless steel. Made from renewable resources, they are biodegradable and more environmentally friendly than conventional plastics [97]. Their sustainability is enhanced through the use of green modification techniques [93]. Carboxymethyl cellulose/LDH nanocomposite films offer high transparency and excellent barrier properties, making them suitable for packaging applications [96]. LDH/cellulose bionanocomposites provide a sustainable, versatile alternative for industrial applications by combining the mechanical and functional advantages of both components [98]. In LDH/cellulose bionanocomposites, cellulose enhances LDH dispersion and prevents aggregation through hydroxyl interactions, improving mechanical stability, elastic modulus, and tensile strength. For example, bacterial cellulose composites reinforced with MoS_2 and carbon nanotubes showed strength and modulus increases of 148% and 333% compared to pure bacterial cellulose films [99]. Adding LDHs to cellulose composites introduces extra adsorption sites, enhancing pollutant removal due to LDHs' layered structure and exchangeable anions. Cellulose/LDH bionanocomposites show improved adsorption of dyes and antibiotics; for example, CoFe LDH/cellulose composites achieved maximum adsorption capacities of 208 mg g^{-1} for cefixime and 272.13 mg g^{-1} for sulfamethoxazole [100].

LDH/cellulose bionanocomposites are biocompatible and suitable for biomedical applications like tissue engineering and drug delivery, promoting cell viability with low cytotoxicity. For example, bacterial cellulose/MoS_2/HCNTs films maintained over 70% cell viability, highlighting their biomedical potential [99]. The interaction between cellulose hydroxyl groups and LDH layers promotes homogeneous LDH dispersion, preventing aggregation and stabilizing the composite. Ultrasonically treated regenerated cellulose/LDH films exhibited 100 nm-wide LDH nanoplatelets and showed 135% higher tensile strength and 234% higher Young's modulus compared to pure cellulose films [101]. LDHs' layered structures with exchangeable anions provide numerous adsorption sites, making LDH-based composites highly effective for removing heavy metals from wastewater due to their adsorption efficiency and structural flexibility [101]. Biocompatible and biodegradable LDH/cellulose bionanocomposites are suitable for tissue engineering and drug delivery. Green synthesis, such as plant extract-modified LDHs, enhances biocompatibility and enables efficient anticancer drug delivery with minimal harm to healthy cells [102]. Green chemistry approaches, including solution intercalation and in situ polymerization, reduce environmental impact. Combined with the biodegradability of the composites, these sustainable methods make them environmentally friendly materials [103].

When LDHs are integrated into cellulose matrices, their positive charges and ion-exchange sites interact with the hydroxyl groups of cellulose, promoting stable anchoring of the inorganic lamellae in the organic matrix; increased active surface area and accessibility of adsorption sites; and greater selectivity for metal ions and polar molecules through a combination of hydrogen bonds and electrostatic interactions. Table 1 provides a comparative analysis between LDHs and cellulose.

2.1.1. Polymorphs, crystallinity and reactivity of cellulose

Cellulose is a natural linear polymer formed by β-D-glucose units linked by β(1→4) bonds. Despite its uniform chemical composition, it has several crystalline polymorphs (cellulose I, II, III, and IV), which differ in the organization of microfibrils and the orientation of adjacent chains [104,105]. Cellulose occurs naturally in plants and is subdivided into Iα (dominant in algae and bacteria) and Iβ (predominant in wood). It has high crystallinity and a highly ordered structure, conferring rigidity and mechanical stability. Cellulose II is obtained by reheating or mercerization, with antiparallel chains; it has reduced crystallinity and greater chemical accessibility [106]. Cellulose III/IV derivatives are obtained through chemical and thermal treatments, generally used to modify mechanical properties and reactivity [107]. Crystallinity is crucial for mechanical strength, thermal stability, and molecular interaction capacity. The amorphous regions of cellulose, in contrast, are more amenable to chemical modification and interaction with inorganic species such as LDHs [92]. In addition to the classic polymorphs, cellulose can be processed into different nanometric forms, each with distinct properties [108]. Cellulose nanocrystals (CNCs) are obtained by acid hydrolysis of plant fibers; they have a high crystallinity (60–90%), typically measuring 5–20 nm in diameter and 100–300 nm in length, and a large surface area [109]. They are rigid and have numerous

Table 1
Comparative properties of LDHs and cellulose and their synergistic interactions in composite materials.

Property	LDHs	Cellulose	Synergy in the composite
Structure	Layered, with M^{2+}/M^{3+} cations and intercalated anions	Linear β-D-glucose polymer	Combination of inorganic layers within an organic matrix, enhancing structural stability
Surface area	Moderate to high (dependent on synthesis)	Relatively low	Cellulose acts as a support, preventing LDH aggregation and increasing active surface area
Functional groups	Hydroxyl groups on layers, positive surface charges	Abundant hydroxyl groups (–OH)	Hydrogen bonding and stable ionic interactions
Charge density	High positive charge density on layers	Neutral, but rich in polar groups	Establishes electrostatic interactions, improving selectivity for anionic pollutants
Biodegradability	Not biodegradable, but partially soluble in acidic media	Highly biodegradable	Reduces environmental persistence of the material
Thermal stability	High, resistant to elevated temperatures	Moderate, decomposes around 300 °C	Composite is more stable and functional under different conditions
Environmental function	Ion exchange and selective anion adsorption	Adsorption via hydrogen bonding and surface interactions	Multifunctional hybrid adsorbent, effective for metals and dyes

exposed hydroxyl groups, favoring hydrogen bonding and electrostatic interactions with LDHs. Bacterial cellulose (BC) is synthesized by bacteria (e.g., *Gluconacetobacter xylinus*); it has a highly pure and porous nanofibrillar network, without lignin or hemicellulose, and has excellent water retention capacity [110]. The three-dimensional matrix allows for uniform dispersion of LDH particles, resulting in composites with high stability and homogeneity [111]. Structural diversity allows for the adjustment of the morphology and density of active sites for adsorption or chemical modification, optimizing composite performance [29].

The hydroxyl (–OH) groups of cellulose are responsible for much of its chemical reactivity. Hydrogen bond formation occurs through interactions with oxygen or hydroxyl groups of the LDH lamellae, stabilizing the dispersion of the inorganic layers in the organic matrix [112].

Electrostatic interactions and ionic complexation, where chemical modifications (carboxylation, sulfation), generate anionic groups that can interact directly with LDH metal cations, increasing their affinity for pollutants or improving the structural integration of the composite [113]. Finally, compatibilization and dispersion, in this case the amorphous regions and exposed nanocrystals, allow for the physical and chemical anchoring of the LDH lamellae, preventing aggregation and increasing the surface area available for adsorption. The structural diversity of cellulose directly influences the performance of the composite (Table 2).

3. Synthesis strategies of LDH–cellulose composites

3.1. In situ precipitation: co-formation of LDHs on cellulose surfaces

In situ precipitation is a common method for producing LDH–cellulose beads, forming LDH crystals directly on cellulose fibers. This ensures close contact and uniform dispersion, enhancing interfacial interactions and preventing agglomeration [114]. The process involves dispersing cellulose in metal salt solutions, adjusting pH to promote LDH nucleation, and maintaining controlled temperature and pH, followed by washing and drying to yield a functional composite [44]. Hydrogen bonding between cellulose hydroxyl groups and LDH layers strengthens interfacial adhesion, improving stability and mechanical properties. LDHs also add functionalities such as enhanced pollutant adsorption and flame retardancy. This method enables efficient production of LDH–cellulose composites for applications in biomedicine, packaging, and environmental remediation [115].

A study examined how well LDH/cellulose nanocomposite spheres (CNS) removed amoxicillin from water in Mg-Al layers made using in situ coprecipitation techniques [116]. LDH@CNS is an effective water treatment adsorbent due to its high porosity (94.7%), large surface area (76.46 $m^2\ g^{-1}$), and high-water content (92%), with a maximum adsorption capacity of 138.3 mg g^{-1}. Electrostatic interactions between negatively charged amoxicillin and positively charged LDH@CNS, via O═C—O···M (Al/Mg) bonds, enable efficient removal, highlighting its potential in water purification [116]. In the LDH@CNS cellulose sphere nanocomposite, the porous cellulose matrix acted as a microreactor, allowing LDH particle loading while limiting aggregation, and its high-water content enabled effective in situ coprecipitation of LDH from metal salt solutions. At natural pH (~7), amoxicillin carried a negative carboxyl group, which electrostatically interacted with positively charged LDH, as confirmed by XPS and ζ potential analyses. Adsorption kinetics fit a pseudo-second order model, indicating chemical regulation, though thermodynamic confirmation of chemical interactions was not performed [117–121]. Lastly, the authors themselves attest that the primary mechanism underlying the process would be physical electrostatic interactions. A schematic illustration of the creation of LDH@CNS nanocomposites and the amoxicillin adsorption that follows is shown in Fig. 3. Making porous cellulose nanocomposite spheres, which act as a strong and extremely hydrated matrix, is the first step in the procedure. By facilitating the inclusion of LDH nanoparticles through in situ coprecipitation, the porous structure reduces particle aggregation and produces a uniform distribution of LDH throughout the cellulose framework. The LDH@CNS nanocomposite offers a large number of active sites for interacting with contaminants once it is produced. Through interaction with the surface metal cations (Al/Mg), negatively charged amoxicillin molecules engage electrostatically with the positively charged LDH layers during adsorption, therefore immobilizing the antibiotic inside the composite structure. Its potential as a cutting-edge adsorbent for water purification applications is highlighted by this hierarchical architecture, which combines the high porosity of cellulose with the adjustable surface chemistry of LDH to improve pollutant capture stability and efficiency [116].

The decrease in specific surface area (86.77 → 74.46 $m^2\ g^{-1}$) reflects partial LDH occupancy within cellulose spheres. Mg—Al LDH cellulose spheres were successfully synthesized via in situ coprecipitation, confirmed by SEM, EDX, and FTIR analyses. XPS and EDX detected S and N from amoxicillin, while the C carboxylate peak shift (288 → 288.5 eV) indicated binding via O═C—O···M (Mg/Al). Amoxicillin adsorption reduced the surface charge from 25 mV to 3.21 mV. These findings demonstrate effective electrostatic-driven removal of penicillin-based antibiotics, highlighting LDH@CB spheres as biodegradable, eco-friendly adsorbents for water purification [116].

LDHs can act as host matrices for inorganic-organic nanocomposites, typically synthesized through coprecipitation, ion exchange, or reconstruction of calcined LDHs in the presence of organic polymers [122]. Biopolymers such as pectin, alginate, xanthan gum, and ι- and κ-carrageenan can intercalate into LDHs and are used to develop sensors for potentiometric ion detection in applications like food analysis, clinical diagnostics, and water quality monitoring [122]. Similarly, various mesoporous materials incorporated into binders have demonstrated high efficiency in separating rare earth elements [123,124]. Despite their potential, LDH-intercalated biopolymer nanocomposites are rarely used for removing heavy metals and rare earth elements. Consequently, a hybrid nanocomposite, Al/CL-Zn LDH, based on cellulose intercalation into LDH, was developed for this purpose [125].

The cellulose solution was made following earlier literature reports in order to synthesize Al/CL-Zn LDH nanocomposites [126]. Al/CL-Zn LDH nanocomposites were synthesized via coprecipitation. A chilled NaOH–urea solution (Solution A) containing cellulose was prepared, and a metal salt solution of $AlCl_3{\cdot}6H_2O$ and $ZnCl_2$ (Solution B, Al:Zn = 1:3) was added dropwise under stirring. The pH was adjusted to 10, and after 18 h aging, the precipitate was washed, dried at 80 °C for 12 h, and ground into fine powder [126]. The Al/CL-Zn LDH nanocomposite exhibited a crystalline, sheet-like structure confirmed by XRD, TEM, and AFM analyses. It showed a pore diameter of 22.7 nm, pore volume of 9.3 $mm^3\ g^{-1}$, and BET surface area of 1.216 $m^2\ g^{-1}$. Equilibrium for Ce^{3+}, Y^{3+}, and La^{3+} was reached in 10 min, following a pseudo-second order kinetic model, with film diffusion as the rate-limiting step. Maximum adsorption capacities at pH 7 were 92.51 mg g^{-1} (La^{3+}), 102.25 mg g^{-1} (Y^{3+}), and 96.25 mg g^{-1} (Ce^{3+}), with adsorption being spontaneous and endothermic. The composite maintained good reusability, with minor reductions after five cycles, and showed slight competition effects in

Table 2
Influence of cellulose structural forms on LDH composite formation and performance.

Form of cellulose	Crystallinity	Interaction with LDHs	Impact on the composite
Microfibrillar cellulose	Moderate to high	Hydrogen bonding in amorphous regions	Good integration, but lower surface area
Nanocrystals (CNCs)	High	Exposed hydroxyl groups, possible functionalization	Higher active surface area, high selectivity, mechanical stability
Bacterial cellulose (BC)	Moderate	Porous network, multiple binding sites	Excellent LDH dispersion, homogeneous and flexible composites

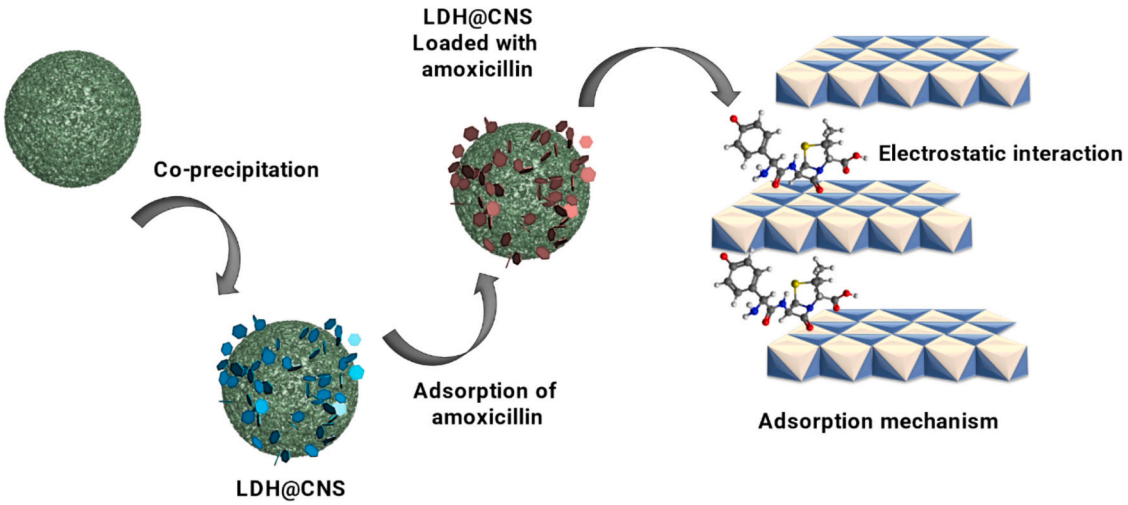

Fig. 3. Diagrammatic representation of the adsorption process between amoxicillin and LDH Mg—Al via electrostatic interaction and the creation of the LDH@CB nanocomposite using the coprecipitation method.

multi-ion systems. Overall, Al/CL-Zn LDH is a promising adsorbent for removing La^{3+}, Y^{3+}, and Ce^{3+} from wastewater [126].

Recent efforts to improve LDH adsorption focus on increasing porosity and stabilizing them on natural or synthetic supports [127]. This study used cellulose nanocrystals, produced via high-temperature acid hydrolysis, and combined them with other materials to create composites with tailored properties. The interaction of many drugs with LDHs has already been described in depth in the literature, including activated carbon [128], metal [129], graphene-based compounds [130,131], and biochar [132]. Likewise, cellulose and other bio-based materials have demonstrated efficacy in cleaning up contaminants found in aqueous media [133,134].

Limited studies exist on using biobased LDH nanoparticles for antibiotic removal. One study evaluated Al—Mg/LDH composites with cellulose nanocrystals for adsorbing tetracycline from water [127]. Cellulose nanocrystal/Al—Mg-LDH composites for tetracycline adsorption were synthesized via coprecipitation. Cellulose nanocrystals were ultrasonically dispersed with Al—Mg-LDH, stirred at 75 °C, and the pH adjusted to 10. After 24 h reflux, the mixture was washed, centrifuged, treated with acetone, and freeze-dried for 48 h to yield the final composite. Pore radius, surface area, and pore volume were characterized for different composites. The composition of the obtained cellulose/Al—Mg nanocrystal composites is displayed in Table 3. The pore radius, specific surface area, and pore volume of the different composites are displayed in Table 4 [127].

The cellulose nanocrystals-MAl-1 composite exhibited a high specific surface area of 101.92 $m^2\ g^{-1}$. Adsorption kinetics followed a pseudo-second-order model, and Langmuir isotherms showed maximum capacities of 153.3 mg g^{-1} (318 K) and 143.5 mg g^{-1} (298 K). Thermodynamic analysis indicated the process was endothermic, spontaneous, and favorable (ΔH^0 = 25 kJ mol^{-1}). The composite maintained over 90% antibiotic removal efficiency after five regeneration cycles [127]. The cellulose nanocrystals/Al—Mg-LDH composite, with its porous surface and abundant functional groups, effectively adsorbs tetracycline. FTIR analysis confirmed the presence of lignocellulosic alkanes and oxide groups, while SEM showed the porous structure facilitating adsorption [127]. Thermodynamic studies indicated spontaneous physical adsorption. At pH 4, tetracycline exists mainly as a zwitterion (84.7%) and partly as a neutral form (15.3%). Tetracycline molecules' adsorption method onto the cellulose nanocrystals/Al—Mg-LDH composite is depicted in Fig. 4. The schematic illustrates how cellulose nanocrystals and LDH layers work in concert to provide a high-surface-area, porous framework that is enhanced with functional groups that can interact in a variety of ways. Tetracycline is primarily found in its zwitterionic form at pH 4, which promotes a variety of adsorption processes [127]. Tetracycline's positively charged amino groups interact electrostatically with the negatively charged areas on the composite surface. Concurrently, π–π stacking interactions and hydrogen bonding reinforce the binding, improving the overall stability of the adsorption process [127]. Additionally, the multilayer LDH structure aids in immobilization by surface complexation, while the cellulose nanocrystals enhance dispersibility and inhibit aggregation. The composite's effectiveness as a material for antibiotic removal is confirmed by these combined effects, which also account for the high adsorption capacity, durability across several regeneration cycles, and sensitivity to ionic strength seen in experiments [127]. In terms of adsorption, it was found that as the concentration of salt in the water increased, less tetracycline was removed from the aqueous phase [127].

LDH-biochar composites are now a viable, appealing, promising, and reasonably priced water purification adsorbent [135–138]. Incorporating biochar as an inexpensive LDH support material not only keeps LDHs from clumping together, but it also significantly improves the composite's chemical-physical properties, enabling better treatment of both organic and inorganic polluted water systems and superior reuse performance [139–141]. For instance, within an hour of the process, biochar-Al—Ni LDH demonstrated quick adsorption towards methyl orange dye, with an adsorption capacity of 412 mg g^{-1} [142]. When compared to pure biochar, the intercalation of Al—Mg layered double hydroxide with biochar demonstrated a high removal of methylene blue cationic dye to about 50%, and equilibrium was attained in half the adsorption time [143]. Additionally, other studies showed that methylene blue (406.47 mg g^{-1}) and methyl orange (412.8 mg g^{-1}) dyes had outstanding adsorption capability on NiAl and MgAl supported biochar, respectively [142,144]. Other anionic contaminants like tetracycline,

Table 3
The cellulose/Al—Mg nanocrystal composite's properties.

Sample number and Al—Mg-LDH (3:1): cellulose nanocrystals	Adsorbent nomenclature
1 and 1:0.2	Cellulose nanocrystals-MAl-1
2 and 1:0.4	Cellulose nanocrystals-MAl-2
3 and 1:0.6	Cellulose nanocrystals-MAl-3
4 and 1:0.8	Cellulose nanocrystals-MAl-4
5 and 1:1	Cellulose nanocrystals-MAl-5

Table 4
The surface textural characteristics of pure cellulose/Al—Mg-LDH nanocrystal composites, Al—Mg-LDH, and cellulose nanocrystals.

Parameter	Al—Mg-LDH (3:1)	Cellulose nanocrystals	Cellulose nanocrystals-MAl-1	Cellulose nanocrystals-MAl-2	Cellulose nanocrystals-MAl-3	Cellulose nanocrystals-MAl-4	Cellulose nanocrystals-MAl-5
BET surface area ($m^2\ g^{-1}$)	9.23	2.19	101.92	82.86	70.73	45.81	8.73
Pore volume ($cm^3\ g^{-1}$)	0.0312	0.0034	1.018	0.366	0.247	0.256	0.0598
Pore radius (nm)	6.86	2.99	18.38	8.5	6.85	7.7	13.7

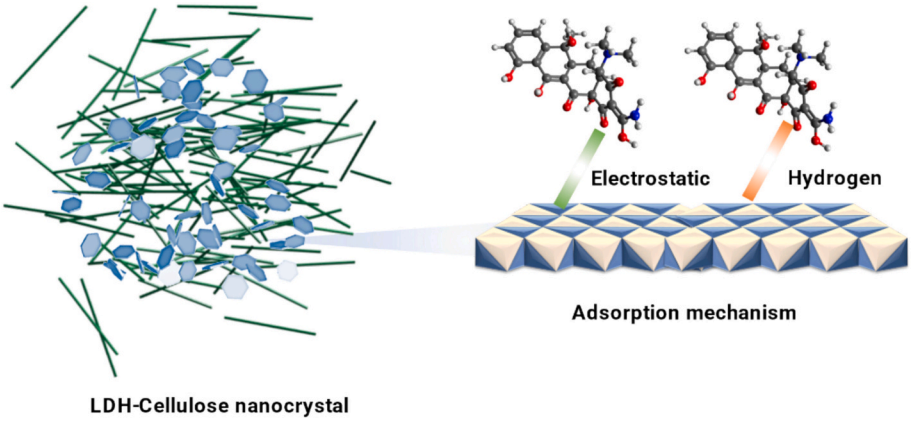

Fig. 4. Suggested method for tetracycline adsorption on the Al—Mg/LDH composite and cellulose nanocrystals.

phosphate, and diclofenac were also effectively removed by the biochar-LDH composites; their highest adsorption capacities were reported to be 2114.43, 487.99, and 1118.2 mg g^{-1}, respectively [145,146]. According to earlier research, biochar-LDH composites are most effective at removing anionic pollutants from water in the acidic pH range. This is mostly due to the several ways that anionic contaminants interact with biochar-LDH composites, including surface adsorption, chemical complexation, electrostatic attraction, and anion exchange [142,147,148].

A viable strategy to enhance the final material's adsorption capabilities and characteristics is the incorporation of functional material into the composite matrix [149]. Crystalline nanocelluloses with superior colloidal and mechanical stability are the cellulose nanocrystals described above [150,151]. Additionally, cellulose nanocrystals' enhanced surface hydroxyl groups facilitate efficient dispersion with the host matrix, linked to hydrogen bonding contact with the composite material [152]. According to reports, cellulose nanocrystals are an extremely effective nanoadsorbent for treating wastewater [153]. According to a recent study, the physical-chemical characteristics and adsorption of organic molecule contaminants significantly improved when chitosan particles were added to CuFe-B [154]. The coupling of CuFe-B with cellulose nanocrystals is therefore anticipated to improve the colloidal stability, which offers an alluring platform for a quicker and more effective interaction between the dye molecules and the composite functions [155]. The synthetic approach and functional synergy of the cellulose-B-CuFe layered double hydroxide biocomposite are schematically depicted in Fig. 5. The integration of CuFe-based LDHs, cellulose nanocrystals, and biochar into a single material is depicted in the figure. The porous and conductive charcoal matrix provides a robust support with many active sites, while cellulose nanocrystals contribute surface hydroxyl groups that promote hydrogen bonding, improve dispersion, and boost colloidal stability.

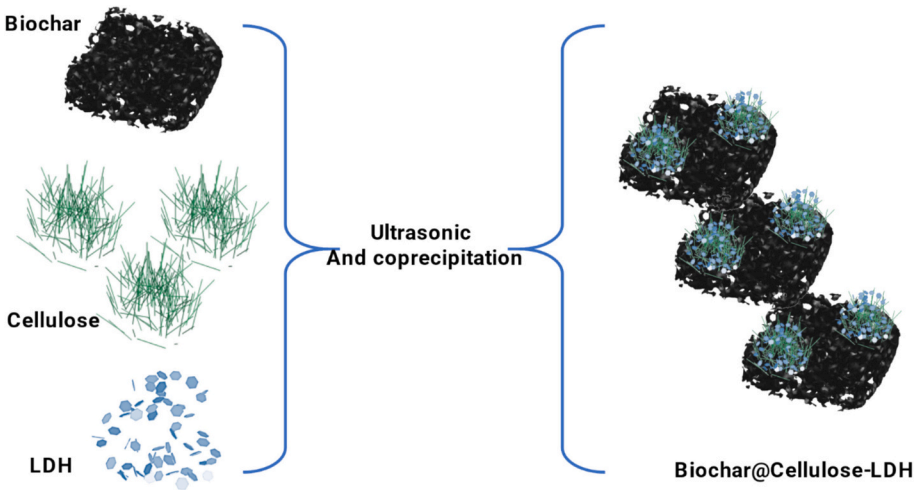

Fig. 5. Biochar-supported layered cellulose double hydroxide nanocrystal composite.

Concurrently, the addition of CuFe-based LDH increases the affinity for negatively charged azo dye molecules like Eriochrome Black T by introducing positively charged layered structures with a high anion-exchange capacity. Each component of the final composite works in concert with the others to create a hierarchical architecture: cellulose nanocrystals improve functional surface interactions, biochar maintains structural integrity, and LDH layers facilitate effective dye uptake. The high adsorption capacity, quick kinetics, and superior reusability noted are explained by this cooperative effect, demonstrating the potential of cellulose-B-CuFe composites as affordable and environmentally friendly adsorbents for wastewater treatment [154]. Layered double hydroxide biocomposites with biochar and cellulose nanocrystals (cellulose-B-CuFe) were synthesized via ultrasonic coprecipitation, producing a 2D rod-like structure with high crystallinity and surface functionality. The biocomposite efficiently adsorbed anionic azo dyes, reaching a maximum Eriochrome Black T adsorption of 876 mg g^{-1} in 45 min at acidic pH (2–5). Adsorption followed pseudo-second-order kinetics and isotherm models (Redlich-Peterson, Freundlich), with excellent reusability over six cycles. Incorporating cellulose nanocrystals and LDHs into biochar provides a cost-effective strategy for enhanced dye removal from wastewater [154].

Using an ultrasound-assisted coprecipitation approach, the aforementioned CuFe-B layered cellulose nanocrystal and LDH biocomposites were created. First, cellulose nanocrystals of 5–25 wt% biochar, which is made from date palm leaf residues at 700 °C for 4 h [156]. The cellulose nanocrystal–biochar mixture was ultrasonically dispersed in water, then combined with Fe^{3+}/Cu^{2+} LDH salts (1:2 molar ratio) at 65 °C under stirring. The pH was gradually adjusted to 9–9.5 with NaOH to initiate coprecipitation, and the mixture was refluxed overnight. The resulting biocomposite was centrifuged, washed with water, and treated with ethanol to remove unreacted salts and NaOH [154]. The biocomposites that were produced were dried for 48 h at 60 °C in an oven.

The addition of cellulose nanocrystals enhanced the surface functionality, structure, and hydrophilicity of the CuFe-B-cellulose nanocrystals biocomposite, increasing dye affinity. For 40 mg L^{-1} Eriochrome Black T, adsorption equilibrium was reached in under 30 min. Adsorption data fit well with Freundlich and Redlich-Peterson models, while Langmuir kinetics also provided a good fit. Maximum adsorption capacities at 25, 35, and 45 °C were 657, 714, and 876 mg g^{-1}, respectively [154]. Adsorption of dyes on 10% CuFe-B-cellulose nanocrystals followed film diffusion and pseudo-second-order models and was spontaneous and endothermic. The biocomposite maintained high adsorption in the presence of NO_3^- and Cl^- but showed reduced capacity with 0.25 M SO_4^{2-} and CO_3^{2-}. It retained excellent performance over six regeneration cycles, demonstrating strong reusability and potential for industrial dye removal [154].

Carboxymethyl cellulose, a polysaccharide of β(1-4)-linked d-glucose units with hydroxyl groups at C2, C3, and C6, enables chemical modifications that enhance adsorption. Its biocompatibility, modifiability, low cost, eco-friendliness, and biodegradability make it an attractive biosorbent, alongside β-cyclodextrin-functionalized materials [157].

Biopolymers like carboxymethyl cellulose and β-cyclodextrin have limited stability, mechanical strength, and selectivity in aquatic applications. To enhance performance, they are often chemically functionalized with materials such as graphene oxide, which offers high surface area, stability, and adsorption capacity. However, its separation from spent adsorbent limits commercial wastewater use [158]. Layered double hydroxides (LDHs) are anionic clays with a 2D brucite-like structure, containing trivalent (M^{3+}, e.g., Al^{3+}) and divalent (M^{2+}, e.g., Fe^{2+}) cations and interlayer anions (A^{n-}). During synthesis, M^{3+} and M^{2+} form octahedral structures with hydroxyl groups, generating a negatively charged surface [116].

FAH-LDH research focuses on integrating reduced graphene oxide with biopolymers to overcome limitations like adsorbent separation and to increase adsorption sites. This aims to develop novel adsorbents with high efficiency, improved regeneration, and superior removal performance [159]. β-Cyclodextrin and carboxymethyl cellulose were incorporated into LDH/reduced graphene oxide composites to create a multifunctional nanocomposite with increased adsorption sites for anionic ions, including selenium. The LDH/reduced graphene oxide-β-cyclodextrin-carboxymethyl cellulose nanocomposite was prepared via ex-situ polymerization, ultrasonic stirring, 24 h colloidal agitation, degassing, centrifugation, and vacuum drying at 50 °C. This functionalization for selenium removal is novel [160]. LDH/reduced graphene oxide composites functionalized with carboxymethyl cellulose and β-cyclodextrin efficiently adsorbed Se(IV), with maximum capacities of 248.75 mg g^{-1} and 275.48 mg g^{-1}, respectively. Adsorption followed the Langmuir isotherm and pseudo-second-order kinetics ($R^2 > 0.98$). Studies on mechanism, regeneration, and coexisting anions confirmed the composites' effectiveness, offering a promising solution for selenium removal from water [159].

In the realm of adsorption, three-dimensional hierarchical porous materials are currently gaining a lot of attention [161]. Three-dimensional hierarchical LDHs feature multi-scale structures with larger pore volumes and surface areas than conventional LDHs, enhancing permeability and mass transfer rates and improving overall adsorption efficiency [162]. Two-dimensional structures could be transformed into three-dimensional ones in a number of ways, such as assembly/delamination [163], model methods [164], and interleaving modification [165]. However, extreme conditions like high pressure and high temperature were necessary for the synthesis of three-dimensional LDH [166]. Three-dimensional LDHs with dynamic pore architectures are highly attractive because their pores can change size and shape in response to external stimuli. Inspired by the sponge's water-absorbing 3D structure, such materials enable novel approaches for mixture separation and controlled adsorption behavior [167]. Adsorbents with dynamic pore architectures improve organic contaminant removal from wastewater by facilitating pollutant diffusion through larger pores. Incorporating a second component into the LDH network enables the creation of 3D structures with dynamic porosity, enhancing practical applications.

Activated carbon fiber made from recycled cotton has been investigated recently as a matrix for creating nanostructured LDHs [168]. Residual cotton fabric is dispersed in a NaOH/urea solution and combined with an LDH formamide suspension to form a homogeneous mixture. After calcination, the product consists of activated carbon fibers and stacked double oxides. LDH/cotton fiber composites are typically prepared via in-situ growth of LDH directly on cotton fibers [169]. No prior studies have built 3D dynamic pore structures of LDHs or activated carbon fibers using calcined cotton fibers. Activated carbon fiber/LDH composites exhibit sponge-like expansion and contraction due to the LDH "memory effect," enhancing adsorption and desorption of organic dyes such as acid red 27 (~760 mg g^{-1}). Adsorption occurs via electrostatic interactions with sulfonic groups and π–π interactions with aromatic rings. The composites' pore structure and surface area recover after regeneration [168]. Activated carbon fiber/LDH adsorbents demonstrated excellent reusability, maintaining acid red adsorption above 650 mg g^{-1} after five cycles. Regeneration at 500 °C restored the LDH layered structure and preserved the 3D network pore architecture formed on calcined cotton fibers. Electron diffraction confirmed partial recovery of LDH nanosheets and MgO crystals. The adsorption–regeneration process involves two stages: structural expansion during adsorption and contraction during regeneration, enabled by the LDH "memory effect" [168].

Pore shape significantly influences adsorption capacity by affecting pollutant diffusion rates. The mesoporous structure of the adsorbent was confirmed by type IV isotherms with hysteresis observed at high relative pressures (0.5–1) [170]. The layered LDH structure in activated carbon fiber/LDH-R composites produced H4-type hysteresis loops, indicating the presence of both small and medium-sized pores [171]. The layered LDH structure in activated carbon fiber/LDH-R composites resulted in H4-type hysteresis loops, revealing the presence of both small and

medium-sized pores [170].

The layered double oxides-R/activated carbon fiber composite exhibited an increased specific surface area due to enhanced microporosity. Conversion to activated carbon fiber/LDH-R decreased micropore volume and total surface area while increasing average pore size through LDH layer reorganization. Pore expansion also generated negative pressure, facilitating dye diffusion into the adsorbent [168]. Stacked double oxides and activated carbon fiber effectively removed water pollutants. During regeneration, particle and pore sizes decreased, but activated carbon fiber/layered double oxides-R1 exhibited the largest surface area due to 3D network pore formation, explaining the peak adsorption in the second cycle. X-ray diffraction confirmed alternating transformations between metal oxides and layered double hydroxides during adsorption–desorption cycles [168]. With increasing adsorption cycles, the pore volume and size of activated carbon fiber/layered double oxides-R decreased due to dye accumulation. FTIR spectra before and after adsorption showed characteristic bands at 1489 and 1605 cm^{-1}, corresponding to the C═C stretching of aromatic rings in both acid red and the adsorbent [172]. The conjugated π system on the activated carbon fiber and the dyes formed π-π stacking, which caused the bands at 1489 cm^{-1} and 1605 cm^{-1} to move to 1499 cm^{-1} and 1615 cm^{-1} after adsorption [173]. Around 1630 cm^{-1}, the azo group's N═N stretching vibrations should have emerged, superimposed on top of the C═C stretching vibration [174]. The O═S═O stretching vibration in the sulfonate group was identified as the cause of the distinctive bands at 1035 cm^{-1} and 1185 cm^{-1} [175]. Bands at 600–700 cm^{-1} indicated substituted benzene rings. Elemental analysis showed minimal changes in carbon content and Al/Mg ratio during adsorption–desorption cycles, demonstrating high stability of the activated carbon fiber/layered double oxides composite compared to pure LDHs. This composite is a promising, cost-effective adsorbent for water pollutants and offers a sustainable strategy for reusing leftover cotton fibers [168].

3.2. Hydrothermal and solvothermal techniques

Comparison between hydrothermal and solvothermal methods, highlighting their definitions, solvents, applications, and main differences (Table 5). Ion exchange, coprecipitation, reconstruction, hydrothermal, salt oxide, and delamination techniques are frequently used to prepare LDH. The most used technique for making LDH is the coprecipitation method [44]. LDHs are commonly synthesized by supersaturating two or more metal ions through physical (evaporation) or chemical (pH adjustment) methods. Among coprecipitation techniques, three types exist: titration coprecipitation (sequential precipitation), where metal cations are gradually added to a basic solution for sequential deposition; and low supersaturation coprecipitation, which ensures simultaneous metal precipitation under controlled temperature, pH, and stirring [44]. The third coprecipitation method, high supersaturation, involves rapidly adding two or more metal cation solutions into a base solution under continuous stirring [176]. *Pseudomonas* sp. strain ADP was immobilized on Mg_2 LDH-Al matrix using a direct coprecipitation technique to degrade the herbicide atrazine [177]. ADP@LDH biohybrids were synthesized at pH 8 using $Mg(NO_3)_2$ and $Al(NO_3)_3$ (Al/Mg = 2), with sodium hydroxide and ADP suspension (mass ratio 2–40). At ratios ≤10, they showed the highest atrazine degradation, retaining biodegradative activity after four reuse cycles and three weeks of storage at 4 °C [177]. The ion exchange method is widely used and relies on replacing interlayer anions through electrostatic interactions with the positively charged host layers [176,178].

LDHs can intercalate various anions, with ion exchange favored under suitable temperature, excess initial anions, high affinity, and pH ≠ 4. The affinity order for monovalent anions is $OH^- > F^- > Cl^- > Br^- > NO_3^- > I^-$ [179]. An earlier investigation detailed the divalent anion as $HPO_4^{2-} > HAsO_4^{2-} > CrO_4^{2-} > SO_4^{2-} > MoO_4^{2-}$ [44]. Examples of various organic anions that are intercalated include amino acids and cellulose [180] and biomolecules [181]. Calcined LDH (layered double oxides) can be reconstructed into LDH under an inert atmosphere by adding ions and water, allowing incorporation of organic anions such as amino acids and peptides [182]. The "memory effect" refers to a structural alteration that decreases with increasing temperature due to the formation of stable spinels [176]. The salt-oxide approach produces LDH by slowly adding a trivalent metal salt to a divalent metal oxide suspension, without maintaining a constant pH [73,183]. For instance, sodium aluminate and magnesium hydroxide or oxide are used to prepare Al/Mg-based LDH [184]. The hydrothermal method synthesizes LDH by dispersing metal oxides in water with target anions and heating the mixture to a specific temperature, such as producing Al—Mg LDH by autoclaving Al_2O_3 and MgO at 110 °C for 5–10 days [180]. Ultrathin LDH nanoplates were produced in a continuous-flow hydrothermal reactor using controlled nucleation, aging, in-line dispersion, and precipitation processes [185]; both approaches were previously created before the application [186,187]. The delamination technique produces LDH nanosheets by dispersing LDH in a polar solvent to solvate intercalated anions, followed by vacuum drying; nanosheets can be formed via top-down or bottom-up approaches. The top-down method entails delaminating LDH in various solvents, including acrylates [188], higher alcohols such as butanol [75], hexanol, pentanol, toluene, carbon tetrachloride, water [189,190], formamide [191], and *N*,*N*-dimethylformamide-ethanol mixture [192]. In the coprecipitation system, the bottom-up method employs 1-butanol as a co-surfactant and dodecyl sulfate as a surfactant in the oil-phase medium [193,194].

All three main synthesis methods (in situ coprecipitation, hydrothermal, and impregnation) have advantages and disadvantages, as well as challenges in the scalability stage. In situ coprecipitation has the advantage of optimizing a homogeneous distribution of LDH particles on the cellulose, increasing the active area and ion exchange efficiency [195]. It is a relatively simple method under mild synthesis conditions; it favors strong interaction between the polymer matrix and the inorganic lamellae [195]. However, controlling the stoichiometry of metal ions can be difficult, resulting in secondary phases or incomplete precipitation; there is a risk of aggregation of particles with excess ionic charge [195]. On an industrial scale, maintaining uniform pH, temperature, and the molar ratio between metal cations is complex; the need for large volumes of solution and washing processes increases costs and generates significant liquid waste [196]. Hydrothermal synthesis, on the other hand, results in composites with greater crystallinity and structural stability; it improves the dispersion and adhesion of LDH to cellulose; it favors more refined control of particle size and morphology [197]. However, it requires specialized equipment (autoclaves) and rigorous operating conditions; high energy consumption; and longer synthesis times compared to methods under mild conditions [198]. High-pressure

Table 5
Comparison between hydrothermal and solvothermal methods.

Aspect	Hydrothermal method	Solvothermal method
Definition	Synthesis in an aqueous medium under high temperature and pressure.	Synthesis in a medium with organic solvents under high temperature and pressure.
Solvent	Water.	Organic solvents (alcohols, ethylene glycol, DMF, etc.).
Solvent role	Acts as both solvent and sometimes reagent.	Controls solubility, nucleation, and particle growth.
Materials obtained	Metal oxides, synthetic clays, crystalline nanomaterials.	Metallic nanoparticles, semiconductors, oxides, hybrids.
Property control	More limited; depends on aqueous chemistry.	Greater control over size, shape, and dispersion through solvent choice.
Advantages	Simple, cost-effective, and more environmentally friendly.	Versatile, allows synthesis of compounds insoluble or unstable in water.
Limitations	Restricted to species soluble/stable in water.	Use of organic solvents may increase cost and toxicity.

operation limits large-scale production due to safety risks, capital costs, and maintenance; the difficulty in reproducing uniform morphologies in large batches can compromise the consistency of the final material [199]. Finally, the impregnation technique offers a simple and straightforward methodology, allowing the incorporation of varying amounts of LDH; it allows selective modification of the cellulose surface without drastically altering its structure; and it has a lower initial cost than hydrothermal synthesis [200]. However, adhesion between LDH and cellulose can be weak, favoring leaching in aqueous media; heterogeneous particle distribution, which reduces efficiency and reproducibility; and less structural integration between phases [201]. Although easier to implement in continuous processes, reproducibility in terms of LDH loading and composite stability is limited; in long-term environmental applications, loss of LDH by detachment is a significant technological barrier.

Each synthesis route offers a trade-off between performance, cost, and scalability. In situ coprecipitation is promising for laboratory applications due to its good phase integration, but faces challenges in achieving uniformity on an industrial scale. Hydrothermal synthesis provides high-quality and stable materials, but faces economic and safety barriers to mass production. Impregnation is simpler and more scalable, but the structural stability of composites remains a challenge. Therefore, transitioning these materials to industrial applications requires the development of hybrid routes, cellulose surface modification strategies, and continuous process optimization to balance cost, performance, and sustainability.

3.3. Other methods

LDH can also be made in a variety of ways, including electrosynthesis, sol-gel [202], urea hydrolysis, and mold [176]. Electrosynthesis is a technique based on the electrochemical deposition of metal layers, in which metal ions present in the solution are reduced or oxidized on an electrode, forming hydroxide layers [203]. In the case of LDH, electrosynthesis allows for the controlled formation of lamellar structures on conductive substrates. The advantage is high purity, control over layer stoichiometry and thickness, and the possibility of direct deposition on conductive supports, useful for applications in electrochemistry and catalysis [204]. However, it is difficult to scale due to the need for specific electrodes and precise control of current and voltage, as well as the relatively high costs compared to large-scale chemical methods [204].

The sol-gel method involves the formation of a three-dimensional network from metal precursors in solution (usually alcoholics), which undergo hydrolysis and condensation to form a gel, subsequently calcined to generate LDH [205]. It allows for fine control over the morphology and homogeneity of the structure and offers the possibility of incorporating dopants or specific ions into the network [206]. However, the process is sensitive to humidity and pH, requiring strict control of conditions, and is difficult to produce on a large scale due to the complexity of gelation and uniform drying [207]. In urea hydrolysis, metal salts are dissolved in aqueous solution along with urea. The thermal decomposition of urea slowly releases hydroxyl ions, promoting the controlled precipitation of LDH [208]. Production is uniform and particle morphology is controlled, and the process is relatively simple and inexpensive. However, the method requires prolonged heating, which can limit large-scale production, and the release of ammonia may require environmental treatments in industrial processes [209]. Finally, the "Mold" (biomimetic) method is inspired by biological processes. This method uses organic structures or biomolecules as templates to guide LDH precipitation, forming structures with specific morphologies (controlled porosity, organized lamellae) [209]. It allows precise control of shape and structure at the nanoscale and has potential for materials with high surface area and improved catalytic or adsorbent properties. Among the challenges, the method requires specific organic precursors or biomolecules, which can increase costs and the process is relatively slow and difficult to standardize on an industrial scale.

Researchers have created a sol-gel process that does not require alkoxide to synthesize Al/Mg-based LDH [210]. In this process, aluminum chloride is hydrolyzed and hydrogel is formed utilizing freshly manufactured magnesium $(HCO_3)_2$ as a moderate neutralizer. To produce pure layered material, the hydrogel was aged for 24 h. Electrochemical synthesis of Cr—Ni-based LDH, Al—Ni-based LDH, Fe—Ni-based LDH, and Mn—Ni-based LDH is possible, and their characteristics are comparable to those achieved using chemical methods. The template approach uses templates that are used in the production of LDH, such as polypeptides, micelle-forming surfactants, polysaccharides, etc. [176]. Because of its high base and weak water solubility, urea can be used to modulate the rate at which it hydrolyzes, making it helpful for precipitating metal hydroxides [176]. Ion exchange, hydrothermal-mechanochemical, usual coprecipitation, and reverse microemulsion were the four methods used to create methotrexate-intercalated LDH hybrids [211,212].

The creation of cellulose LDH composites has made use of a few of the techniques previously discussed. The abundant biopolymer called cellulose makes up all of vegetation's living cells. The carbon cycle revolves around this natural resource. Previously defined as a modified cellulose, carboxymethyl cellulose has carboxymethyl groups ($–CH_2$-COOH) joined to part of the cellulose's –OH groups. It is appropriate for ion exchange applications because of its anionic behavior, water solubility, and chemical reactivity, all of which are caused by the carboxymethyl groups found in carboxymethyl cellulose. Using coprecipitation techniques, researchers have intercalated carboxymethyl cellulose into Al—Mg LDH and Al—Ni LDH [213]. The shift of asymmetric COOH group peaks to higher wavenumbers was seen in the Fourier Transform InfraRed Spectroscopy spectra of Al—Mg LDH/carboxymethyl cellulose, demonstrating the intercalation of carboxymethyl cellulose into the LDH matrix. D-spacing increased for Al—Mg LDH from 0.862 nm to 0.816 nm, for Al—Ni LDH from 1.73 nm to 2.23 nm, and for each of the carboxymethyl cellulose bionanocomposites from 0.862 nm to 2.23 nm. Al—Mg LDH/carboxymethyl cellulose and Al—Ni LDH/carboxymethyl cellulose were found to have non-intercalated and intercalated layers, respectively, according to the results of transmission electron microscopy. Compared to Al—Ni LDH/carboxymethyl cellulose, Al—Mg LDH/carboxymethyl cellulose bionanocomposites exhibited greater heat stability. From pH 2 to pH 10, the swelling behavior of bionanocomposites increased; however, at pH values 10 and higher, a significant rise was noted. Researchers used nanocomposite spheres made with LDH and carboxymethyl cellulose, utilizing the coprecipitation method, to study the drug release of Ibuprofen intercalated with these spheres [214]. The drug release of LDH-ibuprofen was 60% at very acidic pH, whereas the carboxymethyl cellulose/LDH-ibuprofen nanocomposites showed a negligible amount (<10%) because carboxymethyl cellulose contracts in acidic media, but at pH 7.4, it was 40% and higher because of the carboxyl groups in the carboxymethyl cellulose chains. LDH-carboxymethyl cellulose bionanocomposites' pH-sensitive anti-inflammatory release pattern is demonstrated by this activity. Using water as the solvent, carboxymethyl cellulose-Al—Mg LDH bionanocomposite films were created using the solution casting technique, containing 0–8% LDH [213]. Because of the substantial interaction between the LDH sheet and carboxymethyl cellulose, the mechanical properties of the carboxymethyl cellulose-LDH bionanocomposite film, such as its tensile modulus of 1040 MPa and its tensile strength of 25.65 MPa, were 148% and 143% higher than those of the pure carboxymethyl cellulose film at 3 wt% LDH content. Additionally, for the carboxymethyl cellulose-LDH bionanocomposite film, the elongation at break and water vapor permeability decreased by 62% and 37%, respectively.

3.4. Surface functionalization: use of oxidized cellulose or grafting to improve interaction with LDH layers

Functionalizing LDH surfaces with oxidized or grafted cellulose has

proven to be a versatile strategy for improving mechanical properties, increasing drug adsorption capacity, and enhancing biocompatibility for biomedical applications. In the context of mechanical enhancement, the incorporation of cellulose groups and nanocellulose allows for increased structural stability and reduced agglomeration, and is often combined with polymers to form stronger composites [215]. For drug adsorption, oxidized cellulose acts as a loading matrix, increasing affinity for therapeutic molecules and enabling controlled-release systems, often dependent on pH or specific functional groups, such as carboxyl groups [216]. In biomedical applications, functionalization promotes greater biocompatibility and reduces toxicity, enabling the use of LDH in drug delivery systems and tissue engineering, with growing interest in bioinspired surfaces. Furthermore, in environmental adsorption, LDH–cellulose materials have been applied to the removal of metal ions and dyes, often incorporated into biodegradable membranes or hydrogels. In general, trends point toward the use of nanocellulose, the integration of targeted functional groups, the development of multifunctional materials, and the search for sustainable solutions that leverage cellulose's renewable and biodegradable nature. The Table 6 summarizes the different types of LDH functionalization with cellulose, grouped by thematic application. The modifications performed, the main effects obtained, and current research trends are highlighted, highlighting the potential of these materials in areas such as mechanical reinforcement, drug delivery, biomedical applications, and environmental adsorption.

One important tactic to improve its interaction with LDH composites and raise the effectiveness of LDH–cellulose composites in adsorption applications is cellulose surface functionalization. The oxidation of cellulose and the grafting of functional groups onto its backbone are two popular strategies in this regard. Cellulose that has been oxidized to enhance its interaction with LDH. TEMPO-oxidized cellulose nanofibrils (TOCNFs) are produced when cellulose oxidation, especially TEMPO-mediated oxidation, adds carboxyl groups to the cellulose backbone. Stronger electrostatic interactions with the positively charged LDH layers are made possible by these carboxyl groups, which raise the negative charge density of cellulose. This alteration strengthens the composite's structural integrity and adsorption capability in addition to improving LDH's dispersion in the cellulose matrix. For instance, because TOCNFs-LDH composites have more active sites and better interfacial compatibility, they have shown enhanced adsorption capability for heavy metal ions and dyes [217]. By covalently affixing functional monomers to the cellulose backbone, functional groups can be grafted onto cellulose to introduce particular chemical functionalities that can interact with the LDH layers. By using this technique, the characteristics of cellulose can be altered to target particular contaminants. For instance, cellulose's affinity for heavy metal ions can be increased by grafting amino or sulfonic acid groups onto it using chelation or ion exchange processes. It has been demonstrated that these changes increase the cellulose-based composites' adsorption effectiveness for pollutants like lead and cadmium ions [218]. The efficiency of LDH–cellulose composites in adsorption applications is greatly enhanced by cellulose surface functionalization by oxidation or grafting. Stronger interactions with target pollutants are made possible by the added functional groups, which also improve LDH's stability and dispersion in the matrix and increase the quantity and accessibility of active sites. Higher adsorption capacities, quicker adsorption kinetics, and enhanced reusability result from these enhancements, which make the composites extremely useful for environmental remediation projects, especially when it comes to removing organic contaminants and heavy metals from aqueous solutions [219].

LDHs are often introduced directly to composites without modifying their surface in any way [220] or merely through a change using coupling agents [221]. The urea hydrolysis method is one of the most used synthesis procedures for producing LDHs from aqueous solutions containing divalent or trivalent metal cations [79]. In one work, a hybrid filler utilized as reinforcement in polyurethane-based materials was created by using the urea hydrolysis process to precipitate Al/Zn-based LDH on α-cellulose in a single step [222]. It has previously been documented that LDHs can be used to create nanocomposites using a variety of polymers [223,224]. Table 3 provides a few studies on LDH reinforced polyurethane composites, however. Given the enhanced qualities provided by the inorganic filler, research on various economical methods and approaches for incorporating inorganic fillers into the polyurethane polymer matrix is highly desirable. Effective inorganic component dispersion within the matrix is essential for achieving good compatibility at the organic-inorganic interface. Several techniques (including surface modification and in situ polymerization) have been used to do this in order to ensure that the inorganic filler is sufficiently dispersed throughout the polymer matrix [225]. In order to perhaps enhance the dispersion of inorganic LDHs in polyurethane-based matrices, precipitated LDH was prepared on cellulose fibers in this investigation. One naturally occurring organic substance that is widely accessible and prevalent in plant fibers is cellulose [36]. To create a hybrid filler, the study sought to find an inexpensive biodegradable substance that might serve as a support for LDH and enhance compatibility with polyurethane matrices through sustainable approach [222]. As far as we are aware, no reports exist about cellulose fiber composites coated with LDH as a filler in a matrix made of polyurethane (Table 7). The produced filler's thermal, spectroscopic, morphological, and barrier characteristics were thoroughly examined. Additionally, the reinforced polyurethane composites' mechanical, thermal, and barrier qualities were examined and contrasted with those of the unfilled material. The inherent polarity of LDH led to a minor improvement in the polyurethane's heat stability as well as improved hydrophilicity. At a filler loading of 10 wt%, the polyurethane composites' elastic modulus rose to 48 MPa. While effective deposition was shown by examining X-ray diffraction spectra, Fourier transform infrared spectroscopy, and X-ray spectroscopy maps that displayed the distribution of zinc and aluminum, scanning electron micrographs verified the presence of LDH platelets. Additional information about the characteristics of the modified cellulose was provided by its sorption characteristics and point of zero charge. The produced hybrid filler was subsequently included in polyurethane composites as reinforcement. Characterization showed that the

Table 6
Synthesize the different types of LDH functionalization with cellulose, grouped by thematic application.

Theme/application	Type of functionalization	Main effect/benefit	Observed trends
Mechanical enhancement	Grafting of cellulose groups, oxidized cellulose	Increased structural stability, improved compressive strength, reduced agglomeration	Use of nanofibrillated cellulose and nanocrystals for reinforcement; integration with polymers for advanced composites
Drug adsorption	Oxidized cellulose as a loading matrix	Higher affinity for pharmaceutical molecules, controlled release	Development of LDH–cellulose for prolonged and pH-responsive release; incorporation of carboxyl functional groups for specific affinity
Biomedical/ biocompatibility	Grafting of modified cellulose	Improved biocompatibility and reduced toxicity	Applications in drug delivery systems, tissue engineering; growing interest in bioinspired surfaces
Environmental adsorption/ pollutant removal	Oxidized or grafted cellulose	Enhanced interaction with metal ions or dyes	Trend toward integrating functionalized LDH into membranes or hydrogels for water purification; focus on biodegradable and sustainable materials

Table 7
Recent research on composites based on LDH and polyurethane.

Effect of LDH	Type of LDH filler	Reference
Increase in LOI value, higher thermal stability, and improvement in tensile strength.	Dodecyl sulfate intercalated AlMg LDH	[226]
Thermal stability, Young's modulus, and improvement in tensile strength	Dodecyl sulfate intercalated CoAl LDH	[227]
Optical transmittance, thermal stability, elongation at break, and improvement in tensile strength	Dodecyl sulfate intercalated AlMg-LDH	[228]
Thermal stability, smoke suppression, and improvement in flame retardancy	Graphene oxide/lanthanum doped AlMg-LDH	[229]
Antibacterial activity, water resistance, and improvement in mechanical properties	p-Hydroxybenzoic anionic intercalated AlMg-LDH	[230]
Antibacterial activity, water resistance, and improvement in mechanical properties	ZnO/AlNi-LDH	[231]
Combustion behavior and improvement in thermal stability	ZnAl-LDH/carbon nanotubes	[232]
Thermal stability, as well as ultraviolet absorption ability, mechanical behavior, and improvement in damping property	γ-Aminopropyltriethoxysilane-dodecyl sulfonate intercalated AlMg-LDH	[233]
Smoke suppression effect and improvement in flame retardant	Graphene oxide/europium doped AlMg-LDH	[234]

presence of LDH caused a modest increase in sorption properties, while inorganic Zn and Al were mostly responsible for the slight improvement in thermal properties. Furthermore, up to 10% w/w of reinforcement was used to increase mechanical performance. Lastly, research on the ultraviolet and light barrier (up to 700 nm) revealed a striking decrease in the percentage of transmission as the cell's LDH content rises. In conclusion, a polyurethane-based composite reinforced with modified green cellulose that has better physical qualities was designed and made [222]. Surface functionalization of LDH with oxidized cellulose or grafted cellulose represents a versatile strategy to enhance the interaction between the polymeric layer and the inorganic LDH structure. In terms of cost, using standard cellulose derived from natural sources is relatively low-cost, but the use of nanocellulose or chemically modified cellulose increases expenses due to additional processing steps, purification, or oxidation reactions. Regarding process complexity, simple adsorption of cellulose onto LDH is straightforward and requires minimal specialized equipment, whereas chemical grafting or oxidation demands precise control of pH, temperature, and reaction conditions, making the procedure more sophisticated. Concerning biodegradability, functionalization with natural or nanocellulose generally maintains or improves environmental compatibility, as cellulose is inherently biodegradable. However, extensive chemical modification or grafting with synthetic polymers can reduce the overall biodegradability of the material, depending on the nature and density of the functional groups introduced.

3.5. Comparison: efficiency, cost, scalability, and environmental impact of each method

Incorporating LDH–cellulose composites into adsorption technology offers a viable substitute for traditional adsorbents. In terms of effectiveness, affordability, scalability, and environmental impact, these composites have special benefits. To assess their potential for use in water remediation applications, a comparison with more conventional adsorbents, such as metal-organic frameworks (MOFs), zeolites, activated carbon, and biochar, is necessary [235]. In terms of adsorption efficiency, it is found that LDH–cellulose composites have a high adsorption capacity because of the complementary action of cellulose's many functional groups and LDH's anion exchange capabilities. For instance, ZnFe-LDH composites outperformed some traditional adsorbents, including activated carbon made from coconut leaves, which showed adsorption capacities of about 73.83 mg g^{-1}, with adsorption capacities of up to 152.35 mg g^{-1} for the removal of caffeine [236]. Traditional adsorbents, on the other hand, have variable efficiencies. For example, activated carbon can have high efficiencies (up to 90–95%) for organic molecules, but surface fouling and pore blockage may cause performance to decline with repeated usage [236]. For cationic pollutants in particular, zeolites typically offer moderate to high efficiency; however, they are less effective for organic contaminants [237]. While biochar often offers economic and sustainability benefits along with moderate efficiency (50–70%), its adsorption capabilities are typically lower than those of LDH–cellulose composites [235]. Lastly, MODs are highly effective against a range of contaminants, but there may be issues with their stability in aquatic conditions [238].

For large-scale applications, adsorbents' economic feasibility is essential [235]. The utilization of plentiful and renewable resources, including cellulose and inexpensive metal salts, for LDH synthesis implies a cost-effective strategy for LDH–cellulose compounds, despite the lack of precise cost data. Furthermore, its economic viability is increased by the possibility of regeneration and reuse [239]. Production prices for activated carbon vary from 1.100 to 1.700 US$/ton, depending on the energy-intensive activation procedures [240]. Production costs for biochar materials are substantially cheaper, with prices starting at 350 US $/ton, particularly when they are made from leftover biomass [235]. Lastly, the cost of zeolites and MOFs varies greatly; natural zeolites are normally less expensive, but synthetic zeolites and MOFs can be costly because of intricate production processes [239]. The availability of raw ingredients and the ease of synthesis determine scalability. Given the widespread availability of cellulose and metal salts, it has been found that the in situ coprecipitation approach for synthesizing LDH on cellulose substrates is quite easy to scale up for LDH–cellulose composites [44]. Large-scale production of activated carbon is already established; however, the procedure uses a lot of energy and could not be long-term viable [235]. Biochars are a good fit for decentralized water treatment systems since they are reasonably easy to scale and can use a variety of biomass sources [241]. Lastly, because of their intricate and costly manufacturing processes, zeolites and MOFs have synthetic variations and struggle with scalability [239].

When evaluating the environmental impact, one must take into account the sustainability of raw materials, production energy consumption, and disposal at the end of their useful life. LDH–cellulose composites have less of an impact on the environment because they may be made in moderate settings and employ renewable resources. Their ecological sustainability is further enhanced by their capacity for regeneration and biodegradation. Production of activated carbon requires a lot of energy, and regeneration procedures may produce secondary pollutants [242]. Although biochars are thought to be environmentally benign materials, particularly when made from leftover biomass, their effectiveness varies depending on the raw material and the circumstances of production [235]. Additionally, synthetic zeolites, MOFs, might entail toxic chemicals and produce trash during synthesis, whereas natural zeolites have no effect on the environment [243]. As a result, LDH–cellulose composites become a desirable substitute for traditional adsorbents due to their high adsorption efficiency, affordability, scalability, and advantageous environmental profile. Surface functionalization techniques can be used to adjust their

performance, and their synthesis makes use of plentiful and renewable materials. LDH–cellulose composites offer a sustainable and effective way to address new pollutants in wastewater, even if conventional adsorbents like activated carbon and biochar have consolidated roles in water treatment. All of the factors covered are compiled in Table 8.

4. Performance of LDH–cellulose and adsorption mechanisms

4.1. Adsorption processes and the performance of LDH–cellulose in the removal of pollutants

Sun et al. synthesized MgAl-LDO (layered double oxide) by a template approach employing cellulose [248]. The LDO was synthesized by calcining Mg-Al LDH to remove Cd^{2+}, Pb^{2+}, and Cu^{2+} [248]. A symbiotic interplay among cation exchange, deposition/precipitation, and the LDH memory effect (transformation from LDO) enhances removal. Divalent heavy metal ions (Cd^{2+}, Pb^{2+}, Cu^{2+}) replace Mg^{2+} ions in the LDH structure formed when MgAl-LDO is hydrated in water [248]. The ICP-MS experimental investigation indicated an increase in Mg^{2+} in the solution, whereas Al^{3+} remained unchanged, hence confirming the exchange of Mg^{2+}. An XRD study indicated an increased interlayer distance in the LDH post-adsorption due to the larger ionic radii of Cd (II), Pb (II), and Cu (II), resulting in the formation of Mg(M)Al-LDH [248]. Simultaneously, heavy metal ions (M = Cd, Pb, and Cu) react with OH^- (derived from LDH dissolution) to form Cd $(OH)_2$, $Pb_3(CO_3)_2(OH)_2$, and $Cu_4(SO_4)$ $(OH)_6{\cdot}2H_2O$. Characterization experiments, including SEM, XRD, and XPS, disclosed the subsequent alterations [248]. XPS confirms the formation of Cd—OH, Pb—OH, and Cu—OH bonds, while EDS elemental mapping validates precipitation on LDH flakes. The third mechanism enabling elimination was the LDH memory effect, in which MgAl-LDO reverts to LDH upon contact with water, thereby allowing the cation-exchange process [248]. Density functional theory confirmed the thermodynamic feasibility of Mg^2 replacement with Cd^{2+}, Pb^{2+}, and Cu^2. The calculations demonstrated fluctuations in charge density, and the binding energy suggested strengthened M-OH interactions. The conversion of LDO to LDH and the subsequent Mg^{2+}/HMI cation exchange were affected by the solution's pH. The ideal pH for sorption was 6.5 for $Cd^{2+}$and Pb^{2+} and 5.0 for Cu^{2+} [248]. At approximately mildly acidic to neutral pH, MgAl-LDO converts into LDH, utilizing the "memory effect." The chemisorption process was completed in around 10 h and followed a pseudo-second-order (PSO) kinetics model. The Langmuir isotherm (R^2 = 0.976) accurately described the equilibrium isotherm data, indicating monolayer adsorption with capacities of 1422.3, 1336.8, and 1135.4 mg g^{-1} for Cd^{2+}, Pb^{2+}, and Cu^{2+}, respectively [248]. The adsorption efficiency and reusability were significant, owing to the collaborative impact of the ultra-thin nanoflake structure obtained from cellulose templating and the Mg–OH active sites [248].

Similarly, Priya et al. synthesized an LDH/reduced graphene oxide nanocomposite by using carboxymethyl cellulose for the removal of As (V). The doping of CE into the FE-Al-rGO composite improved the adsorption capacity [157]. The mechanisms responsible for the removal of As(V) from solution were anion exchange, surface complexation, electrostatic interaction, and hydrogen bonding [157]. The removal was ascribed to an electrostatic interaction between the protonated functional groups ($–OH^{2+}$) and ($–COOH^{2+}$) and the arsenate ion, then succeeded by inner-sphere complexation with Fe—Al atoms on the surface (As—O—Fe and As—O—Al). Moreover, pore filling occurs as arsenate ions penetrate the internal pores of Fe-AL-rGO/CE, indicating that physical adsorption and volume exclusion are additional mechanisms for elimination, as confirmed by SEM, BET, and other characterization processes [157]. The zeta potential of the adsorbent was found to be approximately between 7 and 9 pH. Adsorption of As(V) was maximum between pH 2 and 7, whereas it was lowest at pH 8 and above [157]. The adsorption behavior of carboxymethyl cellulose-incorporated FAH-rGO nanocomposites was pH-dependent due to electrostatic interactions between anionic arsenate species and protonated functional groups, with optimal As(V) adsorption occurring at pH 7. The PSO model effectively represented the kinetic (R^2 = 0.9996), indicating chemisorption [157]. The maximal sorption capacity of FAH-rGO/CE-4 is 258.39 mg g^{-1}, and isotherm tests validated monolayer adsorption, supporting the Langmuir model. The remediation of arsenic in wastewater was significantly improved by these composites owing to their structural stability, elevated surface area, and plentiful oxygen-containing functional groups, which contributed to their exceptional adsorption capacity and reusability [157].

LDH integrated into cellulose and activated biochar obtained from

Table 8
Comparative analysis of LDH–cellulose composites adsorbents with conventional adsorbents based on various aspects.

Aspect	LDH–cellulose composites	Activated carbon	Zeolites	Biochar (e.g., from biomass)
Adsorption efficiency	High, due to synergistic anion-exchange from LDH layers plus functional groups from cellulose. For instance, Co–Fe LDH/cellulose showed excellent removal of pharmaceuticals (sulfamethoxazole, cefixime) with strong capacity and kinetics [100].	Excellent toward organics (90–95% removal), though may suffer pore-blocking over repeated use [244].	Good for cationic species; less so for organics unless modified (e.g. surfactant-grafted zeolites enhanced dye removal capacity ~5 mg g^{-1}) [245].	Moderate (50–70%) variability; lower capacities than LDH–cellulose, but adequate for some pollutants [244].
Cost	Uses low-cost metal salts and abundant cellulose; potential for cost-effective production and regeneration [100].	Expensive: $1100–1700/ton; energy-intensive activation required [244,246].	Natural zeolites are affordable; synthetic variants may be costly depending on treatment/grafting [245].	Inexpensive: $350/ton from waste biomass [246].
Scalability	Scalable: co-precipitation methods are straightforward using widespread cellulose and salt precursors [100].	Highly scalable: global supply exists, but production remains energy-intensive.	Natural: scalable; engineered versions may have complex production.	Very scalable: can be tailor-made from local biomass.
Environmental impact	Low: uses renewable cellulose; mild synthesis; biodegradable and regenerable [100].	Moderate to high: activation consumes energy; regeneration may produce secondary pollutants.	Natural zeolites low impact; synthetic ones may involve harsh chemicals [245].	Low: especially if derived from waste, though inconsistent performance across feedstocks [244,247].
Selectivity and functionality	Customizable through oxidation/grafting; excellent selectivity for heavy metals, dyes, and pharmaceuticals.	Broad but non-selective; best for organics.	Selective for cationic species; can be modified for anions.	Limited selectivity; works via non-specific adsorption and pore capture.
Regeneration and reuse	Promising regeneration due to reversible LDH intercalation and cellulose stability [246].	Can be regenerated thermally/chemically, but costly and can degrade performance.	Depends on the composition; regeneration is generally feasible but may require chemical treatment.	Regeneration is possible, but efficacy depends on product consistency.
Operational stability	Good mechanical stability from cellulose scaffold; stable LDH dispersion [100].	Fragile dust production and pore structure loss over cycles.	Mechanically robust; structure stable, but surface may clog.	Structural integrity varies; ash content can impact performance.

grape stalks was synthesized for the removal of mercury Hg(II). $MnFe_2O_4$@Zn—Al LDHs@Cel@AGB efficiently eliminated Hg(II), likely via an intraparticle diffusion process [249]. The methods of adsorption for the removal of Hg(II) encompassed pore filling, ionic interaction, van der Waals forces, and coordination interactions [249]. The adsorption efficiency of $MnFe_2O_4$@Zn—Al LDHs@Cel@AGB was markedly affected by pH, achieving optimal Hg (II) removal at pH 2 due to the development of anionic complexes and the attraction of positive surface charges [249]. The Hg (II) results conformed to the PSO kinetic model, signifying chemisorption. Intra-particle diffusion transpired in two phases: external surface adsorption and gradual pore diffusion to equilibrium [249]. The Freundlich isotherms more accurately depict the adsorption behavior, suggesting multilayer adsorption on a heterogeneous surface [249]. The composite exhibited substantial absorption capacities; 1283 mg g^{-1} for Hg(II); rendering it an efficient and reusable adsorbent for the concurrent elimination of heavy metals from aqueous solutions [249].

Peng et al. developed a CuAl-LDH/CCF composite for the efficient removal of phosphates from aqueous media, which is supported on carbon cellulose fiber [250]. Conventional adsorbents, including kaolinite, fly ash, and biochar, were outperformed by the material, which demonstrated a high sorption ability of 105.26 mg g^{-1} at 15 °C [250]. The adsorption mechanism was discovered to be a synergistic interplay of chemisorption and physisorption, with ligand exchange, anion exchange, and electrostatic interaction being the dominant pathways [250]. The SEM imaging revealed a uniform flower-like hierarchical distribution of LDH nanosheets, which facilitated enhanced surface adsorption and intraparticle diffusion [250]. The XRD analysis revealed characteristic reflections at 10°, 20°, and 25.8°, which are attributed to the (003), (006), and (009) planes, respectively. This confirms the presence of a well-developed LDH phase [250]. Post-adsorption, a decrease in peak intensity and broadening suggested structural distortion as a result of phosphate intercalation. This further supports the LDH memory effect and anion exchange between CO_3^{2-} and phosphate species ($H_2PO_4^-$, HPO_4^{2-}). The optimal phosphate uptake was observed at pH 8, which was consistent with the favourable electrostatic conditions [250]. The Langmuir model was the most appropriate fit for the isotherm data ($R^2 > 0.9998$), confirming monolayer adsorption, while the pseudo-second-order model was favoured in kinetic modelling, suggesting chemisorption. Intraparticle diffusion was not the sole rate-limiting factor, despite its contribution to the overall absorption. This suggests a multi-step adsorption mechanism [250]. Moreover, the material maintained an efficacy of over 85% during five adsorption–desorption cycles, and the process was exothermic and spontaneous, underscoring its practical potential for sustainable water purification technologies [250].

MgAl-LDH-modified sphagnum moss cellulose gel (MgAl/LDH@SMCG) was recently studied for its ability to remove Cr(VI) [251]. Cr(VI) was removed by a combination of methods, including surface complexation, hydrogen bonding, ion exchange, and electrostatic interaction [251]. The FTIR study indicates the attachment of Cr(VI) species to the surface. After Cr(VI) adsorption, the appearance of supplementary peaks at 891 and 779 cm^{-1} confirms the Cr═O stretching vibration and the Cr—O bond stretching, signifying that Cr is binding. The alteration in the O—H and C—O peaks signifies that Cr(VI) is exchanging ligands and hydrogen bonds with hydroxyl and carboxyl groups on the composite [251]. XPS analyses reveal a redox process in which the composite surface partially reduces Cr(VI) to Cr(III). Surface complexation (Cr(III) interacts with oxygenated functional groups and modifications in functional groups suggest the likelihood of direct involvement in adsorption and reduction mechanisms [251]. The MgAl/LDH@SMCG nanocomposite exhibited enhanced Cr removal efficiency, mainly driven by electrostatic interactions, chemical, and reduction processes. Adsorption demonstrated a significant reliance on pH, peaking at pH 6, when Cr(VI) was primarily present as favorably adsorbed anions ($HCrO_4^-$, $Cr_2O_7^{2-}$) [251]. The kinetic data adhered to a PSO model, with a saturation time of 60 min, thereby signifying chemisorption as the rate-limiting mechanism [251]. The intraparticle diffusion model indicated a tri-phasic process: Swift surface adsorption, progressive intraparticle diffusion, and the ultimate equilibrium phase (saturation). The Langmuir isotherm fitting indicated monolayer adsorption with a maximal sorption capacity of 62.66 mg g^{-1} at 30 °C [251]. The composite's porous structure, functional surface chemistry, and LDH loading significantly enhanced adsorption capacity, offering a feasible, environmentally conscious approach for Cr(VI) remediation [251].

The phosphate removal method employing the La/MgFe-LDH(LS)@WAs composite incorporates both physical and chemical interactions [252]. Phosphate adsorption transpires through a synergistic method encompassing chemical adsorption, specifically inner-sphere complexation via exchange of ligand, interaction between oppositely charged ions, hydrogen bonding, and van der Waals forces [252]. XPS research verifies the formation of La—O—P bonds, signifying chemical adsorption by inner-sphere complexation between La $(OH)_3$ and phosphate. A ligand exchange mechanism in which hydroxyl groups on La $(OH)_3$ are substituted by phosphate ions, resulting in the formation of stable complexes. Lignosulfonate (LS), comprising sulfonic acid, hydroxyl, and carboxyl groups, engages in hydrogen bonding with phosphate [252]. DFT simulations and interaction region indicator (IRI) analysis demonstrate that hydrogen from the hydroxyl group in LS makes hydrogen bonds with the deprotonated oxygen in phosphate [252]. These interactions facilitate secondary binding and stabilization of phosphate on the surface. The Zeta potential measurement indicated that for pH < 5.16, the adsorbent surface possesses a positive charge, facilitating the adsorption of negatively charged phosphate ions ($H_2PO_4^-$ and HPO_4^{2-}). Electrostatic interaction facilitates fast surface adhesion, particularly under acidic to neutral environments. Molecular Dynamics (MD) simulation demonstrates that LS molecules assimilate into the surface of LDHs, with sulfonic groups establishing robust electrostatic and hydrogen bond interaction [252]. RDF graphs exhibit significant peaks for atom pairs such as O—Fe, O—Mg, and O—H, thereby validating a consistent adsorption mechanism [252]. The optimal pH for phosphate adsorption was determined to be 4.0, resulting in a sorption capacity of 139.49 mg g^{-1}. Zeta potential analyses indicated the isoelectric point (pHpzc) of La/MgFe-LDH(LS)@Was to be 5.16. At a pH below 5.16, the surface possesses a positive charge, which amplifies electrostatic attraction to negatively charged phosphate species, primarily $H_2PO_4^-$ [252]. At pH levels exceeding 5.16, the presence of a negative surface charge and heightened competition from OH^- ions lead to a reduction in adsorption effectiveness. Adsorption diminished markedly at pH 10 (by approximately 64.7%), attributable to heightened repulsion and site competition from hydroxyl ions. Kinetic modelling validated pseudo-second-order kinetics (equilibrium time: 6 h), indicating chemisorption, but intraparticle diffusion studies uncovered a multi-stage mechanism [252]. The Langmuir model yielded the optimal fit, suggesting monolayer adsorption on uniform active sites. The theoretical adsorption capacity closely matched the observed measurement. In actual wastewater treatment (starting P = 2.71 mg/L), the material attained 46.86 mg P/g after 40 h of cyclic operation. The Langmuir isotherm fitting demonstrated monolayer adsorption, corroborated by thermodynamic parameters ($\Delta G^\circ < 0$, $\Delta H^\circ > 0$), affirming spontaneity and endothermicity [252]. The bio-based composite demonstrates exceptional efficacy in both actual wastewater and model solutions, providing a sustainable dual-purpose approach for water purification and agricultural phosphorus recovery via its slow-release fertilizer functionality [252].

Mg—Al LDH/cellulose (LDH@CB) nanocomposite beads were fabricated using an in-situ co-precipitation technique for the removal of amoxicillin. The removal of amoxicillin (AMX) was mostly due to electrostatic interactions between the negatively charged AMX molecules and the positively charged Mg—Al LDH particles included in cellulose beads [253]. At natural pH levels, AMX mostly occurs in an anionic state

due to the deprotonation of its carboxyl and phenolic hydroxyl groups. The LDH@CB adsorbent, distinguished by a net positive surface charge, efficiently attracted the anionic species [253]. Spectroscopic and surface analyses, encompassing FTIR, XPS, and zeta-potential measurements, validated that adsorption predominantly took place via the interaction between the carboxylate groups (–COO–) of AMX and the metal centers (Mg^{2+}/Al^{3+}) of the LDH, resulting in the establishment of O—C═O—M (Mg/Al) linkages [253]. The mechanism highlights the significance of surface charge, functional groups, and the organized porosity architecture of the nanocomposite beads in promoting effective AMX elimination from aqueous systems. The trials were performed under natural pH conditions. Amoxicillin (AMX) functions as a weak polyprotic acid characterized by three pKa values (2.67, 7.11, and 9.55), with its charge fluctuating according to pH levels. At neutral pH, AMX primarily resides in its anionic state. The LDH@CB nanocomposite has a positive charge at this pH (ζ potential: +25 mV), facilitating electrostatic interaction between AMX and the adsorbent. Adsorption kinetic tests were conducted for an adequate duration to achieve a plateau at each temperature [253]. The pseudo-second-order model exhibited a strong fit across the whole-time range to equilibrium, with R^2 exceeding 0.96, so validating the accurate representation of saturation behavior [253]. The intraparticle diffusion model results indicated multi-stage diffusion. Surface adsorption is succeeded by progressive pore diffusion. The R^2 value for the intraparticle model was lower (e.g., 0.8791 at 318 K), indicating that pore diffusion is present but not rate-limiting [253]. The Freundlich isotherm demonstrated the most accurate fit, indicating multilayer adsorption on heterogeneous surfaces [253]. The greatest adsorption capacity attained was 138.3 mg g^{-1} at 318 K, exceeding the majority of documented adsorbents. These findings establish LDH@CB as a potential material for the efficient removal of antibiotics in aquatic settings [253].

ZNF-HS@CMC employs a synergistic approach for the elimination of ciprofloxacin and tetracycline that includes electrostatic interaction, hydrogen bonding, surface complexation, and π-π stacking [254]. The interactions are enabled by the porous structure of the LDH, its extensive surface area, and the functionalized cellulose support, which together make ZNF-HS@CMC an efficient and recyclable adsorbent for antibiotics [254]. The adsorptive removal of tetracycline (TC) and ciprofloxacin (CIP) via ZNF-HS@CMC aerogels is contingent upon many synergistic interactions [254]. The ZnNiFe-layered double hydroxide (ZNF-HS) surface possesses a positive charge, facilitating robust electrostatic interaction with TC and CIP antibiotics, particularly at elevated pH levels [254]. Furthermore, surface complexation transpires via coordination between the metal ions (Zn^{2+}, Ni^{2+}, Fe^{3+}) of ZNF-HS and oxygen-containing functional groups, including –COOH, –OH, and ═O present in the antibiotics. Hydrogen bonding occurs among the groups of hydroxyl and amine of the antibiotics and the –OH and –COOH groups on ZNF-HS@CMC, hence augmenting the stability of the zeta potential of these compounds post-adsorption [254]. Furthermore, improved attachment is facilitated by π–π interactions between the aromatic rings of the medicines and those in the adsorbent [254]. Consequently, its distinctive hollow mesoporous architecture and many active sites within the composite enhance mass transfer, resulting in a significant improvement in total adsorption efficiency [254]. The pH of the environment markedly affected the removal efficacy of tetracycline TC and ciprofloxacin CIP. The evaluated pH range ranged from 2 to 10. Research on zeta potential demonstrated that the surface of ZNF-HS@CMC consistently displayed a positive charge over the full spectrum [254]. As pH increased, antibiotics converted into negatively charged forms, resulting in augmented electrostatic interaction between the antibiotics and the positively charged adsorbent. The greatest removal efficiencies are: at a pH of 10, the total concentration (TC) is 96.49%, and the chemical oxygen demand (COD) is 90.53%. A pH level of 10 was used for the remaining studies [254]. The adsorption process exhibited an initial rapid phase (0–100 min), a subsequent slower phase (100–400 min), and reached equilibrium at approximately 400 min, conforming to a pseudo-second-order model (R^2 = 0.995 for TC, 0.998 for CIP), signifying that chemisorption was the predominant mechanism. The Langmuir isotherm fitting validated monolayer adsorption, revealing maximal capacities of 642.77 mg g^{-1} for TC and 497.91 mg g^{-1} for CIP [254]. The removal method encompassed synergistic effects of surface complexation, π–π interactions, and electrostatic attraction. ZNF-HS@CMC has remarkable reusability and thermal endurance, making it a viable adsorbent for the treatment of antibiotic wastewater in practical applications [254].

Zubair et al. synthesized a B–CuFe–CNC biocomposite for the Eriochrome Black T (EBT) dye through the ultra-co-precipitation technique [255]. The removal of the anionic azo dye occurs via a multi-interaction mechanism and a physico-chemical adsorption process [255]. The B–CuFe–CNC surface acquires a positive charge at an acidic pH (<7.81), corresponding to its isoelectric point, as a result of protonated $–OH_2^+$ groups. This facilitates a robust electrostatic interaction with the negatively charged $–SO_3^-$ groups present on EBT molecules. Complexation mechanisms take place in both the outer and inner spheres [255]. The decrease in the intensity of the MMO (mixed metal oxide) peak (~590 cm^{-1}) in FTIR analysis indicates the direct involvement of metal centres. Shifts in the Cu 2p and Fe 2p peaks, confirmed by XPS analysis post-adsorption, indicate the involvement of metal sites in complexation. The functional groups of EBT interact with hydroxyl (–OH) and sulfonic acid ($–SO_3H$) groups present on both CNC and biochar through hydrogen bonding [255]. Post-adsorption, the $–SO_3H$ (~1230 cm^{-1}) and –OH peaks exhibit broadening and shifts in the FTIR spectra [255]. The porous two-dimensional rod-like structure, resulting from CNC integration, offers an extensive surface and numerous sites for external adsorption [255]. The mesoporous texture, characterized by an average pore size of 12.5–19.6 nm and an increased surface area of approximately 297 m^2 g^{-1}, is validated through SEM and BET analyses. The B–CuFe–CNC bio composite demonstrated significant EBT dye adsorption capabilities, reaching a maximal sorption capacity of 876.2 mg g^{-1} at 45 °C [255]. Optimal elimination was observed at pH 2.5, attributed to the strong electrostatic interaction between protonated surface groups and anionic dye species. Kinetic modelling demonstrated pseudo-second-order behaviour, with equilibrium attained within 30 to 45 min, suggesting chemisorption [255]. Isotherm analyses indicated multilayer and heterogeneous adsorption, optimally characterized by the Freundlich and Redlich–Peterson models [255]. The composite exhibits a high surface area, porous structure, and enriched functional groups, which enhance its adsorption capacity and recyclability, indicating significant potential for sustainable wastewater treatment [255].

The adsorption of ciprofloxacin onto CLZ-1 aerogel is mostly accomplished through surface complexation, which encompasses unsaturated metal bonding, π–π stacking, and electrostatic interaction [256]. The adsorption mechanisms work in conjunction with the porosity and surface area of the aerogel to produce a synergistic effect. Because of this strategy, the one-of-a-kind CLZ-1 materials are able to attain an excellent adsorption of 1397.5 mg g^{-1}, which makes them efficient and adaptable sorbents for the effective elimination of antibiotics in the process of water treatment [256]. Through the use of BET and pore distribution studies, the uptake of antibiotics is further validated. This research demonstrates multi-scale porous structures that are conducive to the quantitative and qualitative retention of large antibiotic molecules. Through a process known as advanced π–π stacking, the aromatic regions of ciprofloxacin participate in interactions with the imidazole components of ZIF-8 [256]. It is because of this that the antibiotic can adhere more easily to the surface of the aerogel. A reduction in C═C/C—C bonds is observed using X-ray photoelectron spectroscopy (XPS), which is followed by peak shifts (754 → 833 cm^{-1}) that are linked with the vibrational modes of imidazole rings. These peak shifts reinforce the π–π stacking hypothesis [256]. It is possible for the $–NH_2$ and –COOH groups of CIP to form bonds with the functional groups that are located on the surface of CLZ-1. These functional groups include carboxyl, hydroxyl, and imidazole structures. Based on the FTIR

data, there are shifts that show involvement. These shifts are caused by the weakening of the (–OH/NH) from 3497 cm^{-1} to 3450 cm^{-1}. This weakening suggests that these surfaces have a crucial role in the removal process, and it also confirms the presence of this particular type of hydrogen bonding [256]. Because of the favorable interactions with zwitterionic CIP species, the adsorption of ciprofloxacin by CLZ-1 was significantly dependent on the pH of the environment, with the highest effectiveness occurring at a pH of 6.0. Adsorption decreased below pH 2 as a result of ZIF-8 degradation, but electrostatic repulsion occurred at pH 8.66 as a result of both the adsorbent and CIP becoming negatively charged [256]. The isoelectric point (pHpzc) of CLZ-1 was 7.2, which had an effect on the behavior of surface charge across the pH range. The equilibrium period for the kinetic study of ciprofloxacin (CIP) adsorption by CLZ-1 (CMC/CoNiFe-LDH/ZIF-8 composite) was around 300 min, which is equivalent to 5 h [256]. Because of its huge surface area (388.51 m^2g^{-1}), hierarchical porous structure, and numerous functional groups, the CLZ-1 composite was able to reach a remarkable sorption capacity of 1397.5 mg g^{-1} for CIP Multiple processes, such as hydrogen bonding, π–π stacking, electrostatic interactions, and metal–ligand complexation, were responsible for driving the adsorption process [256].

The chemical breakdown of diquat herbicide by Al—Cu-LDH/CMC-Alg hydrogel beads involves electrostatic interaction, bonding by hydrogen, integration with metal ions (Al^{3+} and Cu^{2+}), and pore-filling processes [257]. The interaction between diquat molecules and the negatively charged adsorbent surface occurs as a result of the positive charge of diquat. Hydrogen bonding arises from molecular bonds between –OH and –COOH groups [257]. The coordination of diquat's electron-rich sites by metal ions within the layered double hydroxide structure significantly enhances adsorption [257]. BET analysis indicated substantial pore occupancy by diquat, implying physical entrapment. Intraparticle diffusion investigations revealed that adsorption occurred through rapid surface adsorption, intraparticle diffusion, and a subsequent equilibrium adsorption phase [257]. The adsorption mechanism demonstrates that Al—Cu-LDH/CMC-Alg hydrogel beads are highly effective for the environmentally friendly, specific, and reusable extraction of diquat herbicide from water sources. The pHpzc for the adsorbent was found to be 6.79. When the pH exceeds 6.79, the adsorbent surface acquires a negative charge, enhancing electrostatic interaction with the positively charged DQ herbicide. Below the pHpzc, the surface exhibits a positive charge, resulting in repulsion with DQ. The adsorption efficiency exhibited a consistent increase from pH 2 to 8, achieving optimal performance at pH 8 [257]. The sorption process adhered to PSO kinetics, suggesting chemisorption, with equilibrium reached in 100 min. Isotherm analysis indicated that the Langmuir model most accurately represented the monolayer adsorption behavior, demonstrating a maximal sorption of 303.2 mg g^{-1} at pH 8.0 [257]. This finding is further corroborated by favorable thermodynamic parameters that confirm the endothermic and spontaneous characteristics of the process [257]. The composite is positioned as a promising, regenerable adsorbent for wastewater contaminated by herbicides because of its mesoporous structure and functional groups, which allow for effective electrostatic coupling, hydrogen bonding, and pore filling [257].

The TPA/CuCr-LDH@BC nanocomposite, formed by integrating terephthalic acid-loaded CuCr-layered double hydroxides with bacterial cellulose, exhibits a flexible adsorption approach for the removal of mixed pesticide residues [258]. A highly porous crystalline material exhibiting increased interlayer spacing and a high density of functional groups was verified through imaging microscopy, transmission electron microscopy, X-ray diffraction (XRD), Fourier-transform infrared spectroscopy (FTIR), scanning electron microscopy (SEM), Brunauer-Emmett-Teller (BET) analysis, and energy-dispersive X-ray spectroscopy (EDX). Multiple pathways contribute to the efficiency of adsorption [258]. The interactions include (i) electrostatic interaction between negatively charged pesticide groups and positively charged LDH sheets; (ii) hydrogen bonds linking hydroxyl and carboxyl sites of BC and TPA to the polar regions of the pesticide; (iii) pi-pi stacking between the aromatic rings of TPA and the pesticide; (iv) van der Waals attractions facilitated by a rough and varied surface; and (v) physical filling of mesopores, supported by a surface area of 238.3 m^2 g^{-1} and an average pore size of 13.5 nm [258]. The downward shift of the (003) peak during adsorption indicates that the LDH layers expand, facilitating the passage of pesticide molecules between them. The apparent eco-friendliness of the composite and its effective broad-spectrum pesticide capture results [258].

The binding of phenol onto a Zn/Al LDH (Zn/Al-cellulose) composite primarily occurs through surface-mediated mechanisms, including electrostatic interaction, hydrogen bonding, and physical adsorption [259]. Characterizations obtained from structural and spectroscopic analyses provide substantial support for this assertion. The XRD patterns validate the occurrence of the layered-double-hydroxide phase, as evidenced by peaks at 10.3°, 20.3°, 34.8°, and 60.4° [259]. In contrast, peaks at 15.5°, 22.4°, and 34.5° signify the existence of the unmodified cellulose phase, collectively illustrating the coexistence of both components within the material. The significant bands at 3442 cm^{-1} and 1642 cm^{-1} suggest the existence of OH groups and interlayer water. The features observed between 1440 and 1620 cm^{-1} correspond to carboxylate vibrations, which are capable of forming hydrogen bonds with phenol [259]. The FTIR spectrum indicates that the adsorption pathway is preserved. Additional bands around 400–800 cm^{-1} confirm the presence of Zn—O and Al—O connections within the LDH layers. The BET analysis shows that the specific surface area of the composite material rises from 1.968 m^2 g^{-1} for the bare Zn/Al LDH to 13.615 m^2 g^{-1} for the composite material [259]. The composite material demonstrates increased pore volume and reduced pore size, underscoring its enhanced textural properties that improve contaminant retention [259]. Kinetic studies indicated that phenol adsorption adhered to the PSO model, suggesting that chemisorption was the primary rate-limiting factor. The Langmuir indicated that the Zn/Al-cellulose composite had a sorption capacity of 35.34 mg g^{-1} [259]. This indicates that it adsorbs onto a smooth surface in a monolayer arrangement. Thermodynamic data validated the spontaneity and endothermic characteristics of the process, as evidenced by positive ΔH values and negative ΔG values at elevated temperatures [259]. The composite's extensive surface area, presence of functional groups, and mesoporous architecture enhance adsorption efficiency [259]. This facilitates the diffusion and interaction of phenol molecules with active sites. The structural and mechanistic data indicate that Zn/Al-cellulose composites efficiently remediate phenol from water and exhibit reusability [259].

Because of a combination of ion exchange processes, π–π stacking, and electrostatic interaction, the Co–Fe LDH/cellulose nanocomposite is capable of retaining antibiotics [100]. The Co—Fe LDH is characterized by a layered structure that includes positively charged brucite-like layers. This structure facilitates the adhesion of negatively charged antibiotic species, particularly when the pH is optimal [100]. Electrostatic interactions are crucial, particularly at specific pH levels when the surface of Co—Fe LDH/cellulose acquires a positive charge (as indicated by zeta potential), whereas SMX and CFX molecules deprotonate and attain a negative charge. The disparity in charge results in optimal SMX adsorption at pH 5 and superior CFX removal at pH 9 [100]. FTIR spectroscopy verifies the involvement of –OH, NO_3^-, and metal–oxygen functional groups in the adsorption mechanism. Upon adsorption, notable alterations in the –OH stretching (from 3431 to 3450 cm^{-1}) and NO_3^- vibration bands (from 1383 to 1401 cm^{-1}) indicate the establishment of hydrogen bonds and electrostatic interactions between the pharmaceuticals and the functional groups on the composite. The alignment of the aromatic rings of SMX and CFX with surface locations on the LDH/cellulose framework facilitates π–π stacking interactions [100]. Additionally, ion exchange mechanisms are engaged, particularly at reduced pH levels, when SMX anions substitute interlayer nitrate ions inside the LDH structure. The BET surface area and BJH pore size distribution study indicate that the structure is mesoporous, exhibiting a

surface area of 15.46 $m^2\ g^{-1}$ and an approximate pore width of 15 nm, facilitating the diffusion and entrapment of antibiotic molecules inside the adsorbent matrix [100]. This multipronged adsorption mechanism, comprising electrostatic interaction, hydrogen bonding, π–π stacking, and ion exchange, ensures high efficiency, reusability, and green compatibility of the Co—Fe LDH/cellulose nanocomposite for antibiotic removal from contaminated water systems [100]. Table 9 shows a comparison of different LDH–cellulose adsorbents for the removal of pollutants.

Table 9
A comparison of different LDH–cellulose adsorbents for the removal of pollutants.

Pollutant	Adsorbent	Adsorption parameters	Adsorption capacity (mg g^{-1})	Ref.
Cr (VI)	MgAl/LDH@SMCG	pH:6 Equilibrium time:60 min	62.66	[251]
As (V)	FAH-rGO/CE	pH:7 Equilibrium time: 360 min	258.39	[157]
Cd^{2+}, Pb^{2+}, Cu^{2+}	MgAl-LDO	pH: 6.5 for Cd^{2+}, Pb^{2+} pH: 5 for Cu^{2+} Equilibrium time: 600 min	1422.3 (Cd^{2+}) 1336.8 (Pb^{2+}) 1135.4 (Cu^{2+})	[248]
PO_4^{2-}	CuAl-LDH/CCF composite	pH:8 Equilibrium time:60 min	105.26	[250]
PO_4^{2-}	La/MgFe-LDH(LS) @WAs composite	pH:4 Equilibrium time: 360 min	139.49	[252]
Amoxicillin	Mg-Al LDH/ cellulose nanocomposite beads	pH: 7 Equilibrium time: 1440 min	138.30	[116]
Ciprofloxacin tetracycline	ZNF-HS@CMC	pH: 10 Equilibrium time: ~400 min	642.77 (TC) 497.91 (CIP)	[254]
Methylene blue	$MnFe_2O_4$@ZnAl AlLDHs@Cel@AGB	pH:6 Equilibrium time:25 min	19.28	[249]
Hg (II)	$MnFe_2O_4$@Zn-Al LDHs@Cel@AGB	pH:2 Equilibrium time:25 min	128	[249]
Eriochrome black T	B–CuFe–CNC biocomposite	pH:2.5 Equilibrium time:30-45 min	876.2	[255]
Ciprofloxacin	CMC/CoNiFe-LDH/ ZIF-8 composite	pH 6.0 Equilibrium time:300 min	1397.5	[256]
Diquat	Al-Cu-LDH/CMC-Alg hydrogel beads	pH 8.0 Equilibrium time: 100 min	303.2	[257]
Ethyl paraben	CNC/LDH	pH 8-10 Equilibrium time: 240 min	15.57	[253]
Phenol	Zn/Al-LDH@Cellulose composite	pH:2 Equilibrium time: 120-150 min	35.33	[259]
Malachite green	**Ni/Al–cellulose composite**	pH: 7 Equilibrium time: 150 min	**107.527**	[260]
Sulfamethoxazole Cefixime	Co-Fe LDH/ cellulose composite	pH: 5 Equilibrium time: 50 min	**272.13 (SMX) 208.00 (SFX)**	[100]

Surface adsorption serves as a flexible and effective approach for eliminating various contaminants from water sources. LDHs possess unique structural properties, a high surface area, tunable chemical composition, and ion exchange capability, making them highly effective adsorbents. The various mechanisms that regulate adsorption, such as electrostatic interaction, π–π stacking, ion exchange, and surface complexation, enable LDH-based materials to effectively target both inorganic and organic pollutants with remarkable specificity and capacity. A multitude of studies have confirmed the enhanced performance of LDH composites when they are functionalized with materials like cellulose. The composites demonstrate increased porosity, availability of functional groups, and mechanical stability, which further enhance adsorption kinetics and capacities. The prevalence of pseudo-second-order kinetics and Langmuir isotherm models in various studies suggests a clear indication of chemisorption and monolayer adsorption behavior. Additionally, elements such as pH, surface charge, and composite morphology play a significant role in finding the adsorption pathways and efficiencies. In summary, LDH-based materials present a sustainable and effective method for water purification, adept at tackling both heavy metal and organic pollutant contamination. The ongoing refinement of their physicochemical properties, along with the incorporation of biodegradable and economically viable materials, will significantly improve their usability in practical water treatment applications.

Testing of LDH–cellulose composites in real or spiked natural water matrices reports mixed but promising performance, with both potential and challenges being indicated. In one study, cellulose-supported CoFe-LDH composite was tested on three real water bodies (tap water, river Nile water, and groundwater) [100], each spiked with 5 ppm of the antibiotic sulfamethoxazole (SMX) [100]. Under optimal conditions, removal efficiencies of ~50–60% were realized throughout the natural waters, somewhat less in the ideal laboratory solutions, implying matrix effects (ions, organics, or pH buffering) dampen adsorption in actual waters. In the same research, removal of a second antibiotic (cefixime) under identical real-water conditions realized ~73.6% at pH 9 with a lower adsorbent dose [100]. These findings suggest that while LDH–cellulose or LDH-carbon-cellulose composites can be extremely effective under more practical conditions, their efficacy is dependent to a large extent on conditions like pH, competing ions, pollutant concentration, and adsorbent dose. Additionally, reusability experiments in some of these reports demonstrate good regeneration, albeit with decreased efficiency upon several cycles. Such results only serve to underscore the disparity between laboratory-scale high-value adsorption capacities and actual treatment efficiency in the field, and one is left to appreciate that optimization versus wastewater matrices is the crux of successful translation of LDH–cellulose hybrids into viable water treatment technologies.

4.2. *Adsorption mechanisms*

Adsorption is a highly important process in environmental systems, particularly in the treatment of effluents containing heavy metals, dyes, and persistent organic compounds. The efficiency of this process depends not only on the nature of the adsorbent but also on the intermolecular and interionic mechanisms involved. The main mechanisms include ion exchange, electrostatic interaction, and hydrogen bonding, which act independently or synergistically depending on the type of pollutant and the environmental conditions (pH, ionic strength, polarity). Ion exchange occurs when ions present on the adsorbent surface are replaced by pollutant ions in solution [261]. This mechanism is particularly relevant in materials with ionizable functional groups (e.g., carboxylic groups, sulfonates, protonated amines) or in porous matrices

capable of cation or anion exchange, such as clays, zeolites, and modified biopolymers. Metal ions such as Pb^{2+}, Cd^{2+}, or Cu^{2+} can replace protons (H^+) or other weak cations adsorbed on the material's surface. pH is crucial, as it influences the degree of ionization of the functional groups and the ionic speciation of the pollutant. This is a selective and reversible mechanism, allowing partial regeneration of the adsorbent. Electrostatic interaction results from the interaction between opposite charges of the adsorbent and the pollutant. Unlike ion exchange, which involves substitution, here stabilization occurs primarily through Coulomb forces. For example, in cationic dyes (such as methylene blue), the negatively charged surface of materials rich in deprotonated $–COO^-$ or –OH groups can attract the dyes, favoring removal. In anionic dyes (such as Congo red), protonated surfaces at acidic pH ($–NH_3^+$ or $–OH_2^+$ groups) promote adsorption. Chemical modifications that adjust the surface charge increase the selective affinity for different types of pollutants. The strength of this interaction depends strongly on the ionic strength of the solution; high salt concentrations can compete with electrostatic interactions, reducing efficiency. Finally, hydrogen bonds constitute intermolecular interactions of a physicochemical nature, occurring when there are hydrogen donors (–OH, –NH) and acceptors (–C═O, –O–, –N–) in both the adsorbent and the pollutant. Phenols, pesticides, or pharmaceuticals can establish hydrogen bonds with hydroxyl and carbonyl groups present in biopolymers such as cellulose, chitosan, or agar derivatives. In many systems, hydrogen bonds act as a secondary mechanism, strengthening retention after the initial interaction via electrostatics or ion exchange. Hydrogen bonds influence the availability of lone electron pairs and the protonation state of functional groups, modifying the ability to form hydrogen bonds.

The adsorption processes of pollutants on LDH–cellulose adsorbents are governed through a synergistic effect of physicochemical interactions between both components [28]. LDHs, featuring exchangeable interlayer anions and positively charged brucite-like layers, possess high anion-exchange capacity and tunable surface chemistry [262]. At the same time, cellulose provides a web of excess hydroxyl and carboxyl functional groups, which render the material very hydrophilic and enable hydrogen bonding, electrostatic interaction, and surface complexation [263]. For anionic pollutants such as phosphate, chromate, or dyes, intercalation into the LDH interlayer via ion exchange is a dominant mode in which the pollutant substitutes interlayer anions such as NO_3^- or CO_3^{2-} [263]. On the other hand, for positively charged species like heavy metal ions (e.g., Pb^{2+}, Cu^{2+}), adsorption is mainly on the cellulose matrix by chelation with the hydroxyl and carboxyl groups or surface complexation at defect sites [39]. LDHs are also useful for the precipitation of metal hydroxides in the case of high pH as a second cation removal aid. Hydrogen bonding and van der Waals interactions are also responsible, especially for the adsorption of organic pollutants such as dyes or phenols [66]. Dispersion of LDH particles and inhibition of aggregation are encouraged by cellulose hybridization with LDH, increasing surface area and available active sites [37]. Porosity and flexibility of the cellulose backbone also increase the rate of mass transfer of the pollutants, improving the kinetics. Electrostatic interactions between the composite surface and impurity, controlled by pH and ionic strength, play a key role in controlling adsorption efficiency [264]. In some hybrid composites, capacity and selectivity are also enhanced by functionalities added through chemical modification (e.g., amidation, thiolation, or carboxymethylation) through the creation of new binding sites [265].

About the composite's interactions with the dye, Fig. 6 summarizes the adsorption pathways of Eriochrome Black T by the CuFe-B-cellulose nanocrystals biocomposite. The strong adsorption of Eriochrome Black T on CuFe-B-cellulose nanocrystals occurs via a multi-mechanism process, including surface adsorption, hydrogen bonding, electrostatic attraction, metal complexation, and anion exchange. Negatively charged sulfonate groups interact electrostatically with positively charged hydroxyl groups, while OH^- anions are exchanged with anionic dye species, forming robust interfaces with Fe—O and Cu—O. Cellulose nanocrystals enhance surface porosity and hydrophilicity, facilitating efficient dye capture [154].

Generally, the adsorption mechanism in LDH–cellulose composites is multi-mechanism, including ion exchange, surface complexation, hydrogen bonding, electrostatic interaction, and at times co-precipitation, depending on the circumstances and nature of the

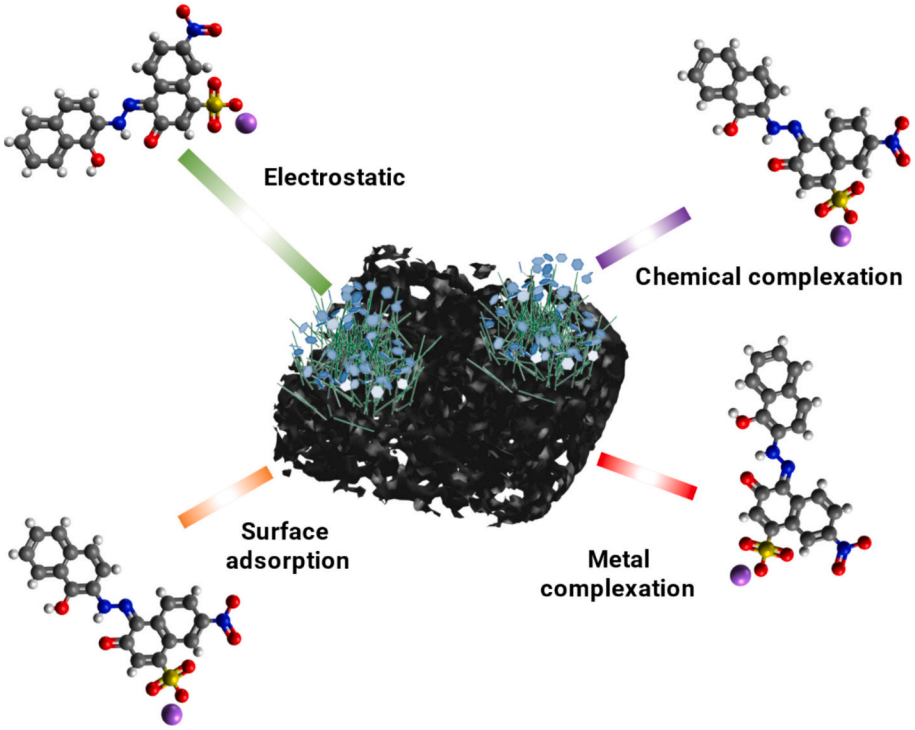

Fig. 6. Eriochrome Black T's adsorption mechanism on the CuFe-B-cellulose nanocrystal biocomposite.

contaminant. Multiplicity of function thus makes LDH–cellulose composites very efficient and versatile in the removal of inorganic and organic pollutants from wastewater and thus potential rivals for sustainable water purification technologies.

4.3. Regeneration and recyclability of adsorbents

LDH–cellulose adsorbents' efficiency of adsorption is a controlling factor in their long-term use for wastewater treatment because it directly influences recyclability, cost-sustainability, and sustainability [266]. Recyclability refers to hybrid adsorbents' capability to be cycled via repeated adsorption-desorption cycles without encountering unacceptable pollutant removal efficiency loss [267]. Theoretically, LDH–cellulose composites would show high recyclability in multi-cycle adsorption due to the abundance of anion-exchange sites from the layer-structure of LDH and mechanical stability and regenerable substrate of cellulose. In practice, recyclability of LDH–cellulose adsorbents are usually limited by site loss on regeneration, structural instability under harsh regeneration conditions, and incomplete release of pollutants. The degree of loss of capacity per cycle largely depends on both the nature of the pollutant and regeneration agent used. For example, strong acids or bases are able to desorb dyes or heavy metals very fast but simultaneously destroy the LDH layers or hydrolyze the cellulose backbone and lead to permanent damage and low efficiency in subsequent cycles. On the other hand, less violent agents such as weaker concentrations of saline (such as NaCl in regenerating ion-exchange) will fail to wash away the strongly bound impurities from the adsorbent, and thus there is congestion buildup and progressive loss in adsorbing capacity. Reduction in adsorbing capacity is an important parameter utilized to calculate efficiency of regeneration, and research tends to report a reduction in capacity by 10–30% after five to ten cycles depending on the pollutant matrix.

This loss is attributed to several factors: blockage of pores by residual impurities, partial degradation or delamination of LDH layers, oxidation or degradation of functional groups of cellulose, and chemisorption of pollutants on surface sites irreversibly [268]. Interestingly, the presence of a concentration of competing ions or complex organic compounds in actual wastewater may result in capacity loss more rapidly than laboratory-controlled trials. In trying to control this issue, researchers have explored surface modification of LDH–cellulose adsorbents such as grafting with functional groups (–COOH, –SH, or $–NH_2$) or protective biopolymer coating, which would enhance chemical stability and enable easier desorption [269]. Besides, mild regeneration methods such as electrochemical desorption, low-temperature thermal processing, or using green solvents (e.g., biodegradable chelating agents) are being proposed instead of harsh extreme chemical washing processes. The ecological impact of regeneration methods has to be taken into account with utmost care because the entire idea of LDH–cellulose adsorbents is to provide a green and sustainable wastewater treatment process.

Traditional regeneration methods using harsh acids, bases, or organic solvents not only inactivate the adsorbent but also create secondary wastes that need further treatment, essentially undoing the environmental benefit of adsorption [267]. On the other hand, environmentally friendly methods such as saline washing, mild pH adjustment, or natural chelator usage, i.e., citric acid, are suitable in the case of low secondary pollution and circular economy applicability but with the trade-off of sacrificing overall desorption efficiency, i.e., adsorbent-efficiency vs. environmental-friendliness trade-off. The test will ultimately be to design regeneration protocols that maximize recyclability, minimum capacity loss, and low environmental footprint so that LDH–cellulose composites are ready to transition from laboratory-scale demonstration to industrial-scale implementation. Optimization of these variables will make the LDH–cellulose adsorbents more economically viable and further enhance their status as next-generation green materials for contaminant removal in wastewater treatment processes.

5. Applications and environmental impact

5.1. Real-world water treatment

5.1.1. Performance in complex matrices

The LDH–cellulose composite is a promising adsorbent attributable to its exceptional characteristics, including structural flexibility, biocompatibility, chemical stability, reusability, simple synthesis, non-toxicity, cost-effectiveness, and high adsorption efficiency [92] (Fig. 7). The dual functionality arises from the high surface area and ion-exchange capacity of LDHs, along with the mechanical stability, porosity, and biodegradability of cellulose (Fig. 7a). These composite adsorption properties are enhanced through metal binding intercalation, surface modification, and hybridization with other substances [270]. Studies report that the functional groups present on the cellulose backbone (such as –OH, –COOH) enhance pollutant interaction and help maintain composite integrity in harsh environments [271] (Fig. 7b).

Ren et al. (2025) designed a modified composite by sphagnum cellulose gel (SMCG) with MgAl-LDH for the removal of Cr(VI). Experimental trials conducted in batch mode achieved up to 97.08% removal of Cr(VI) under optimized parameters (pH 6, 60 min) [251]. Peng et al. developed a carbon-based cellulose fiber composite integrated CuAl-LDH for phosphorus adsorption, achieving a high maximum capacity of 105.26 mg g^{-1}, which is higher than that of pure LDH and CuAl-LDH adsorption [250]. Abduarahman et al. investigated the use of a cellulose fiber-modified MnFe-LDH membrane to investigate the adsorption of arsenic, phosphate (P), and textile dye Acid Green 25 (AG25). The composites exhibited varying adsorption capacities of 82.71 mg g^{-1} for arsenic (V), 106.9 mg g^{-1} for phosphate, and 130.3 mg g^{-1} for AG25 [272]. Priya et al. synthesized carboxymethyl cellulose (CE) with FeAl-LDH and reduced graphene oxide to formulate a very efficient nanocomposite for the adsorption of arsenate (As(V)) ions from wastewater [157]. The incorporation of CE significantly improved the As(V) removal efficiency to 98% and raised the composite's surface area to 156.24 m^2 g^{-1} by an increase in the number of active sites throughout the border layer [157].

Oily wastewater is a serious and troubling issue in wastewater management because of its potential to cause environmental and health hazards. Ning et al. showed that a 3D flower-like LDH-modified bilayered cellulose acetate membrane, featuring high superhydrophilicity and underwater superoleophobicity, achieved an impressive separation flux of 27,346 L m^{-2} h^{-1} bar^{-1} and an efficiency of 98.93%. The excellent anti-fouling performance and cycling stability of these nanofiber membranes indicated a wide range of potential applications in the excellent purification of oily wastewater [273]. Furthermore, pharmaceutical residues are also discovered pollutants in domestic and hospital wastewater, posing significant environmental hazards due to their low concentration presence and tendency to bioaccumulate [274]. Kotp et al. studied a cellulose-based LDH that functions as an efficient adsorbent and nanocarrier for the effective removal of both sulfamethoxazole (SMX) and cefixime (CFX) residues, showing maximum adsorption capacities of 272.13 mg g^{-1} for SMX and 208.00 mg g^{-1} for CFX [100]. Beyki et al. developed the CaAl-LDH–cellulose ionomer for the adsorption of pharmaceutical pollutants, diclofenac sodium [275]. The magnetite ionomer had a fast (2 min) equilibrium period and a maximum absorption of 268 mg g^{-1} [275]. Raicopol et al. developed cellulose acetate–MgAl-LDH nanocomposite membranes for the removal of pharmaceutical contaminants, specifically diclofenac sodium (DS) and tetracycline (TC), from wastewater [276]. The 10% of adsorption capacity for DS was increased compared to neat cellulose acetate, attributed to strong electrostatic interactions between MgAl-LDH layers [276]. Due to hydrogen bonding interactions between the drug molecules and the LDH nanofiller, the adsorption capacity for TC experienced a lesser increase [276].

Synthetic dyes are a major contamination in textile wastewater because of their high color intensity, chemical stability, and resistance to

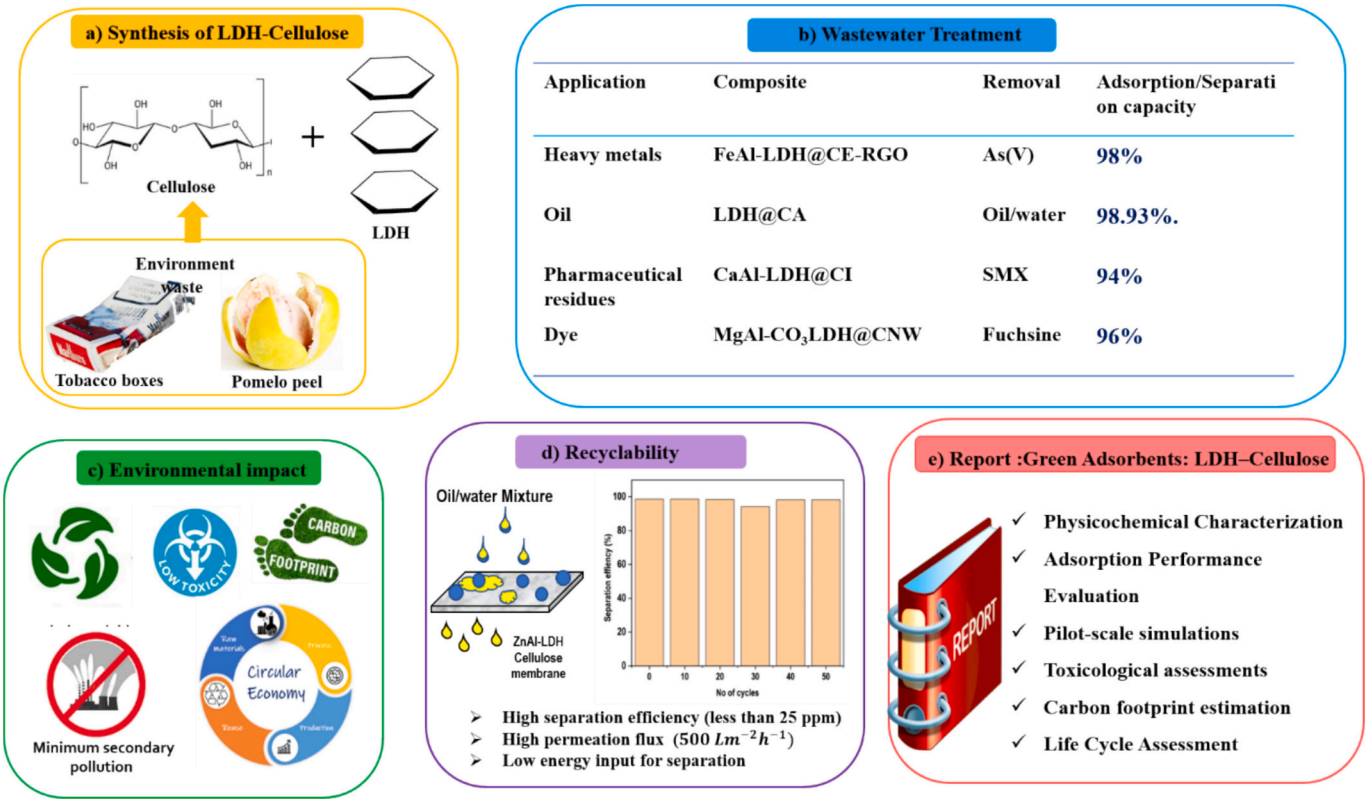

Fig. 7. Applications and environmental impact of LDH–cellulose composite: a) synthesis from environmental cellulose waste and LDH, b) efficient removal of pollutants in wastewater, c) biodegradable with minimal environmental impact, d) high recyclability and low energy use, and e) reporting on green adsorbent evaluation with life cycle assessment

natural degradation processes. LDH–cellulose-based composites have shown impressive results in removing various dyes. Sobhana et al. synthesized ZnAl-CO_3 LDHs using microcrystalline cellulose (MCC) as a soft template [277], achieving enhanced Orange II dye adsorption, the highest capacity (3.4 mmol g^{-1}) due to the large surface area (152 m^2 g^{-1}) of the composite (synthesized using 1.5 wt% MCC) with more active sites [277]. Razani et al. constructed new organic-inorganic hybrid nanomaterials using cellulose nanowhiskers (CNW) and MgAl-CO_3 LDH to remove organic cationic and anionic dyes like methylene blue (MB), malachite green (MG), crystal violet (CV), Fuchsine (Fuc), and Janus green (JG) from wastewater [278]. This nanocomposite hydrogel increased adsorption efficiency due to increased surface area and porosity, abundant negatively charged functional groups for electrostatic interaction, well-dispersed LDH layers that prevent aggregation, and a stable hybrid network structure [278]. The incorporation of LDH into CNW-graft-PAA improved the Fuc removal efficiency from 33% to 96% [278]. Further, these groups are more ionized at high pH, enhancing electrostatic interaction toward cationic dye molecules. Conversely, at low pH, decreasing adsorption efficiency is due to competition between protons and dye cations for adsorption sites [278]. Manalu et al. developed NiCr-LDH/microcrystalline cellulose composites for the adsorption of malachite green dye from industrial wastewater [279]. The adsorption behavior was described by the Freundlich isotherm model, which has a maximum adsorption capacity of 129.870 mg g^{-1} [279]. Wijaya et al. synthesized the cellulose-supported NiAl-LDH composites for the adsorption of malachite green (MG) dye [260]. Compared with other adsorbents, this composite achieved the highest adsorption of 107.527 mg g^{-1} [260]. For the phosphate pollution, Castro et al. (2018) evaluated an MgAl-LDH–cellulose acetate composite for phosphate removal, finding a maximum adsorption capacity of 6.98 mg g^{-1} according to the Langmuir-Freundlich model [280].

However, most of the reviewed studies have been conducted with batch adsorption experiments under optimal lab conditions (e.g., pH 3–7, contact duration 30–90 min, adsorbent dose 0.1–0.5 g L^{-1}). However, these conditions are generally established for fundamental efficiency, but real-world wastewater is far more complex, often containing high ionic strength, organic matter, competing anions, and fluctuating pH [6]. Synthesizing modified LDH composites that are customizable for specific wastewater can greatly enhance adsorption efficiency for particular contaminants found in various wastewater streams.

5.1.2. *Selectivity and competitive adsorption*

In wastewater treatment applications, selectivity and competitive adsorption behavior of LDH are critical due to its direct influence on the efficiency, specificity, and overall effectiveness of contaminant removal processes [114,281]. LDHs-cellulose selectively adsorb specific contaminants, enabling efficient removal of harmful substances while minimizing uptake of benign or non-target species, improving treatment precision, and reducing resource waste. Among the present competing ions, LDH–cellulose can selectively adsorb toxic ions (e.g., heavy metals like Pb^{2+}, Cd^{2+}, Cr^{6+}) [281].Tailored LDHs through metal composition, layer charge density, and interlayer ions to suit diverse wastewater compositions, enhancing their versatility and broadening their practical application scope.

LDH–cellulose composites exhibit high selectivity for specific ions and organic pollutants because of the combined structural and chemical properties of LDHs and cellulose fibers. Iftekhar et al. studied Zn/Al LDH intercalated into cellulose nanocomposites for selective adsorption of rare earth elements, highlighting their ability to preferentially bind these metal ions from mixtures with maximum adsorption of 102.25 mg/g for Y^{3+}, 92.51 mg g^{-1} for La^{3+}, and 96.25 mg g^{-1} for Ce^{3+}, respectively [125]. LDH/cellulose composites show a great deal of promise in oil/water separation due to surface roughness and chemical functionality, making them different wetting behavior surfaces for the

selective separation of water and oil [282]. Abduarahman et al. highlighted that the wCell/Mn-Fe-LDH membrane achieves selective adsorption through two main mechanisms: surface complexation for oxyanions (arsenate and phosphate) and electrostatic interactions for organic dye anions such as AG-25 [272]. The CNW-graft-PAA/LDH nanocomposite hydrogel exhibits selective adsorption primarily toward cationic dyes such as MB, MG, CV, Fuc, and JG, with removal efficiencies reported as 94% for MB, 92% for MG, 90% for CV, 96% for Fuc, and 23% for JG due to ariseed from the presence of ionized carboxylic acid groups (–COO^-) and hydroxyl groups on the cellulose nanowhisker-graft-poly(acrylic acid) chains. In contrast, the nanocomposite shows poor adsorption for anionic dyes like CR, which are not absorbed effectively [278].

Competitive adsorption of LDH–cellulose is critical in wastewater treatment because real wastewater typically contains multiple pollutants simultaneously, and LDHs must selectively adsorb the target contaminants in the presence of competing species. The electrostatic interactions are the main mechanism of the dye adsorption, due to the charges present in the LDH network [283,284]. In mixed dye solutions, the retention performance for a specific dye is generally reduced compared to single-solute systems. Moreover, the extent of competition's impact on individual sorption quantities depends on two key factors: the individual characteristics of the dye itself and the composition of the aqueous solution it's dissolved in [284]. Few studies have focused on the competitive adsorption between LDH and cellulose, with most research concentrating on LDH-based composites [281]. Akanyeti et al. (2023) examined the competitive dye adsorption capabilities of CoAl-LDH concerning methyl orange (MO), Remazol brilliant blue R (RBBR), and Allura red (AR) under varying concentration levels. They found that the highest adsorption capacities were 2.267 mmol g^{-1} for MO, 0.258 mmol g^{-1} for RBBR, and 0.195 mmol g^{-1} for AR, respectively [285]. Normah et al. demonstrated the polyoxometalate (POM)-modified ZnAl-LDH for the competitive removal of heavy metal ions, and achieved maximum adsorption capacities of 92.95 mg g^{-1} for Fe(II) with compared to Cr(VI) 44.44 mg g^{-1} [286]. The absorbent selectivity of LDH–cellulose composites is strongly influenced by pH, ionic strength, and the presence of competing ions in the wastewater environment. H^+ ions can compete for active sites, affecting target anion adsorption and overall selectivity [272]. Functionalizing LDH with cellulose improves surface attributes such as porosity and active site exposure, resulting in higher selectivity [92]. Future study is needed to develop theoretical modeling and in situ characterization methodologies to better understand adsorption mechanisms and the selectivity and competitiveness of adsorption for large-scale wastewater treatment.

5.1.3. Comparative analysis of advanced adsorbent materials: cellulose–LDH composites, biochar, MOFs, and graphene derivatives for pollutant removal

In the field of environmental remediation, the development of efficient and sustainable adsorbent materials is crucial for the removal of heavy metals, dyes, pharmaceuticals, and other emerging pollutants. Traditional materials such as biochar, alongside advanced nanostructured systems like metal–organic frameworks (MOFs) and graphene derivatives, have been widely studied due to their distinct surface properties and adsorption mechanisms. More recently, cellulose–layered double hydroxide (LDH) composites have emerged as promising alternatives, combining the renewability and biocompatibility of cellulose with the ion-exchange capacity of LDHs. The following table provides a comparative overview of these four categories of adsorbents, highlighting their structural features, dominant adsorption mechanisms, main advantages, limitations, and representative applications (Table 10).

5.2. Environmental safety

5.2.1. Toxicological assessments of spent composites

When composites are used for water purification, residual chemicals, fibers, or nanoparticles may remain, posing potential toxicity risks upon release into the environment or through biological exposure. Toxicological assessments usually evaluate acute and chronic toxicity, genotoxicity, inflammatory or cytological changes, and potential bioaccumulation. The LDH–cellulose composites are regarded as environmentally safe materials because of their biocompatibility, biodegradability, and the use of cellulose as a sustainable, non-toxic substrate [92,277] (Fig. 7c). The composites are synthesized through eco-friendly, water-based methods that eliminate the use of toxic reagents, enhancing their sustainable appeal and commitment to a greener future [100]. Additionally, cellulose's biodegradability ensures that spent composites can degrade naturally, reducing long-term environmental burden. While LDH–cellulose composites show great efficiency in pollutant adsorption, their toxicity after being spent is critical for assessing environmental safety and feasibility for large-scale applications. The use of bio-based

Table 10
Comparative analysis of advanced adsorbent materials: cellulose-LDH composites, biochar, MOFs, and graphene derivatives for pollutant removal.

Adsorbent material	Main characteristics	Predominant adsorption mechanisms	Advantages	Limitations	Representative applications	Reference
Cellulose–LDH composites	Layered structures with metallic cations (Mg^{2+}, Al^{3+}, Zn^{2+}, etc.) intercalated into cellulose matrices; high density of hydroxyl groups.	Ion exchange, electrostatic interaction, hydrogen bonding.	Biodegradable, renewable, high ionic selectivity, synergy between organic (cellulose) and inorganic (LDH) phases.	Higher synthesis cost compared to pure cellulose, limited stability in strongly acidic media.	Removal of heavy metals (Pb^{2+}, Cr^{6+}), phosphates, anionic dyes.	[92,287,288]
Biochar	Carbonaceous material obtained by biomass pyrolysis; porous and functionalized surface.	Physical adsorption (π–π), hydrophobic interactions, electrostatic interaction (pH-dependent).	Low cost, abundant, produced from agricultural residues; high surface area.	Lower selectivity; properties vary with biomass type and pyrolysis conditions; limited regeneration.	Adsorption of metals, pesticides, antibiotics, and organic dyes.	[289–292]
MOFs	Highly porous crystalline structures formed by metallic ions coordinated to organic linkers.	Metal–ligand coordination, physical adsorption, electrostatic interactions.	Extremely high surface area (>1000 m^2/g), tunable structure and functionality.	High cost, low stability in aqueous and harsh environmental	Removal of gases (CO_2, SO_2), heavy metals, emerging pharmaceuticals.	[293,294]
Graphene and derivatives (GO, rGO)	Two-dimensional carbon network; graphene oxides contain functional groups (–OH, –COOH, –O–).	π–π interactions, electrostatic interaction, hydrogen bonding, surface complexation.	Very high surface area, strong interaction with aromatic molecules, high potential for chemical modification.	Complex synthesis, high cost, tendency to aggregate in solution.	Removal of aromatic dyes, antibiotics, heavy metals.	[295–297]

components like cellulose might reduce toxicity risks, but systematic toxicological assessments are essential to confirm safety.

Recently, a few studies have specifically addressed LDH–cellulose bio-nanocomposites' impacts on human health. Kotp et al. conducted the MTT assay to describe the cytotoxicity and side effects of cellulose-based CoFe-LDH composite. The treatment of Vero cells with CoFe-LDH/cellulose, CoFe-LDH/cellulose-SMX, and CoFe-LDH/cellulose-CFX at a concentration of 200 μg mL^{-1} for 24 h resulted in an increase in cell viability by 75%, 57.9%, and 56.2%, respectively. After 48 h at the same concentration, cell viability increased by 71%, 52.9%, and 50.2%, respectively. These results confirmed that after 24 and 48 h of exposure, LDH concentrations up to 200 μg mL^{-1} showed no significant impact on the viability of Vero cell lines and demonstrated as cytocompatible biomaterials for water purification applications [100]. Nia et al. conducted cytotoxicity experiments using free amoxicillin (AMX), carboxymethylcellulose-based CuAl-LDH beads, and a composite combined with AMX, utilizing the MTT assay against HUVEC cells [298]. After 24 h of incubation, no obvious cytotoxicity was observed for this composite, even at higher concentrations, and more than 70% of the cells survived after incubation with this carrier at concentrations ranging from 0 to 32 μg mL^{-1} [298]. However, both combined composites with AMX and pure AMX lead to higher cytotoxicity to HUVEC cells compared to the CuAl-LDH composite [298]. Another major toxicological issue such that absorbed contaminants (heavy metals and organic pollutants) leach back into the environment. Long-term leaching tests should be integrated into the evaluation framework for regulatory compliance and risk assessment [299]. Degradation of LDH–cellulose composites under different environmental conditions may lead to the release of metal ions or organic byproducts [300]. For safe large-scale implementation, future research and regulatory frameworks must incorporate thorough and standardized toxicological assessments, such as in vitro and in vivo studies, long-term leaching behavior, and ecotoxicity evaluations.

5.2.2. Biodegradability and recyclability of cellulose backbone

LDH–cellulose composites attracted significant attention for wastewater treatment due to their biodegradability and recyclability, which are critical features for efficient purification [251] (Fig. 7c and d). The specific enzymes of cellulose, called cellulases, produced by microorganisms, hydrolyze these β-1,4 linkages, breaking down cellulose into glucose monomers. The high concentration of hydroxyl groups in cellulose can enhance chemical adsorption by introducing appropriate chemical moieties. The crystallinity index and polymer chain length are key parameters that influence the degree and rate of biodegradation; higher crystallinity generally reduces enzymatic hydrolysis owing to the restricted accessibility of enzymes to tightly packed chains [301]. Chemically modified cellulose, such as cellulose acetate, limits biodegradability by hindering enzyme access; however, partial reversal or controlled modifications can preserve or tailor biodegradability [302]. Environmental factors such as temperature, pH, moisture content, and microbial activity are still crucial for cellulose biodegradation [303,304]. Cellulose not only improves physical properties but also introduces biodegradation pathways for otherwise inorganic materials, reducing long-term environmental burdens after application in wastewater treatment [305]. According to Pulyala et al., non-ionic and anionic polymers moderately adsorbed on wastewater-associated bacterial cells, improving degradation and enzyme activity [306]. Limited research is available on the studies of the biodegradation of LDH–cellulose composites in wastewater treatment. However, LDH–cellulose composites are capable of safe degradation under controlled composting or natural conditions, making them particularly suitable for short-term adsorption applications, such as emergency spill cleanups or decentralized water purification systems. The porous fibrous network of cellulose enhances the diffusion and stabilization of LDH layers, and the structure not only aids in adsorption but also accelerates biodegradation by providing microbial attachment sites. Further, the chemical modification of cellulose as an environmentally friendly composite with LDH is needed both to tune the biodegradability and increase adsorption efficiency [263].

The presence of cellulose in LDH composites positively influences their recyclability by enhancing structural stability, adsorption efficiency, and mechanical integrity across multiple reuse cycles in wastewater treatment. The ability to reuse LDH–cellulose composites directly impacts the economic viability and environmental sustainability as an adsorbent material because it lowers operational costs and waste production. Yue et al. (2018) showed that the oil separation efficiency of ZnAl-LDH/cellulose membranes was more than 94.0% after 50 cycles, indicating the stability of hydrophobicity and good recyclability [282]. Kotp et al. synthesised the CoFe-LDH/cellulose composite as an absorbent for both SMX and CFX residues due to their biodegradability and biocompatibility [100]. The composite analysis showed no detectable loss of removal efficiency over three consecutive cycles, indicating the favorable reusability of this adsorbent [100]. Tan et al. observed a high removal efficiency (96.2%) for Cr(VI) by carboxymethylcellulose (CMC)-LDH beads, and reuse studies showed that even after 10 reuse cycles, with removal efficiency remained at 89.6% [307]. Peng et al. found that during five adsorption-desorption recycling procedures, the CuAl-LDH/CCF retained more than 85% of phosphorus [250]. The recyclability of the CNW-graft-PAA/LDH nanocomposite hydrogel was evaluated through repeating the adsorption–desorption process three times using MB dye. The removal efficiency showed only a slight decrease from 100% to 95%, indicating that the nanocomposite hydrogel maintains stable and reusable adsorption performance over multiple uses [278]. The CaAl-LDH–magnetite cellulose ionomer adsorbent showed the removal efficiencies of 99%, 95%, and 88% after three consecutive adsorption–desorption cycles, respectively. The regeneration was achieved by elution with a NaOH-methanol solution (2.0 mol L^{-1}), which enabled 98% regeneration efficiency by replacing adsorbed diclofenac with OH^- ions and desorbing diclofenac through hydrophobic interaction with methanol [275]. The FAH-rGO/CE-As(V) could be rapidly separated using a strong magnet due to their magnetic nature. After drying, these composite materials retained over 88% removal efficiency even after five consecutive adsorption–desorption cycles, indicating excellent regeneration capacity and strong stability of the synthesized adsorbents [157].

The synergistic coupling of cellulose's mechanical reinforcement and porous, hydrophilic character with LDH's adsorption capabilities ensures structural durability, maintains active sites, ensures ease of regeneration, and utilizes multiple cycles of efficient pollutant removal. And also, it effectively decreases the need for fresh raw materials and energy consumption in wastewater treatment, contributing to greener operational frameworks. This enables the design of "smart" LDH–cellulose composites with tailored degradation timelines depending on the environmental and operational requirements. Establishing a strong regeneration mechanism is crucial to preserving important cellulose-based material resources. More research aimed at improving regeneration methods will be necessary to fully realize the potential of these materials [263].

5.3. Sustainability and economics

5.3.1. Low-cost synthesis, use of agricultural or industrial cellulose waste

The co-precipitation process is a widely used method for synthesizing LDH–cellulose composite due to its simple, inexpensive, and environmentally friendly methods, and can produce high-quality materials. During this process, cellulose is combined with metal salts (like magnesium nitrate, zinc nitrate, or aluminum chloride), a precipitating agent (typically sodium hydroxide or ammonium hydroxide), and an aqueous medium. In this process, required minimum equipment, low energy input, minimal material degradation, and usual operation at low to moderate temperatures (~25–80 °C) and atmospheric pressure make it easy to scale up for application in industrial settings [92]. In contrast

to urea hydrolysis or hydrothermal methods, LDHs can form in a few hours to a few minutes. The cellulose's –OH groups help to anchor the growing LDH particles, fostering good dispersion and interfacial compatibility. Sobhanadhas et al. successfully fabricated a NiFe-LDH hybrid photocatalyst by tailoring it in situ onto anionic cellulose beads for the first time, creating a support for customized waterproof or oil absorption applications [308]. Further, *in situ* co-precipitation offers superior integration and functional performance compared to conventional co-precipitation, making it ideal for the production of advanced LDH-based hybrid materials. This method further requires a lower overall energy input, as it combines synthesis and immobilization in a single step under mild conditions, for example, LDH nucleates directly on the support, ensuring strong interfacial bonding and uniform distribution. Yang et al. synthesized MgAl-LDH/cellulose nanocomposite beads with a large specific surface area (76.46 m^2 g^{-1}), high water content (92.05%), and high porosity (94.75%) by an in situ co-precipitation process to remove amoxicillin in the aqueous phase [116].

Furthermore, reducing synthesis costs is achieved by lowering raw material expenses and minimizing environmental impact through the valorization of agricultural or industrial cellulose waste. Agricultural waste such as sunflower stem pith, sugar beet chips, and other biomass residues provides abundant cellulose sources for synthesizing LDH–cellulose composites [309] (Fig. 7a). Industrial cellulose wastes, such as microcrystalline cellulose (MCC) derived from pulping processes, also serve as sustainable feedstocks for these composites [310,311]. Alkali delignification and peroxide bleaching are common chemical processes used in cellulose extraction that efficiently eliminate non-cellulosic substances, including lignin and hemicellulose, increasing the yield and purity of cellulose. Further characterization with techniques such as X-ray diffraction, FTIR, and SEM confirms cellulose removal and structure, indicating the suitability of isolated cellulose for applications [312]. However, there is a lack of research available on the use of cellulose waste in LDH composites for wastewater treatment. The majority of current research emphasizes agricultural uses, particularly in areas like soil improvement and the development of slow-release fertilizers [313]. Zhang et al. developed a novel slow-release hydrogel fertilizer by graft copolymerizing acrylic acid (AA) with recycled cellulose (PCe) sourced from waste biomass, specifically pomelo peel [314]. Abduarahman et al. utilized waste tobacco boxes to extract cellulose fibers to fabricate a wCell/Mn-Fe-LDH membrane for the sustainable removal of anionic pollutants [272]. This composite offers a practical way to treat wastewater efficiently while also fostering environmental sustainability by turning waste biomass into valuable adsorbent materials.

5.3.2. Energy inputs and life cycle assessment (LCA) considerations

The energy input for LDH cellulose composite mainly depends on synthesis and the application process, which is relatively low compared to other methods, especially considering the co-precipitation process [32]. The co-precipitation method is widely favored due to its straightforward preparation process and relatively low operating temperature [31]. In hydrothermal treatment is often performed at around 100 °C for about 16 h to enable the creation of well-crystallized materials under mild conditions. As an alternative, methods like the sol–gel approach are also valued for their affordability and energy efficiency, as well as enabling fast processing and control over composition [36]. LDH–cellulose composites function effectively as adsorbents under ambient temperature and pressure conditions, significantly reducing energy requirements during water treatment processes. Compared to conventional synthesis, cellulose acetate or LDH–cellulose composite material is typically prepared via membrane casting or nanoparticle coating, using mild conditions and low heat input. Raicopol et al. developed the cellulose acetate-MgAl-LDH nanocomposite membranes for the removal of pharmaceutical contaminants (TC and DS) from wastewater with the highest water flux performance (529 L m^{-2} h^{-1}) compared to the pristine CA membrane (36 L m^{-2} h^{-1}) [276]. Yu et al. described a cost-effective and durable flexible membrane that was created via in situ ZnAl-LDH growth on a cellulose substrate, with a high separation efficiency (>94.4%) for industrial oily effluent [282] (Fig. 7d). The ability to regenerate and reuse LDH-based adsorbents, as shown in some studies, can further decrease the overall energy footprint of the treatment. Combining LDH-based adsorbents with other methods, like photocatalysis, can improve efficiency and potentially lower energy consumption. Bisaria et al. demonstrated that multiple recycling and reuse of the adsorbent significantly increased its negative environmental impact due to additional electricity used for drying before each use [38]. Large-scale applications may require more energy than laboratory-scale studies.

Life Cycle Assessment (LCA) is a structured method to assess the environmental effects of a product in each stage of its entire life span, from raw material extraction to manufacturing, usage, and final disposal [281,315]. Although there has not been much attention on LDH–cellulose composites in LCA, existing research has focused on the synthesis of LCA related to LDA [92]. Bisari et al. followed an LCA of chitosan-modified NiFe-LDH for arsenic(III) in aqueous solution using OpenLCA software and the ReCiPe Midpoint (H) (v1.02) method, enabling the evaluation and comparison of the environmental impacts associated with the applied techniques [316]. LCA analysis confirmed that the use of electricity consumption and the use of chemicals, particularly nickel and ammonia solution, were the primary contributors to environmental impacts such as global warming, human toxicity, freshwater ecotoxicity, and marine ecotoxicity [316]. Cellulose derived from renewable biomass enhances the sustainability benefits of LDHs by offering a biodegradable scaffold, which decreases the overall carbon footprint compared to solely synthetic adsorbents. When data are collected from laboratory-scale experiments, they carry potential errors due to involving controlled environmental conditions that do not fully replicate real-world scenarios, leading to discrepancies in the assessment results [316]. Furthermore, the use of advanced computational tools, such as artificial intelligence, can further support sustainability assessments and LCAs by improving data analysis, ensuring compliance with environmental standards, and promoting the development of environmentally friendly materials [92] (Fig. 7e).

LDH–cellulose hybrids are in the offing at the crossroads of biomedical and environmental applications, but the drivers of design and performance criteria are vastly different in the two fields [317,318]. Biomedically, the hybrids are explored as drug carriers, tissue engineering scaffolds, wound dressings, and antimicrobial coatings due to LDHs providing controlled release of bioactive species, whereas cellulose contributes biocompatibility, non-toxicity, and tunable porosity [30,319]. Specifications such as cytocompatibility, sterility, degradation rate, and pH-sensitive release overwhelm the performance requirements. By comparison, environmental applications are for contaminant remediation and wastewater treatment, where LDH–cellulose composites are engineered to maximize adsorption capacity, ion-exchange capacity, and chemical stability under harsh effluents [320]. In these situations, high surface area, reusability, cost effectiveness, and fouling or competitive ion resistance are most important, while stringent biomedical safety requirements are less relevant. These varied demands dictate the synthesis pathways, functionalization models, and testing protocols employed. Yet, biomedical application wisdom; i.e., surface functionalization and controlled release; can be transferred to the development of environmentally stable adsorbents, and pollutant adsorption experience can contribute to improved toxin removal or detoxification platforms in medicine. This tool transfer emphasizes LDH–cellulose composites as a universal platform with applicability to medical as well as environmental issues.

5.4. Cytotoxicity and biodegradability

Cellulose is intrinsically biocompatible and non-toxic, being widely used in biomedical and environmental applications. LDHs, in turn, are

considered relatively safe, especially those based on cations such as Mg^{2+}, Al^{3+}, and Zn^{2+}. However, toxicity can vary depending on the metal composition; composites containing less biocompatible cations (Ni^{2+}, Cr^{3+}, Co^{2+}) can release potentially toxic ions into aquatic environments [321]. In vitro studies suggest that excess LDH particles can induce oxidative stress, cellular inflammation, and damage to biological membranes, especially at high concentrations or when there is uncontrolled release of metal ions. Therefore, cytotoxicity assessment should consider both the chemical composition of the LDH and its stability in real-world environments. The cellulose matrix is highly biodegradable, undergoing enzymatic degradation by microorganisms, which favors the natural decomposition of the composite after use. The inorganic fraction of LDH is not biodegradable in the classical sense, but it can undergo partial dissolution in acidic media, releasing intercalated metal ions and anions [92]. This process can be beneficial, as it prevents persistent accumulation in the environment, but it can also pose a risk if the released ions are ecotoxic. The cellulose-LDH combination tends to reduce the mobility of inorganic nanomaterials, acting as a natural barrier that limits the uncontrolled release of LDH particles into the environment. The biodegradability of cellulose and the relative biocompatibility of certain LDHs (Mg—Al, Zn—Al) make these composites more sustainable and less persistent than purely synthetic adsorbents, such as MOFs or graphene. The release of metal ions during degradation can cause secondary contamination; the impact depends strongly on the type of cation present in the LDH. It is essential to conduct full-scale ecotoxicological tests, simulating environmental conditions (pH, ionic strength, presence of natural organic matter), to predict the stability and toxicity of composites. The development of cellulose-LDH composites with environmentally safe cations (Mg, Ca, Zn) and functionalization that controls the degradation rate can expand their potential use without compromising environmental safety.

Thus, in addition to the technical advantages of adsorption, the discussion on cytotoxicity and biodegradability reinforces that the development of these composites must be aligned with environmental safety and public health criteria, otherwise it could generate new sources of risk.

6. Challenges and future perspectives

This review presents a detailed overview of the synthesis and application of LDH–cellulose composites and identification of key challenges and developing future research needs for their practical use. The most pressing among these is the structural stability of the composites, particularly in harsh environmental conditions. LDHs, though chemically tunable and highly efficient in anion exchange, are prone to dissolution or phase transition in highly acidic industrial wastewaters or highly alkaline wastewater. This renders them to operate less effectively in the long term and decreases recyclability. Additionally, leaching of LDH is a very critical environmental concern because metal ions like Mg^{2+}, Al^{3+}, or Zn^{2+} can leach into treated water during adsorption or desorption operations and lead to secondary contamination as well as loss of material integrity.

The other key limitation is the scalability and complexity of synthesis techniques. Current fabrication techniques; such as hydrothermal, in situ co-precipitation, and impregnation; often entail high temperatures, lengthy reaction times, and multi-step processing not amenable to scalability to industrial-scale applications. Uniform dispersion of LDH in the cellulose matrix, particle size control, and retention of the composite structure upon scale-up are difficult to achieve. In addition, source and quality variability of cellulose, especially if derived from natural biomass or wastes, can result in composite variability in properties and performance. The latter affects reproducibility and standardization—essential parameters for commercialization.

From the application point of view, low regeneration and reusability also restrict the broad application of LDH–cellulose composites. Though the materials exhibit high initial adsorption capacity, repeated cycles of pollutant adsorption/desorption may result in damage to both the LDH network and cellulose chain, resulting in reduced activity and increased material cost. Moreover, the majority of the reported work is conducted in laboratory-scale controlled settings and using simulated wastewater. Its operation under normal conditions in normal wastewater systems, e.g., a blend of organic, inorganic, and biologic substances, remains to be comprehensively examined. Realistic, not restrictive, conditions of varying ionic strength, turbidity, and interfering ions must be considered to truly assess the pragmatic value.

Despite their promising performance under laboratory conditions, LDH–cellulose adsorbents also experience some limitations in application to actual wastewater treatment. Another of the grand challenges is the complexity of real wastewater matrices, which in most instances comprises mixed pollutants, fluctuating pH, high salinity, and high concentrations of competing ions or organic matter that can clog or occupy adsorption sites and thus reduce the removal efficiency compared to synthetic single-solute systems. Another limitation is the stability of the composite material during prolonged exposure to aggressive chemical media, e.g., acid or alkaline industrial wastewater, which may lead to partial dissolution of LDH layers or hydrolysis of cellulose and thereby shorten the operational life of the adsorbent. In addition, the production scalability is also finite, as it remains cost- and energy-intensive to produce uniform LDH–cellulose composites with controlled morphology and functional group distribution at industrial levels. Regeneration and recycling of the materials in real conditions also present challenges: desorption agents that work well in the lab can be less effective in wastewater of complicated compositions. Their use may also generate secondary waste streams requiring further treatment. In addition, mechanical strength is an issue, as multiple cycles of stirring, pumping, or filtration can result in attrition or particle breakdown, compromising recovery and reuse. Finally, long-term pilot-scale performance data, regeneration efficiency, and economic feasibility are not available, making full-scale adoption by water utilities challenging. Addressing these challenges through improved material design, low-cost fabrication, and field-scale demonstration will be the key to transforming LDH–cellulose adsorbents from promising research concepts to practical wastewater treatment technologies.

The future study can expect to encounter enhancement of composite stability, particularly under multi-contaminant and high pH conditions. This can be made possible through surface engineering, crosslinking, or introduction of other nanomaterials (e.g., graphene oxide, biochar, or metal–organic frameworks) for structural stability and durability of long-term adsorption. By comparison, sustainable, low-energy, green, and high-throughput synthesis routes from waste or renewable cellulose feedstocks and low-energy processing conditions are required to allow for sustainable manufacturing. Implementation of new functionalization protocols to allow selectivity towards target pollutants, e.g., endocrine-disrupting chemicals or medications, would further increase the utility and diversity of these materials.

Besides that, future studies should combine life cycle assessment (LCA) and techno-economic analysis (TEA) to explore the economic and environmental sustainability of LDH–cellulose composites from production cycles, use cycles, and waste disposal cycles. Blends of these materials with advanced monitoring and regenerating mechanisms, including electrochemical or photocatalytic systems, may also provide real-time regulation and sustainable operation. Lastly, interaction among materials science, environmental engineering, and process industrial engineering from different disciplines will be necessary for bridging the gap between laboratory discovery and field implementation. In summary, although LDH–cellulose composites represent an enormously promising platform for efficient, sustainable, and next-generation water-filtering materials, overcoming the limitation of stability, regeneration, scale-up, and in-field validation is very important to effectively achieve their full potential.

7. Conclusion

This review highlights the future of LDH–cellulose composites as new generation hybrid adsorbents for efficient wastewater treatment of inorganic and organic pollutants. When optimized, such composites have demonstrated maximum adsorption capacities in excess of ≈270 mg g^{-1} for pharmaceuticals (e.g., sulfamethoxazole) and over 400 mg g^{-1} for dyes (e.g., methylene blue), showcasing high affinity toward diverse contaminants. Their surface areas are often in the tens to hundreds of m^2 g^{-1}; for example, BET surface areas of ~15–60 m^2 g^{-1} in cellulosic LDH composites and up to ~700–750 m^2 g^{-1} in LDH–carbon systems, which substantially improve adsorption performance and kinetics. Regeneration cycles have shown promising performance, with many composites maintaining > 80-90% of their adsorption efficiency over 4-5 reuse cycles. The review categorizes synthesis strategies in an orderly manner, clarifies adsorption mechanisms, and dissects performance in various environmental conditions, showing the overall structure–function relationship of these hybrid materials. Despite all their advantages, problems such as LDH leaching, loss of structural stability at extreme pH levels, regeneration limitations, and scale-up challenges are still significant obstacles to practical use. Future research should therefore focus on **tailored surface functionalization**; for instance, grafting selective functional groups (–SH, –COOH, $–NH_2$) or biomimetic ligands to improve pollutant selectivity and stability; and on engineering **hierarchical or porous architectures** that enhance mass transfer, adsorption kinetics, and mechanical robustness under real wastewater conditions. Another promising direction is the **integration of LDH–cellulose composites with membrane or filter systems** to create hybrid separation–adsorption modules that combine high flux, low fouling, and easy regeneration. At the same time, these materials should be developed with broader societal and industrial considerations in mind. Using green, low-energy or solvent-free synthesis not only improves their environmental credentials but also aligns with circular-economy principles by valorizing cellulose from agricultural or industrial residues. Their relatively low-cost, biodegradable nature makes them particularly attractive for low-income regions where centralized treatment infrastructure is lacking. Incorporating life-cycle assessment, techno-economic modeling, and compliance with evolving regulatory frameworks can guide industrial-scale implementation and ensure public acceptance. In parallel, pilot-scale testing under realistic conditions will provide critical performance data. Overall, LDH–cellulose hybrid composite materials remain an efficient, multifunctional, and prospective sustainable system for effective wastewater treatment, and continuous interdisciplinary research combining materials science, process engineering, and environmental assessment will be key to unlocking their full potential and achieving global water quality and environmental resilience.

CRediT authorship contribution statement

Noureddine El Messaoudi: Writing – original draft, Investigation, Conceptualization. **Youssef Miyah:** Writing – review & editing, Visualization. **Jordana Georgin:** Writing – review & editing, Conceptualization. **Dison S.P. Franco:** Writing – review & editing, Investigation. **B. V.N. Sewwandi:** Writing – review & editing, Methodology. **Neha Singh:** Writing – review & editing, Validation. **Salah Knani:** Writing – review & editing, Project administration.

Declaration of competing interest

The authors declare that they have no known competing financial interests or personal relationships that could have appeared to influence the work reported in this paper.

Acknowledgment

The authors extend their appreciation to the Deanship of Scientific Research at Northern Border University, Arar, KSA for funding this research work through the project number "NBU-FPEJ-2025-2483-08".

Data availability

Data will be made available on request.

References

[1] F. Lyu, Research on the current status of global water pollution and corresponding countermeasures, Highl. Sci. Eng. Technol. 141 (2025) 14–19, https://doi.org/10.54097/E3M5TW49.
[2] L. Lin, H. Yang, X. Xu, Effects of water pollution on human health and disease heterogeneity: a review, Front. Environ. Sci. 10 (2022) 880246, https://doi.org/10.3389/FENVS.2022.880246/BIBTEX.
[3] P. Saravanan, V. Saravanan, R. Rajeshkannan, G. Arnica, M. Rajasimman, G. Baskar, A. Pugazhendhi, Comprehensive review on toxic heavy metals in the aquatic system: sources, identification, treatment strategies, and health risk assessment, Environ. Res. 258 (2024) 119440, https://doi.org/10.1016/J.ENVRES.2024.119440.
[4] S.F. AbuQamar, M.T. El-Saadony, S.S. Alkafaas, M.I. Elsalahaty, S.S. Elkafas, B. T. Mathew, A.N. Aljasmi, H.S. Alhammadi, H.M. Salem, T.A. Abd El-Mageed, R. A. Zaghloul, W.F.A. Mosa, A.E. Ahmed, A.S. Elrys, A.M. Saad, F.A. Alsaeed, K. A. El-Tarabily, Ecological impacts and management strategies of pesticide pollution on aquatic life and human beings, Mar. Pollut. Bull. 206 (2024) 116613, https://doi.org/10.1016/J.MARPOLBUL.2024.116613.
[5] M. Hameed, Z.K. Dijoo, R.A. Bhat, I. Qayoom, Concerns and threats of heavy metals' contamination on aquatic ecosystem, Bioremediat. Biotechnol. Technol. Noxious Subst. Remediat. 4 (2020) 1–19, https://doi.org/10.1007/978-3-030-48690-7_1.
[6] Y. Chen, H. Xu, M.S. Khan, S. Han, S. Zhu, Recent advances in layered double hydroxides for pharmaceutical wastewater treatment: a critical review, Crit. Rev. Environ. Sci. Technol. 55 (2025) 1097–1123, https://doi.org/10.1080/10643389.2025.2488808.
[7] O.V. Obayomi, D.C. Olawoyin, O. Oguntimehin, L.S. Mustapha, S.O. Kolade, P. O. Oladoye, S. Oh, K.S. Obayomi, Exploring emerging water treatment technologies for the removal of microbial pathogens, Curr. Res. Biotechnol. 8 (2024) 100252, https://doi.org/10.1016/J.CRBIOT.2024.100252.
[8] N. Taoufik, W. Boumya, F.Z. Janani, A. Elhalil, F.Z. Mahjoubi, N. Barka, Removal of emerging pharmaceutical pollutants: a systematic mapping study review, J. Environ. Chem. Eng. 8 (2020) 104251, https://doi.org/10.1016/J.JECE.2020.104251.
[9] A. Jamrah, T.M. Al-Zghoul, M.M. Darwish, A comprehensive review of combined processes for olive mill wastewater treatments, Case Stud. Chem. Environ. Eng. 8 (2023) 100493, https://doi.org/10.1016/J.CSCEE.2023.100493.
[10] G. Kooijman, M.K. de Kreuk, C. Houtman, J.B. van Lier, Perspectives of coagulation/flocculation for the removal of pharmaceuticals from domestic wastewater: a critical view at experimental procedures, J. Water Process Eng. 34 (2020), https://doi.org/10.1016/J.JWPE.2020.101161.
[11] P.S. Nishmitha, K.A. Akhilghosh, V.P. Aiswriya, A. Ramesh, M. Muthuchamy, A. Muthukumar, Understanding emerging contaminants in water and wastewater: a comprehensive review on detection, impacts, and solutions, J. Hazard. Mater. Adv. 18 (2025) 100755, https://doi.org/10.1016/J.HAZADV.2025.100755.
[12] R. Kumar, M. Qureshi, D.K. Vishwakarma, N. Al-Ansari, A. Kuriqi, A. Elbeltagi, A. Saraswat, A review on emerging water contaminants and the application of sustainable removal technologies, Case Stud. Chem. Environ. Eng. 6 (2022) 100219, https://doi.org/10.1016/J.CSCEE.2022.100219.
[13] K.P. Sharma, B. Pokharel, A. Subedi, U. Neupane, Assessment of heavy metal contamination in wastewater surrounding the Butwal industrial area, Butwal Campus J. 7 (2024) 15–24, https://doi.org/10.3126/BCJ.V7I2.73172.
[14] W. Halecki, T. Sionkowski, K. Chmielowski, A. Kowalczyk, K. Kalarus, Municipal wastewater quality control: heavy metal comparative analysis — case study, Ochr. Sr. Zasobow Nat. 34 (2023) 127–134, https://doi.org/10.2478/OSZN-2023-0023.
[15] M. Uddin, F. Bin Alam, Health risk assessment of the heavy metals at wastewater discharge points of textile industries in Tongi, Shitalakkhya, and Dhaleshwari, Bangladesh, J. Water Health 21 (2023) 586–600, https://doi.org/10.2166/WH.2023.284.
[16] H. Ghazal, E. Koumaki, J. Hoslett, S. Malamis, E. Katsou, D. Barcelo, H. Jouhara, Insights into current physical, chemical and hybrid technologies used for the treatment of wastewater contaminated with pharmaceuticals, J. Clean. Prod. 361 (2022) 132079, https://doi.org/10.1016/J.JCLEPRO.2022.132079.
[17] S. Ahmad, G. Mujtaba, M. Zubair, M.U.H. Shah, M. Daud, N.D. Mu'azu, M.A. Al-Harthi, A review of performance, mechanism, and challenges of layered double hydroxide-based biocomposites for the adsorptive removal of dye contaminants from water and wastewater, J. Water Process Eng. 70 (2025) 106837, https://doi.org/10.1016/J.JWPE.2024.106837.
[18] A.L. Johnston, E. Lester, O. Williams, R.L. Gomes, Interactions between antibiotic removal, water matrix characteristics and layered double hydroxide sorbent

material, Chemosphere 367 (2024) 143546, https://doi.org/10.1016/J.CHEMOSPHERE.2024.143546.
[19] X. Wang, M.A. Khan, M. Xia, S. Zhu, W. Lei, F. Wang, Synthesis of RGO and g-C_3N_4 hybrid with WO_3/Bi_2WO_6 to boost degradation of nitroguanidine under visible light irradiation, J. Mater. Sci. Mater. Electron. 30 (2019) 5503–5515, https://doi.org/10.1007/s10854-019-00844-w.
[20] M.E. Mahmoud, R.M. El-Sharkawy, E.A. Allam, G.M. Nabil, F.R. Louka, M. Sillanpää, S.M. Elsayed, Layered double hydroxide nanocomposites as promising nanomaterials for removal of inorganic pollutants from aquatic systems: a review, J. Solid State Chem. 346 (2025) 125289, https://doi.org/10.1016/J.JSSC.2025.125289.
[21] M.E. Mahmoud, R.M. El-Sharkawy, E.A. Allam, G.M. Nabil, F.R. Louka, M. A. Salam, S.M. Elsayed, Recent progress in water decontamination from dyes, pharmaceuticals, and other miscellaneous nonmetallic pollutants by layered double hydroxide materials, J. Water Process Eng. 57 (2024) 104625, https://doi.org/10.1016/J.JWPE.2023.104625.
[22] G.M. Nabil, M.K. Obada, M.E. Mahmoud, Implementation of integrated palygorskite with copper–aluminum layered double hydroxides composite in superior nitrate pollutant removal from wastewater, J. Ind. Eng. Chem. 151 (2025) 605–617, https://doi.org/10.1016/J.JIEC.2025.04.032.
[23] M.E. Mahmoud, N.K. Kamel, M.F. Amira, N.A. Fekry, Nitrate removal from wastewater by a novel co-biochar from guava seeds/beetroot peels-functionalized-Mg/Al double-layered hydroxide, Sep. Purif. Technol. 344 (2024) 127067, https://doi.org/10.1016/J.SEPPUR.2024.127067.
[24] J. Mittal, Recent progress in the synthesis of layered double hydroxides and their application for the adsorptive removal of dyes: a review, J. Environ. Manag. 295 (2021) 113017, https://doi.org/10.1016/J.JENVMAN.2021.113017.
[25] S. Kumari, V. Sharma, S. Soni, A. Sharma, A. Thakur, S. Kumar, K. Dhama, A. K. Sharma, S.K. Bhatia, Layered double hydroxides and their tailored hybrids/composites: progressive trends for delivery of natural/synthetic-drug/cosmetic biomolecules, Environ. Res. 238 (2023) 117171, https://doi.org/10.1016/J.ENVRES.2023.117171.
[26] S. Zhu, H. Xu, M.S. Khan, M. Xia, F. Wang, Y. Chen, Enhanced removal of Ni^{2+} and Co^{2+} from wastewater using a novel 2-hydroxyphosphonoacetic acid modified Mg/Fe-LDH composite adsorbent, Water Res. 272 (2025) 122997, https://doi.org/10.1016/j.watres.2024.122997.
[27] R. Keyikoglu, A. Khataee, Y. Yoon, Layered double hydroxides for removing and recovering phosphate: recent advances and future directions, Adv. Colloid Interf. Sci. 300 (2022) 102598, https://doi.org/10.1016/J.CIS.2021.102598.
[28] J. Bai, X. Zhang, C. Wang, X. Li, Z. Xu, C. Jing, T. Zhang, Y. Jiang, The adsorption-photocatalytic synergism of LDHs-based nanocomposites on the removal of pollutants in aqueous environment: a critical review, J. Clean. Prod. 436 (2024) 140705, https://doi.org/10.1016/J.JCLEPRO.2024.140705.
[29] M. Mohapi, J.S. Sefadi, M.J. Mochane, S.I. Magagula, K. Lebelo, Effect of LDHs and other clays on polymer composite in adsorptive removal of contaminants: a review, Crystals 10 (2020) (2020) 957, https://doi.org/10.3390/CRYST10110957.
[30] J. Luo, Y. Cui, L. Xu, J. Zhang, J. Chen, X. Li, B. Zeng, Z. Deng, L. Shao, Layered double hydroxides for regenerative nanomedicine and tissue engineering: recent advances and future perspectives, J. Nanobiotechnol. 23 (2025) 370, https://doi.org/10.1186/S12951-025-03448-1.
[31] R. Zhang, Y. Ai, Z. Lu, Application of multifunctional layered double hydroxides for removing environmental pollutants: recent experimental and theoretical progress, J. Environ. Chem. Eng. 8 (2020), https://doi.org/10.1016/J.JECE.2020.103908.
[32] B.M.V. da Gama, R. Selvasembian, D.A. Giannakoudakis, K.S. Triantafyllidis, G. McKay, L. Meili, Layered double hydroxides as rising-star adsorbents for water purification: a brief discussion, Molecules 27 (2022), https://doi.org/10.3390/MOLECULES27154900.
[33] O. Platnieks, S. Beluns, S. Briede, M. Jurinovs, S. Gaidukovs, Cellulose synergetic interactions with biopolymers: functionalization for sustainable and green material design, Ind. Crop. Prod. 204 (2023) 117310, https://doi.org/10.1016/J.INDCROP.2023.117310.
[34] R. Kundu, P. Mahada, B. Chhirang, B. Das, Cellulose hydrogels: green and sustainable soft biomaterials, Curr. Res. Green Sustain. Chem. 5 (2022) 100252, https://doi.org/10.1016/J.CRGSC.2021.100252.
[35] G.M. Nabil, R.H. Althomali, M.E. Mahmoud, Pioneering nanobiosorbent of doped cellulose-gelatin hydrogel into carbon quantum dots and magnesium ferrite for effective removal of Cr(VI), Int. J. Biol. Macromol. 323 (2025) 147119, https://doi.org/10.1016/J.IJBIOMAC.2025.147119.
[36] S. Mandal, S. Mayadevi, Cellulose supported layered double hydroxides for the adsorption of fluoride from aqueous solution, Chemosphere 72 (2008) 995–998, https://doi.org/10.1016/J.CHEMOSPHERE.2008.03.053.
[37] M. Pavlovic, A. Szerlauth, S. Muráth, G. Varga, I. Szilagyi, Surface modification of two-dimensional layered double hydroxide nanoparticles with biopolymers for biomedical applications, Adv. Drug Deliv. Rev. 191 (2022) 114590, https://doi.org/10.1016/J.ADDR.2022.114590.
[38] D. Wu, P.R. Chang, X. Ma, Preparation and properties of layered double hydroxide- carboxymethylcellulose sodium/glycerol plasticized starch nanocomposites, Carbohydr. Polym. 86 (2011) 877–882, https://doi.org/10.1016/J.CARBPOL.2011.05.030.
[39] T. Zhao, Z. Chen, W. Xiao, Y. Zhou, B. Zhan, Y. Lyu, S. Li, Y. Liu, Cellulose aerogels in water pollution treatment: preparation, applications and mechanism, Adv. Bionics (2025), https://doi.org/10.1016/J.ABS.2025.06.003.
[40] R. Rukaramato, D. Babatunde, T. Madanhire, N. Mketo, N. Magwa, Nanocellulose-based materials for the removal of metal ions, pharmaceuticals, pesticides, dyes, and other pollutants from aqueous environments: a review, J. Ind. Eng. Chem. (2025), https://doi.org/10.1016/J.JIEC.2025.05.028.
[41] Z. Chen, H. Zheng, J. Yi, T. Liu, H. Lai, S. Zhang, W. Huang, Y. Yin, X. Huang, Y. Tong, D. Liang, R. Li, L. Zhong, C. Zhang, H. Zhang, Advanced cellulose-based materials for flexible energy storage systems, Resour. Chem. Mater. 4 (2025) 100120, https://doi.org/10.1016/J.RECM.2025.100120.
[42] A.K. Rana, E. Mostafavi, W.F. Alsanie, S.S. Siwal, V.K. Thakur, Cellulose-based materials for air purification: a review, Ind. Crop. Prod. 194 (2023) 116331, https://doi.org/10.1016/J.INDCROP.2023.116331.
[43] O.A. Oyewo, A.M. Muliwa, S.S. Makgato, D.C. Onwudiwe, Research progress on green adsorption process for water pollution control applications, Hybrid Adv. 8 (2025) 100338, https://doi.org/10.1016/J.HYBADV.2024.100338.
[44] A. Chatterjee, P. Bharadiya, D. Hansora, Layered double hydroxide based bionanocomposites, Appl. Clay Sci. 177 (2019) 19–36, https://doi.org/10.1016/j.clay.2019.04.022.
[45] M.D. Solikhah, Y.G. Wibowo, D. Anwar, A. Andriani, A. Pamungkas, F.T. Pratiwi, S.S. Wirawan, S.N.A. Jenie, H. Prasetia, H.T.B.M. Petrus, A comprehensive review of potential utilization of novel flame-resistant hydrogel composites using alginate-cellulose-LDH Zn/Al-carbon nanotubes for water removal from biofuel, Inorg. Chem. Commun. 180 (2025) 114986, https://doi.org/10.1016/J.INOCHE.2025.114986.
[46] V. Mittal, Polymer layered silicate nanocomposites: a review, Materials (Basel) 2 (2009) 992–1057, https://doi.org/10.3390/ma2030992.
[47] G. Huang, A. Zhuo, L. Wang, X. Wang, Preparation and flammability properties of intumescent flame retardant-functionalized layered double hydroxides/polymethyl methacrylate nanocomposites, Mater. Chem. Phys. 130 (2011) 714–720, https://doi.org/10.1016/j.matchemphys.2011.07.047.
[48] C.M.C. Pereira, M. Herrero, F.M. Labajos, A.T. Marques, V. Rives, Preparation and properties of new flame retardant unsaturated polyester nanocomposites based on layered double hydroxides, Polym. Degrad. Stab. 94 (2009) 939–946, https://doi.org/10.1016/j.polymdegradstab. 2009.03.009.
[49] L. Du, B. Qu, M. Zhang, Thermal properties and combustion characterization of nylon 6/MgAl-LDH nanocomposites via organic modification and melt intercalation, Polym. Degrad. Stab. 92 (2007) 497–502, https://doi.org/10.1016/j.polymdegradstab. 2006.08.001.
[50] H. Benaddi, D. Benachour, Y. Grohens, No title, J. Polym. Eng. 36 (2016) 681–693, https://doi.org/10.1515/polyeng-2015-0162.
[51] M. Dinari, A.R. Rajabi, Structural, thermal and mechanical properties of polymer nanocomposites based on organosoluble polyimide with naphthyl pendent group and layered double hydroxide, High Perform. Polym. 29 (2017) 951–959, https://doi.org/10.1177/0954008316665678.
[52] S. Elbasuney, Surface engineering of layered double hydroxide (LDH) nanoparticles for polymer flame retardancy, Powder Technol. 277 (2015) 63–73, https://doi.org/10.1016/j.powtec.2015.02.044.
[53] P.K. Kaul, A.J. Samson, G.T. Selvan, I.V.M.V. Enoch, P.M. Selvakumar, Synergistic effect of LDH in the presence of organophosphate on thermal and flammable properties of an epoxy nanocomposite, Appl. Clay Sci. 135 (2017) 234–243, https://doi.org/10.1016/j.clay.2016.09.031.
[54] C. Manzi-Nshuti, P. Songtipya, E. Manias, M.M. Jimenez-Gasco, J.M. Hossenlopp, C.A. Wilkie, Polymer nanocomposites using zinc aluminum and magnesium aluminum oleate layered double hydroxides: Effects of LDH divalent metals on dispersion, thermal, mechanical and fire performance in various polymers, Polymer (Guildf.) 50 (2009) 3564–3574, https://doi.org/10.1016/j.polymer.2009.06.014.
[55] D. Scarpellini, C. Falconi, P. Gaudio, A. Mattoccia, P.G. Medaglia, A. Orsini, R. Pizzoferrato, M. Richetta, Morphology of Zn/Al layered double hydroxide nanosheets grown onto aluminum thin films, Microelectron. Eng. 126 (2014) 129–133, https://doi.org/10.1016/j.mee.2014.07.007.
[56] F. Leroux, J. Besse, Polymer interleaved layered double hydroxide: a new emerging class of nanocomposites, Chem. Mater. 13 (2001) 3507–3515, https://doi.org/10.1021/CM0110268.
[57] L. Guo, W. Wu, Y. Zhou, F. Zhang, R. Zeng, J. Zeng, Layered double hydroxide coatings on magnesium alloys: a review, J. Mater. Sci. Technol. 34 (2018) 1455–1466, https://doi.org/10.1016/J.JMST.2018.03.003.
[58] A.L.M.D. de Sousa, W.M. dos Santos, M.L. de Souza, L.C.P.B.B. Silva, A.E.H. K. Yun, C.S.B. Aguilera, B.F. Chagas, L.A. Rolim, R.M.F. da Silva, P.J.R. Neto, Layered double hydroxides as promising excipients for drug delivery purposes, Eur. J. Pharm. Sci. 165 (2021) 105922, https://doi.org/10.1016/J.EJPS.2021.105922.
[59] G. Arrabito, A. Bonasera, G. Prestopino, A. Orsini, A. Mattoccia, E. Martinelli, B. Pignataro, P.G. Medaglia, Layered double hydroxides: a toolbox for chemistry and biology, Crystals 9 (2019) (2019) 361, https://doi.org/10.3390/CRYST9070361.
[60] F. Cavani, F. Trifirò, A. Vaccari, Hydrotalcite-type anionic clays: preparation, properties and applications, Catal. Today 11 (1991) 173–301, https://doi.org/10.1016/0920-5861(91)80068-K.
[61] D.G. Evans, R.C.T. Slade, Structural aspects of layered double hydroxides, in: X. Duan, D.G. Evans (Eds.), Layer. Double Hydroxides, Springer Berlin Heidelberg, Berlin, Heidelberg, 2006, pp. 1–87, https://doi.org/10.1007/430_005.
[62] V. Rives, Characterisation of layered double hydroxides and their decomposition products, Mater. Chem. Phys. 75 (2002) 19–25, https://doi.org/10.1016/S0254-0584(02)00024-X.
[63] J.M. Bouzaid, R.L. Frost, W.N. Martens, Thermal decomposition of the composite hydrotalcites of iowaite and woodallite, J. Therm. Anal. Calorim. 89 (2007) 511–519, https://doi.org/10.1007/s10973-006-7562-x.

[64] S.J. Palmer, H.J. Spratt, R.L. Frost, Thermal decomposition of hydrotalcites with variable cationic ratios, J. Therm. Anal. Calorim. 95 (2009) 123–129, https://doi.org/10.1007/s10973-008-8992-4.
[65] V.K. Porwal, E. André, A. Carof, A. Bastida Pascual, C. Carteret, F. Ingrosso, Structural and vibrational properties of carboxylates intercalated into layered double hydroxides: a joint computational and experimental study, Molecules 29 (2024) 1853, https://doi.org/10.3390/MOLECULES29081853/S1.
[66] R. Sharma, G.G.C. Arizaga, A.K. Saini, P. Shandilya, Layered double hydroxide as multifunctional materials for environmental remediation: from chemical pollutants to microorganisms, Sustain. Mater. Technol. 29 (2021) e00319, https://doi.org/10.1016/J.SUSMAT.2021.E00319.
[67] L.Y. Wang, D.S. Tong, L.Z. Zhao, F.G. Liu, N. An, W.H. Yu, C.H. Zhou, Utilization of alum sludge for producing aluminum hydroxide and layered double hydroxide, Ceram. Int. 40 (2014) 15503–15514, https://doi.org/10.1016/j.ceramint.2014.07.012.
[68] J.T. Kloprogge, D. Wharton, L. Hickey, R.L. Frost, No title, Am. Miner. 87 (2002) 623–629, https://doi.org/10.2138/am-2002-5-604.
[69] Q. Tao, B.J. Reddy, H. He, R.L. Frost, P. Yuan, J. Zhu, Synthesis and infrared spectroscopic characterization of selected layered double hydroxides containing divalent Ni and Co, Mater. Chem. Phys. 112 (2008) 869–875, https://doi.org/10.1016/j.matchemphys.2008.06.060.
[70] A.I. Khan, D. O'Hare, Intercalation chemistry of layered double hydroxides: recent developments and applications, J. Mater. Chem. 12 (2002) 3191–3198, https://doi.org/10.1039/B204076J.
[71] M.V.P.O. Cunha, J.A.M. Corrèa, Síntese e caracterização de hidróxidos duplos a partir da lama vermelha (Synthesis and characterization of layered double hydroxides from red mud), Cerâmica 57 (2011) 85–93.
[72] G.W. Brindley, S. Kikkawa, Thermal behavior of hydrotalcite and of anion-exchanged forms of hydrotalcite, Clay Clay Miner. 28 (1980) 87–91, https://doi.org/10.1346/CCMN.1980.0280202.
[73] S. Komarneni, N. Kozai, R. Roy, Novel function for anionic clays: selective transition metal cation uptake by diadochy, J. Mater. Chem. 8 (1998) 1329–1331, https://doi.org/10.1039/A801631C.
[74] M. Bujoli-Dœuff, L. Force, V. Gadet, M. Verdaguer, K. El Malki, A. de Roy, J. P. Besse, J.P. Renard, A new two-dimensional approach to molecular-based magnets: nickel(II)-chromium(III) double hydroxide systems, Mater. Res. Bull. 26 (1991) 577–587, https://doi.org/10.1016/0025-5408(91)90100-Z.
[75] M. Adachi-pagano, C. Forano, J. Besse, M. Inorganiques, C. Esa, U.B. Pascal, A. Cedex, Adachipagano2000.Pdf, 2000, pp. 91–92.
[76] K.K.H. Choy, J.F. Porter, G. McKay, Langmuir isotherm models applied to the multicomponent sorption of acid dyes from effluent onto activated carbon, J. Chem. Eng. Data 45 (2000) 575–584, https://doi.org/10.1021/je9902894.
[77] V. Ambrogi, G. Fardella, G. Grandolini, L. Perioli, Intercalation compounds of hydrotalcite-like anionic clays with antiinflammatory agents — I. Intercalation and in vitro release of ibuprofen, Int. J. Pharm. 220 (2001) 23–32, https://doi.org/10.1016/S0378-5173(01)00629-9.
[78] K.M. Tyner, M.S. Roberson, K.A. Berghorn, L. Li, R.F. Gilmour, C.A. Batt, E. P. Giannelis, Intercalation, delivery, and expression of the gene encoding green fluorescence protein utilizing nanobiohybrids, J. Control. Release 100 (2004) 399–409, https://doi.org/10.1016/j.jconrel.2004.07.035.
[79] U. Costantino, F. Marmottini, M. Nocchetti, R. Vivani, New synthetic routes to hydrotalcite-like compounds — characterisation and properties of the obtained materials, Eur. J. Inorg. Chem. (1998) 1439–1446, https://doi.org/10.1002/(sici)1099-0682(199810)1998:10<1439::aid-ejic1439>3.0.co;2-1.
[80] M. Ogawa, H. Kaiho, Homogeneous precipitation of uniform hydrotalcite particles, Langmuir 18 (2002) 4240–4242, https://doi.org/10.1021/la0117045.
[81] J. Livage, M. Henry, C. Sanchez, Sol-gel chemistry of transition metal oxides, Prog. Solid State Chem. 18 (1988) 259–341, https://doi.org/10.1016/0079-6786(88)90005-2.
[82] F. Prinetto, G. Ghiotti, P. Graffin, D. Tichit, Synthesis and characterization of sol-gel Mg/Al and Ni/Al layered double hydroxides and comparison with co-precipitated samples, Microporous Mesoporous Mater. 39 (2000) 229–247, https://doi.org/10.1016/S1387-1811(00)00197-9.
[83] M.A. Aramendía, V. Borau, C. Jiménez, J.M. Marinas, J.R. Ruiz, F.J. Urbano, Comparative study of Mg/M(III) (M = Al, Ga, In) layered double hydroxides obtained by coprecipitation and the sol-gel method, J. Solid State Chem. 168 (2002) 156–161, https://doi.org/10.1006/jssc.2002.9655.
[84] M. Jitianu, M. Bālāsoiu, M. Zaharescu, A. Jitianu, A. Ivanov, Comparative study of sol-gel and coprecipitated Ni-Al hydrotalcites, J. Sol-Gel Sci. Technol. 19 (2000) 453–457, https://doi.org/10.1023/A:1008703714841.
[85] T. Lopez, P. Bosch, E. Ramos, R. Gomez, O. Novaro, D. Acosta, F. Figueras, Synthesis and characterization of sol-gel hydrotalcites. Structure and texture, Langmuir 12 (1996) 189–192, https://doi.org/10.1021/la940703s.
[86] E. Conterosito, L. Palin, D. Antonioli, M.P. Riccardi, E. Boccaleri, M. Aceto, M. Milanesio, V. Gianotti, On the rehydration of organic layered double hydroxides to form low-ordered carbon/LDH nanocomposites, Inorganics 6 (2018) 1–16, https://doi.org/10.3390/inorganics6030079.
[87] K. Zhu, Y. Gao, X. Tan, C. Chen, Polyaniline-modified Mg/Al layered double hydroxide composites and their application in efficient removal of Cr(VI), ACS Sustain. Chem. Eng. 4 (2016) 4361–4369, https://doi.org/10.1021/acssuschemeng.6b00922.
[88] A.M. Youssef, H. Moustafa, A. Barhoum, A.E.F.A.A. Hakim, A. Dufresne, Evaluation of the morphological, electrical and antibacterial properties of polyaniline nanocomposite based on Zn/Al-layered double hydroxides, ChemistrySelect 2 (2017) 8553–8566, https://doi.org/10.1002/slct.201701513.
[89] G.I. Edo, W. Ndudi, A.B.M. Ali, E. Yousif, A.N. Jikah, E.F. Isoje, U.A. Igbuku, A. N. Mafe, R.A. Opiti, C.J. Madueke, A.E.A. Essaghah, D.S. Ahmed, H. Umar, Biopolymers: an inclusive review, Hybrid Adv. 9 (2025) 100418, https://doi.org/10.1016/J.HYBADV.2025.100418.
[90] D. Dutta, N. Sit, A comprehensive review on types and properties of biopolymers as sustainable bio-based alternatives for packaging, Food Biomacromol. 1 (2024) 58–87, https://doi.org/10.1002/FOB2.12019.
[91] S. Petrovic, B. Bita, M.E. Barbinta-Patrascu, Nanoformulations in pharmaceutical and biomedical applications: green perspectives, Int. J. Mol. Sci. 25 (2024) 5842, https://doi.org/10.3390/IJMS25115842.
[92] V.S. Munagapati, H.Y. Wen, J.C. Wen, K.Y.A. Lin, Y. Gutha, A.R.K. Gollakota, V. Yarramuthi, K. Rudravarapu, S. Sangaraju, H.Y. Choi, Biopolymer-inorganic hybrid composites: the expanding role of cellulose/layered double hydroxides (LDHs) in advanced applications, Inorg. Chem. Commun. 179 (2025) 114795, https://doi.org/10.1016/J.INOCHE.2025.114795.
[93] M.M. Reddy, S. Vivekanandhan, M. Misra, S.K. Bhatia, A.K. Mohanty, Biobased plastics and bionanocomposites: current status and future opportunities, Prog. Polym. Sci. 38 (2013) 1653–1689, https://doi.org/10.1016/j.progpolymsci.2013.05.006.
[94] M.N. Norizan, S.S. Shazleen, A.H. Alias, F.A. Sabaruddin, M.R.M. Asyraf, E. S. Zainudin, N. Abdullah, M.S. Samsudin, S.H. Kamarudin, M.N.F. Norrrahim, Nanocellulose-based nanocomposites for sustainable applications: a review, Nanomaterials 12 (2022) 1–51, https://doi.org/10.3390/nano12193483.
[95] E. Aigaje, A. Riofrio, Impact of nanocellulose/biopolymer composites: a review, Polymers (Basel) 15 (2023) 1219.
[96] P. Kaur, N. Sharma, M. Munagala, R. Rajkhowa, B. Aallardyce, Y. Shastri, R. Agrawal, Nanocellulose: resources, physio-chemical properties, current uses and future applications, Front. Nanotechnol. 3 (2021) 1–17, https://doi.org/10.3389/fnano.2021.747329.
[97] D. Tahir, M. Ramzan, A. Karim, H. Hu, S. Naseem, M. Rehan, M. Ahmad, M. Zhang, Applications of nanocellulose and nanocellulose-based composites: a review, Polymers (Basel) 14 (2022) 4468.
[98] S. Kalia, A. Dufresne, B.M. Cherian, B.S. Kaith, L. Avérous, J. Njuguna, E. Nassiopoulos, Cellulose-based bio- and nanocomposites: a review, Int. J. Polym. Sci. 2011 (2011), https://doi.org/10.1155/2011/837875.
[99] V. Tunsound, T. Krasian, D. Daranarong, W. Punyodom, K. Jantanasakulwong, S. Ross, P. Tipduangta, P. Rachtanapun, G. Ross, P. Jantrawut, S. Amnuaypanich, P. Worajittiphon, Enhanced mechanical properties and biocompatibility of bacterial cellulose composite films with inclusion of 2D MoS_2 and helical carbon nanotubes for use as antimicrobial drug carriers, Int. J. Biol. Macromol. 253 (2023) 126712, https://doi.org/10.1016/j.ijbiomac.2023.126712.
[100] A.A. Kotp, A.A. Allam, A.M. Salah, W. Kamal, D. Essam, S.M. Mahgoub, M. A. Mohamed, Z.E. Eldin, H.E. Alfassam, H.A. Rudayni, A.S. Alawam, F.A. Nasr, R. Mahmoud, Cellulose-based Co–Fe LDH composite as a nano-adsorbent for sulfamethoxazole and cefixime residues: evaluation of performance, green metrics and cytotoxicity, J. Contam. Hydrol. 264 (2024), https://doi.org/10.1016/J.JCONHYD.2024.104364.
[101] G. Li, Y. Hu, X. Yang, Q. Yang, H. Tian, Z. Shi, C. Xiong, Regenerated cellulose/layered double hydroxide nanocomposite films with improved mechanical property, J. Appl. Polym. Sci. 138 (2021) 1–8, https://doi.org/10.1002/app.51448.
[102] M. Kiani, M. Bagherzadeh, A.M. Ghadiri, P. Makvandi, N. Rabiee, Multifunctional green synthesized Cu–Al layered double hydroxide (LDH) nanoparticles: anti-cancer and antibacterial activities, Sci. Rep. 12 (2022) 1–14, https://doi.org/10.1038/s41598-022-13431-7.
[103] J. Nandhini, E. Karthikeyan, S. Rajeshkumar, Eco-friendly Bio-nanocomposites: Pioneering Sustainable Biomedical Advancements in Engineering, Springer US, 2024, https://doi.org/10.1186/s11671-024-04007-7.
[104] M. Kostag, O.A. El Seoud, Sustainable biomaterials based on cellulose, chitin and chitosan composites — a review, Carbohydr. Polym. Technol. Appl. 2 (2021) 100079, https://doi.org/10.1016/J.CARPTA.2021.100079.
[105] A. Etale, A.J. Onyianta, S.R. Turner, S.J. Eichhorn, Cellulose: a review of water interactions, applications in composites, and water treatment, Chem. Rev. 123 (2023) 2016–2048, https://doi.org/10.1021/acs.chemrev.2c00477.
[106] F. Xu, J. Yu, T. Tesso, F. Dowell, D. Wang, Qualitative and quantitative analysis of lignocellulosic biomass using infrared techniques: a mini-review, Appl. Energy 104 (2013) 801–809, https://doi.org/10.1016/j.apenergy.2012.12.019.
[107] H. Seddiqi, E. Oliaei, H. Honarkar, J. Jin, L.C. Geonzon, R.G. Bacabac, J. Klein-Nulend, Cellulose and its derivatives: towards biomedical applications, Cellulose 28 (2021) 1893–1931, https://doi.org/10.1007/S10570-020-03674-W/FIGURES/6.
[108] J. Verma, M. Petru, S. Goel, Cellulose based materials to accelerate the transition towards sustainability, Ind. Crop. Prod. 210 (2024) 118078, https://doi.org/10.1016/J.INDCROP.2024.118078.
[109] K.Y. Foo, B.H. Hameed, Insights into the modeling of adsorption isotherm systems, Chem. Eng. J. 156 (2010) 2–10, https://doi.org/10.1016/j.cej.2009.09.013.
[110] T.G. Volova, S.V. Prudnikova, E.G. Kiselev, I.V. Nemtsev, A.D. Vasiliev, A. P. Kuzmin, E.I. Shishatskaya, Bacterial cellulose (BC) and BC composites: production and properties, Nanomaterials 12 (2022) 192, https://doi.org/10.3390/NANO12020192.
[111] A.M. Tucker-Quiñónez, B.F. Rivadeneira-Mendoza, M.L. Gorozabel-Mendoza, I. B. Pérez-Almeida, A.J. García-Guerrero, A.A. Dueñas-Rivadeneira, K.K. Yadav, L. A. Zambrano-Intriago, J.M. Rodríguez-Díaz, Challenges and potential of layered double hydroxides as electrocatalytic materials for hydrogen production from

water: a review of recent advances and applications, Energy Nexus 17 (2025) 100399, https://doi.org/10.1016/J.NEXUS.2025.100399.
[112] Q. Yang, X. Pan, Introducing hydroxyl groups as cellulose-binding sites into polymeric solid acids to improve their catalytic performance in hydrolyzing cellulose, Carbohydr. Polym. 261 (2021) 117895, https://doi.org/10.1016/J.CARBPOL.2021.117895.
[113] S.T. Lin, H.N. Tran, H.P. Chao, J.F. Lee, Layered double hydroxides intercalated with sulfur-containing organic solutes for efficient removal of cationic and oxyanionic metal ions, Appl. Clay Sci. 162 (2018) 443–453, https://doi.org/10.1016/J.CLAY.2018.06.011.
[114] D. Gao, W. Zhang, H. Dong, Y. Yu, W. Liu, H. Luo, Z. Jing, B. Liang, L. Peng, B. Wu, T. Huang, H. Cheng, Phosphorus removal from water by the layered double hydroxides (LDHs)-based adsorbents: a review for structure, mechanism, and current progress, Environ. Technol. Innov. 37 (2025) 104003, https://doi.org/10.1016/J.ETI.2024.104003.
[115] M.J. Mochane, S.I. Magagula, J.S. Sefadi, Morphology, thermal stability, and flammability properties of polymer-layered double hydroxide (LDH) nanocomposites: a review, Crystals (2020).
[116] C. Yang, L. Wang, Y. Yu, P. Wu, F. Wang, S. Liu, X. Luo, Highly efficient removal of amoxicillin from water by Mg-Al layered double hydroxide/cellulose nanocomposite beads synthesized through in-situ coprecipitation method, Int. J. Biol. Macromol. 149 (2020) 93–100, https://doi.org/10.1016/j.ijbiomac.2020.01.096.
[117] N. El Messaoudi, Y. Miyah, J. Georgin, M. Wasilewska, R.J.A. Felisardo, H. Moukadiri, M.S. Manzar, A.A. Aryee, S. Knani, M.M. Rahman, Recent developments in the synthesis of tetraethylenepentamine-based nanocomposites to eliminate heavy metal pollutants from wastewater through adsorption, Bioresour. Technol. Rep. 28 (2024) 101982, https://doi.org/10.1016/J.BITEB.2024.101982.
[118] J. Georgin, D. Stracke Pfingsten Franco, C. Gindri Ramos, H. Nguyen Tran, A. Benettayeb, G. Imanova, I. Ali, Recent advances in removing glyphosate herbicide and its aminomethylphosphonic acid metabolite in water, J. Mol. Liq. 402 (2024), https://doi.org/10.1016/j.molliq.2024.124786.
[119] J.O. Ighalo, S.B. Kurniawan, B. Khongthaw, J. Buhari, P.K. Chauhan, J. Georgin, D.S. Pfingsten Franco, Bisphenol A (BPA) toxicity assessment and insights into current remediation strategies, RSC Adv. 14 (2024) 35128–35162, https://doi.org/10.1039/d4ra05628k.
[120] D.S.P. Franco, J. Georgin, D.G. Piccilli, L. Meili, M. Silanpää, T. Kon Kova, O.M. L. Alharbi, G. Imanova, J.Y. Al-Humaidi, I. Ali, Diuron removal from water by adsorption: fundamentals, mechanism, desorption, and future perspectives, Sep. Purif. Rev. 00 (2024) 1–17, https://doi.org/10.1080/15422119.2024.2401848.
[121] J. Georgin, L. Meili, D. Franco, A review of the application of low-cost adsorbents as an alternative method for biosorption of contaminants present in water, LADEE 4 (2023) 1–20, https://doi.org/10.17981/ladee.04.02.2023.1.
[122] M. Park, C.L. Choi, Y.J. Seo, S.K. Yeo, J. Choi, S. Komarneni, J.H. Lee, Reactions of Cu^{2+} and Pb^{2+} with Mg/Al layered double hydroxide, Appl. Clay Sci. 37 (2007) 143–148, https://doi.org/10.1016/j.clay.2006.12.006.
[123] M.R. Awual, T. Yaita, H. Shiwaku, Design a novel optical adsorbent for simultaneous ultra-trace cerium(III) detection, sorption and recovery, Chem. Eng. J. 228 (2013) 327–335, https://doi.org/10.1016/j.cej.2013.05.010.
[124] M.R. Awual, T. Kobayashi, Y. Miyazaki, R. Motokawa, H. Shiwaku, S. Suzuki, Y. Okamoto, T. Yaita, Selective lanthanide sorption and mechanism using novel hybrid Lewis base (N-methyl-N-phenyl-1,10-phenanthroline-2-carboxamide) ligand modified adsorbent, J. Hazard. Mater. 252–253 (2013) 313–320, https://doi.org/10.1016/j.jhazmat.2013.03.020.
[125] S. Iftekhar, V. Srivastava, M. Sillanpää, Synthesis and application of LDH intercalated cellulose nanocomposite for separation of rare earth elements (REEs), Chem. Eng. J. 309 (2017) 130–139, https://doi.org/10.1016/J.CEJ.2016.10.028.
[126] M.G. Ma, F. Deng, K. Yao, Manganese-containing cellulose nanocomposites: the restrain effect of cellulose treated with NaOH/urea aqueous solutions, Carbohydr. Polym. 111 (2014) 230–235, https://doi.org/10.1016/j.carbpol.2014.04.080.
[127] M.S. Manzar, H.A. Aziz, L. Meili, I. Ihsanullah, P. Palaniandy, M.A. Al-Harthi, Insights into the adsorption of tetracycline onto cellulose nanocrystal structured MgAl/LDH composite, Mater. Chem. Phys. 299 (2023) 127247, https://doi.org/10.1016/j.matchemphys.2022.127247.
[128] M. Djellali, M. Kameche, H. Kebaili, M.M. Bouhent, A. Benhamou, Synthesis of nickel-based layered double hydroxide (LDH) and their adsorption on carbon felt fibres: application as low cost cathode catalyst in microbial fuel cell (MFC), Environ. Technol. (United Kingdom) 42 (2021) 492–504, https://doi.org/10.1080/09593330.2019.1635652.
[129] L. Yang, Z. Liu, S. Zhu, L. Feng, W. Xing, Ni-based layered double hydroxide catalysts for oxygen evolution reaction, Mater. Today Phys. 16 (2021) 100292, https://doi.org/10.1016/j.mtphys.2020.100292.
[130] F. Golmohammadi, M. Amiri, Biomass-derived graphene-based nanocomposite: a facile template for decoration of ultrathin nickel–aluminum layered double hydroxide nanosheets as high-performance supercapacitors, Int. J. Hydrog. Energy 45 (2020) 15578–15588, https://doi.org/10.1016/j.ijhydene.2020.04.044.
[131] J. Deng, L. Xiao, S. Yuan, W. Wang, X. Zhan, Z.-H. Hu, Activation of peroxymonosulfate by CoFeNi layered double hydroxide/graphene oxide (LDH/GO) for the degradation of gatifloxacin, Sep. Purif. Technol. 255 (2021) 117685, https://doi.org/10.1016/j.seppur.2020.117685.
[132] P.V. dos Santos Lins, D.C. Henrique, A.H. Ide, C.L. de Paiva e Silva Zanta, L. Meili, Evaluation of caffeine adsorption by MgAl-LDH/biochar composite, Environ. Sci. Pollut. Res. 26 (2019) 31804–31811, https://doi.org/10.1007/s11356-019-06288-3.
[133] M. Hadid, H. Noukrati, H. Ben Youcef, A. Barroug, H. Sehaqui, Phosphorylated cellulose for water purification: a promising material with outstanding adsorption capacity towards methylene blue, Cellulose 28 (2021) 7893–7908, https://doi.org/10.1007/s10570-021-04012-4.
[134] L. Lu, M. Liu, Y. Chen, Y. Luo, Effective removal of tetracycline antibiotics from wastewater using practically applicable iron(III)-loaded cellulose nanofibres, R. Soc. Open Sci. 8 (2021), https://doi.org/10.1098/rsos.210336.
[135] H. He, N. Zhang, N. Chen, Z. Lei, K. Shimizu, Z. Zhang, Efficient phosphate removal from wastewater by MgAl-LDHs modified hydrochar derived from tobacco stalk, Bioresour. Technol. Rep. 8 (2019) 100348, https://doi.org/10.1016/j.biteb.2019.100348.
[136] Z. Zhang, L. Yan, H. Yu, T. Yan, X. Li, Adsorption of phosphate from aqueous solution by vegetable biochar/layered double oxides: fast removal and mechanistic studies, Bioresour. Technol. 284 (2019) 65–71, https://doi.org/10.1016/j.biortech.2019.03.113.
[137] H. Wang, W. Zhao, Y. Chen, Y. Li, Nickel aluminum layered double oxides modified magnetic biochar from waste corncob for efficient removal of acridine orange, Bioresour. Technol. 315 (2020) 123834, https://doi.org/10.1016/j.biortech.2020.123834.
[138] M. Zubair, I. Ihsanullah, H. Abdul Aziz, M. Azmier Ahmad, M.A. Al-Harthi, Sustainable wastewater treatment by biochar/layered double hydroxide composites: progress, challenges, and outlook, Bioresour. Technol. 319 (2021) 124128, https://doi.org/10.1016/j.biortech.2020.124128.
[139] K.W. Jung, S. Lee, Y.J. Lee, Synthesis of novel magnesium ferrite ($MgFe_2O_4$)/biochar magnetic composites and its adsorption behavior for phosphate in aqueous solutions, Bioresour. Technol. 245 (2017) 751–759, https://doi.org/10.1016/j.biortech.2017.09.035.
[140] P. Gholami, L. Dinpazhoh, A. Khataee, A. Hassani, A. Bhatnagar, Facile hydrothermal synthesis of novel Fe-Cu layered double hydroxide/biochar nanocomposite with enhanced sonocatalytic activity for degradation of cefazolin sodium, J. Hazard. Mater. 381 (2020) 120742, https://doi.org/10.1016/j.jhazmat.2019.120742.
[141] Y. Jia, Y. Zhang, J. Fu, L. Yuan, Z. Li, C. Liu, D. Zhao, X. Wang, A novel magnetic biochar/MgFe-layered double hydroxides composite removing Pb^{2+} from aqueous solution: isotherms, kinetics and thermodynamics, Colloids Surf. A Physicochem. Eng. Asp. 567 (2019) 278–287, https://doi.org/10.1016/j.colsurfa.2019.01.064.
[142] S. Chen, Y. Huang, X. Han, Z. Wu, C. Lai, J. Wang, Q. Deng, Z. Zeng, S. Deng, Simultaneous and efficient removal of Cr(VI) and methyl orange on LDHs decorated porous carbons, Chem. Eng. J. 352 (2018) 306–315, https://doi.org/10.1016/j.cej.2018.07.012.
[143] M. Zubair, M.S. Manzar, N.D. Mu'azu, I. Anil, N.I. Blaisi, M.A. Al-Harthi, Functionalized MgAl-layered hydroxide intercalated date-palm biochar for enhanced uptake of cationic dye: kinetics, isotherm and thermodynamic studies, Appl. Clay Sci. 190 (2020) 105587, https://doi.org/10.1016/j.clay.2020.105587.
[144] L. Meili, P.V. Lins, C.L.P.S. Zanta, J.I. Soletti, L.M.O. Ribeiro, C.B. Dornelas, T. L. Silva, M.G.A. Vieira, MgAl-LDH/Biochar composites for methylene blue removal by adsorption, Appl. Clay Sci. 168 (2019) 11–20, https://doi.org/10.1016/j.clay.2018.10.012.
[145] M. Zhang, B. Gao, Y. Yao, M. Inyang, Phosphate removal ability of biochar/MgAl-LDH ultra-fine composites prepared by liquid-phase deposition, Chemosphere 92 (2013) 1042–1047, https://doi.org/10.1016/j.chemosphere.2013.02.050.
[146] X. Tan, S. Liu, Y. Liu, Y. Gu, G. Zeng, X. Cai, Z.L. Yan, C. Yang, X. Hu, B. Chen, One-pot synthesis of carbon supported calcined-Mg/Al layered double hydroxides for antibiotic removal by slow pyrolysis of biomass waste, Sci. Rep. 6 (2016) 1–12, https://doi.org/10.1038/srep39691.
[147] R. Li, J.J. Wang, B. Zhou, M.K. Awasthi, A. Ali, Z. Zhang, L.A. Gaston, A.H. Lahori, A. Mahar, Enhancing phosphate adsorption by Mg/Al layered double hydroxide functionalized biochar with different Mg/Al ratios, Sci. Total Environ. 559 (2016) 121–129, https://doi.org/10.1016/j.scitotenv.2016.03.151.
[148] S.Y. Lee, J.W. Choi, K.G. Song, K. Choi, Y.J. Lee, K.W. Jung, Adsorption and mechanistic study for phosphate removal by rice husk-derived biochar functionalized with Mg/Al-calcined layered double hydroxides via co-pyrolysis, Compos. Pt. B Eng. 176 (2019) 107209, https://doi.org/10.1016/j.compositesb.2019.107209.
[149] T. Selkälä, T. Suopajärvi, J.A. Sirviö, T. Luukkonen, P. Kinnunen, A.L.C.B. De Carvalho, H. Liimatainen, Surface modification of cured inorganic foams with cationic cellulose nanocrystals and their use as reactive filter media for anionic dye removal, ACS Appl. Mater. Interfaces 12 (2020) 27745–27757, https://doi.org/10.1021/acsami.0c05927.
[150] P. Moharrami, E. Motamedi, Application of cellulose nanocrystals prepared from agricultural wastes for synthesis of starch-based hydrogel nanocomposites: efficient and selective nanoadsorbent for removal of cationic dyes from water, Bioresour. Technol. 313 (2020) 123661, https://doi.org/10.1016/j.biortech.2020.123661.
[151] M. Nasir, M.A. Aziz, M. Zubair, M.S. Manzar, N. Ashraf, N.D. Mu'azu, M.A. Al-Harthi, Recent review on synthesis, evaluation, and SWOT analysis of nanostructured cellulose in construction applications, J. Build. Eng. 46 (2022) 103747, https://doi.org/10.1016/j.jobe.2021.103747.
[152] Z. Karim, A.P. Mathew, M. Grahn, J. Mouzon, K. Oksman, Nanoporous membranes with cellulose nanocrystals as functional entity in chitosan: removal of dyes from water, Carbohydr. Polym. 112 (2014) 668–676, https://doi.org/10.1016/j.carbpol.2014.06.048.
[153] N. Grishkewich, N. Mohammed, J. Tang, K.C. Tam, Recent advances in the application of cellulose nanocrystals, Curr. Opin. Colloid Interface Sci. 29 (2017) 32–45, https://doi.org/10.1016/j.cocis.2017.01.005.

[154] M. Zubair, H.A. Aziz, I. Ihsanullah, M.A. Ahmad, M.A. Al-Harthi, Enhanced removal of Eriochrome Black T from water using biochar/layered double hydroxide/chitosan hybrid composite: performance evaluation and optimization using BBD-RSM approach, Environ. Res. 209 (2022) 112861, https://doi.org/10.1016/j.envres.2022.112861.
[155] R.C. da Silva, S.B. de Aguiar, P.L.R. da Cunha, R.C.M. de Paula, J.P.A. Feitosa, Effect of microwave on the synthesis of polyacrylamide-g-chitosan gel for azo dye removal, React. Funct. Polym. 148 (2020) 104491, https://doi.org/10.1016/j.reactfunctpolym.2020.104491.
[156] M. Zubair, N.D. Mu'azu, N. Jarrah, N.I. Blaisi, H.A. Aziz, M.A. Al-Harthi, Adsorption behavior and mechanism of methylene blue, crystal violet, eriochrome black T, and methyl orange dyes onto biochar-derived date palm fronds waste produced at different pyrolysis conditions, Water Air Soil Pollut. 231 (2020) 240, https://doi.org/10.1007/s11270-020-04595-x.
[157] V.N. Priya, M. Rajkumar, J. Mobika, S.P.L. Sibi, Adsorption of As (V) ions from aqueous solution by carboxymethyl cellulose incorporated layered double hydroxide/reduced graphene oxide nanocomposites: isotherm and kinetic studies, Environ. Technol. Innov. 26 (2022) 102268, https://doi.org/10.1016/j.eti.2022.102268.
[158] M. Yusuf, M. Kumar, M.A. Khan, M. Sillanpääillanpa, H. Arafat, A review on exfoliation, characterization, environmental and energy applications of graphene and graphene-based composites, Adv. Colloid Interf. Sci. 273 (2019) 1–23, https://doi.org/10.1016/j.cis.2019.102036.
[159] V.N. Priya, M. Rajkumar, V. Rajendran, J. Mobika, S.P.L. Sibi, B. Veena, V. Vijayalakshmi, P. Ahila, Sustainable selenium ions adsorption of cyclodextrin and cellulose functionalized layered double hydroxide/reduced graphene oxide nanocomposites, J. Water Process Eng. 69 (2025) 106580, https://doi.org/10.1016/j.jwpe.2024.106580.
[160] V.N. Priya, M. Rajkumar, J. Mobika, S.P.L. Sibi, Removal of As (V) in water using β-cyclodextrin intercalated Fe-Al layered double hydroxide/reduced graphene oxide nanocomposites, Synth. Met. 270 (2020) 116595, https://doi.org/10.1016/j.synthmet.2020.116595.
[161] C. Lei, M. Pi, C. Jiang, B. Cheng, J. Yu, Synthesis of hierarchical porous zinc oxide (ZnO) microspheres with highly efficient adsorption of Congo red, J. Colloid Interface Sci. 490 (2017) 242–251, https://doi.org/10.1016/j.jcis.2016.11.049.
[162] X. Guo, Y. Li, M. Zhang, K. Cao, Y. Tian, Y. Qi, S. Li, K. Li, X. Yu, L. Ma, Colyliform crystalline 2D covalent organic frameworks (COFs) with quasi-3D topologies for rapid I2 adsorption, Angew. Chem. Int. Ed. 59 (2020) 22697–22705, https://doi.org/10.1002/anie.202010829.
[163] M. Shao, M. Wei, D.G. Evans, X. Duan, Hierarchical structures based on functionalized magnetic cores and layered double-hydroxide shells: concept, controlled synthesis, and applications, Chemistry 19 (2013) 4100–4108, https://doi.org/10.1002/chem.201204205.
[164] P. Zhang, S. Ouyang, P. Li, Y. Huang, R.L. Frost, Enhanced removal of ionic dyes by hierarchical organic three-dimensional layered double hydroxide prepared via soft-template synthesis with mechanism study, Chem. Eng. J. 360 (2019) 1137–1149, https://doi.org/10.1016/j.cej.2018.10.179.
[165] Y.H. Jia, Z.H. Liu, Preparation of borate anions intercalated MgAl-LDHs microsphere and its calcinated product with superior adsorption performance for Congo red, Colloids Surf. A Physicochem. Eng. Asp. 575 (2019) 373–381, https://doi.org/10.1016/j.colsurfa.2019.05.032.
[166] J. Cao, Z. Feng, H. Liang, X. Lu, W. Wang, Oriented self-assembly of anisotropic layered double hydroxides (LDHs) with 2D-on-3D hierarchical structure, Chem. Eng. J. 472 (2023) 144872, https://doi.org/10.1016/j.cej.2023.144872.
[167] J. Lu, J. Li, J. Xu, H. Tang, Z. Lv, E. Du, L. Wang, M. Peng, Kinetics, structural effects and transformation pathways for norfloxacin oxidation using the UV/chlorine process, J. Water Process Eng. 44 (2021) 102324, https://doi.org/10.1016/j.jwpe.2021.102324.
[168] C. Wang, D. Yin, R. Zhang, F. Chen, Efficient removal of organic pollutants on sponge-type inorganic adsorbent derived from spent cotton fiber/layered double hydroxides, Appl. Clay Sci. 260 (2024) 107541, https://doi.org/10.1016/j.clay.2024.107541.
[169] R. Aladpoosh, M. Montazer, Functionalization of cellulose fibers alongside growth of 2D LDH platelets through urea hydrolysis inspired Taro wettability, Carbohydr. Polym. 275 (2022) 118584, https://doi.org/10.1016/j.carbpol.2021.118584.
[170] Q. Tian, Z. Zuo, F. Qiu, Z. Li, D. Yang, T. Zhang, Toxic waste sludge derived hierarchical porous adsorbent for efficient phosphate removal, Sci. Total Environ. 830 (2022) 154765, https://doi.org/10.1016/j.scitotenv.2022.154765.
[171] J. Ge, L. Lian, X. Wang, X. Cao, W. Gao, D. Lou, Coating layered double hydroxides with carbon dots for highly efficient removal of multiple dyes, J. Hazard. Mater. 424 (2022) 127613, https://doi.org/10.1016/j.jhazmat.2021.127613.
[172] S.H. Kim, D.S. Kim, H. Moradi, Y.Y. Chang, J.K. Yang, Highly porous biobased graphene-like carbon adsorbent for dye removal: preparation, adsorption mechanisms and optimization, J. Environ. Chem. Eng. 11 (2023) 109278, https://doi.org/10.1016/j.jece.2023.109278.
[173] C. Bo, Z. Jia, B. Liu, X. Dai, G. Ma, Y. Li, Copolymer-type magnetic graphene oxide with dual-function for adsorption of variety of dyes, J. Taiwan Inst. Chem. Eng. 138 (2022) 104499, https://doi.org/10.1016/j.jtice.2022.104499.
[174] B. Aljafari, S. James, G. Ahalya, S. Anandan, Acid red 88 dye doped polyaniline framed by soft template method: a potential candidate for dye-sensitized solar cells, J. Saudi Chem. Soc. 26 (2022) 101574, https://doi.org/10.1016/j.jscs.2022.101574.
[175] S. Sanati, Z. Rezvani, Co-intercalation of Acid Red-27/sodium dodecyl sulfate in a Ce-containing Ni-Al-layered double hydroxide matrix and characterization of its luminescent properties, J. Mol. Liq. 249 (2018) 318–325, https://doi.org/10.1016/j.molliq.2017.10.145.
[176] J. He, M. Wei, B. Li, Y. Kang, D.G. Evans, X. Duan, Preparation of layered double hydroxides, Struct. Bond. 119 (2006) 89–119, https://doi.org/10.1016/s1573-4285(04)80047-4.
[177] M. Halma, C. Mousty, C. Forano, M. Sancelme, P. Besse-Hoggan, V. Prevot, Bacteria encapsulated in layered double hydroxides: towards an efficient bionanohybrid for pollutant degradation, Colloids Surf. B: Biointerfaces 126 (2015) 344–350, https://doi.org/10.1016/j.colsurfb.2014.11.029.
[178] D.L. Bish, Anion-exchange in takovite: applications to other hydroxide minerals, Bull. Miner. 103 (1980) 170–175, https://doi.org/10.3406/bulmi.1980.7392.
[179] Y. Israeli, C. Taviot-Guého, J.P. Besse, J.P. Morel, N. Morel-Desrosiers, Thermodynamics of anion exchange on a chloride-intercalated zinc-aluminum layered double hydroxide: a microcalorimetric study, J. Chem. Soc. Dalton Trans. (2000) 791–796, https://doi.org/10.1039/a906346c.
[180] Fudalá, I. Pálinkó, I. Kiricsí, Preparation and characterization of hybrid organic-inorganic composite materials using the amphoteric property of amino acids: amino acid intercalated layered double hydroxide and montmorillonite, Inorg. Chem. 38 (1999) 4653–4658, https://doi.org/10.1021/ic981176t.
[181] J.H. Choy, S.Y. Kwak, J.S. Park, Y.J. Jeong, J. Portier, Intercalative nanohybrids of nucleoside monophosphates and DNA in layered metal hydroxide [11], J. Am. Chem. Soc. 121 (1999) 1399–1400, https://doi.org/10.1021/ja981823f.
[182] H. Nakayama, N. Wada, M. Tsuhako, Intercalation of amino acids and peptides into Mg-Al layered double hydroxide by reconstruction method, Int. J. Pharm. 269 (2004) 469–478, https://doi.org/10.1016/j.ijpharm.2003.09.043.
[183] B.H. Boehm, J. Steinle, Z.X. Ci, The Subsequent Steps Are Once Again a Wittig reaction With Methoxycarbonylmethylenephosphorane and Hydrolysis of the Dithing of the Epoxide With Methyldithiane Anion and Formylation at the Initially Introduced Dithiane Center Affords the Aldehyde vol. 646, 1977, pp. 265–266.
[184] L. Li, Q. Luo, X. Duan, Clean route for the synthesis of hydrotalcites and their property of selective intercalation with benzenedicarboxylate anions, J. Mater. Sci. Lett. 21 (2002) 439–441, https://doi.org/10.1023/A:1015314119011.
[185] Q. Wang, S.V.Y. Tang, E. Lester, D. O'Hare, Synthesis of ultrafine layered double hydroxide (LDHs) nanoplates using a continuous-flow hydrothermal reactor, Nanoscale 5 (2013) 114–117, https://doi.org/10.1039/c2nr32568c.
[186] Y. Zhao, F. Li, R. Zhang, D.G. Evans, X. Duan, Preparation of layered double-hydroxide nanomaterials with a uniform crystallite size using a new method involving separate nucleation and aging steps, Chem. Mater. 14 (2002) 4286–4291, https://doi.org/10.1021/cm020370h.
[187] S. Abelló, J. Pérez-Ramírez, Tuning nanomaterials' characteristics by a miniaturized in-line dispersion-precipitation method: application to hydrotalcite synthesis, Adv. Mater. 18 (2006) 2436–2439, https://doi.org/10.1002/adma.200600673.
[188] S. O'Leary, D. O'Hare, G. Seeley, Delamination of layered double hydroxides in polar monomers: new LDH-acrylate nanocomposites, Chem. Commun. 2 (2002) 1506–1507, https://doi.org/10.1039/b204213d.
[189] E. Gardner, K.M. Huntoon, T.J. Pinnavaia, Direct synthesis of alkoxide-intercalated derivatives of hydrotalcite-like layered double hydroxides: precursors for the formation of colloidal layered double hydroxide suspensions and transparent thin films, Adv. Mater. 13 (2001) 1263–1266, https://doi.org/10.1002/1521-4095(200108)13:16<1263::AID-ADMA1263>3.0.CO;2-R.
[190] T. Hibino, M. Kobayashi, Delamination of layered double hydroxides in water, J. Mater. Chem. 15 (2005) 653–656, https://doi.org/10.1039/b416913a.
[191] T. Hibino, W. Jones, New approach to the delamination of layered double hydroxides, J. Mater. Chem. 11 (2001) 1321–1323, https://doi.org/10.1039/b101135i.
[192] C.R. Gordijo, V.R. Leopoldo Constantino, D. de Oliveira Silva, Evidences for decarbonation and exfoliation of layered double hydroxide in N,N-dimethylformamide-ethanol solvent mixture, J. Solid State Chem. 180 (2007) 1967–1976, https://doi.org/10.1016/j.jssc.2007.05.003.
[193] G. Hu, D. O'Hare, Unique layered double hydroxide morphologies using reverse microemulsion synthesis, J. Am. Chem. Soc. 127 (2005) 17808–17813, https://doi.org/10.1021/ja0549392.
[194] G. Hu, N. Wang, D. O'Hare, J. Davis, One-step synthesis and AFM imaging of hydrophobic LDH monolayers, Chem. Commun. 1 (2006) 287–289, https://doi.org/10.1039/b514368c.
[195] S. Patil, S. Jagadale, Co-precipitation methods for the synthesis of metal oxide nanostructures, Solut. Methods Met. Oxide Nanostruct. (2023) 39–60, https://doi.org/10.1016/B978-0-12-824353-4.00016-6.
[196] T.E. Oladimeji, M. Oyedemi, M.E. Emetere, O. Agboola, J.B. Adeoye, O. A. Odunlami, Review on the impact of heavy metals from industrial wastewater effluent and removal technologies, Heliyon 10 (2024) e40370, https://doi.org/10.1016/J.HELIYON.2024.E40370/ASSET/D56635D9-3862-4238-A94C-2EBBFBD7FF1E/MAIN.ASSETS/GR3.JPG.
[197] Y.Y. Xi, D. Li, A.B. Djurišić, M.H. Xie, K.Y.K. Man, W.K. Chan, Hydrothermal synthesis vs electrodeposition for high specific capacitance nanostructured NiO films, Electrochem. Solid-State Lett. 11 (2008), https://doi.org/10.1149/1.2903345.
[198] K. Chen, W. Dong, Y. Huang, F. Wang, J.L. Zhou, W. Li, Photocatalysis for sustainable energy and environmental protection in construction: a review on surface engineering and emerging synthesis, J. Environ. Chem. Eng. 13 (2025) 117529, https://doi.org/10.1016/J.JECE.2025.117529.
[199] E. Olorundaisi, P.A. Olubambi, The prospect and limitation of high entropy alloy as 4th industrial material, Mater. Today Sustain. 31 (2025) 101163, https://doi.org/10.1016/J.MTSUST.2025.101163.

[200] A.M. Omer, G.S. Elgarhy, G.M. El-Subruiti, E.M. Abd El-Monaem, A.S. Eltaweil, Construction of efficient Ni-FeLDH@MWCNT@cellulose acetate floatable microbeads for Cr(VI) removal: performance and mechanism, Carbohydr. Polym. 311 (2023) 120771, https://doi.org/10.1016/J.CARBPOL.2023.120771.
[201] M. He, C. Chang, N. Peng, L. Zhang, Structure and properties of hydroxyapatite/cellulose nanocomposite films, Carbohydr. Polym. 87 (2012) 2512–2518, https://doi.org/10.1016/J.CARBPOL.2011.11.029.
[202] A.B. Béléké, E. Higuchi, H. Inoue, M. Mizuhata, Effects of the composition on the properties of nickel-aluminum layered double hydroxide/carbon (Ni-Al LDH/C) composite fabricated by liquid phase deposition (LPD), J. Power Sources 225 (2013) 215–220, https://doi.org/10.1016/j.jpowsour.2012.10.048.
[203] E. Musella, I. Gualandi, M. Giorgetti, E. Scavetta, F. Basile, A. Rivalta, E. Venuti, F. Corticelli, M. Christian, V. Morandi, D. Tonelli, Electrosynthesis and characterization of layered double hydroxides on different supports, Appl. Clay Sci. 202 (2021) 105949, https://doi.org/10.1016/J.CLAY.2020.105949.
[204] A.C. Bouali, M. Serdechnova, C. Blawert, J. Tedim, M.G.S. Ferreira, M. L. Zheludkevich, Layered double hydroxides (LDHs) as functional materials for the corrosion protection of aluminum alloys: a review, Appl. Mater. Today 21 (2020) 100857, https://doi.org/10.1016/J.APMT.2020.100857.
[205] S. Esposito, "Traditional" sol-gel chemistry as a powerful tool for the preparation of supported metal and metal oxide catalysts, Materials (Basel) 12 (2019), https://doi.org/10.3390/MA12040668.
[206] A.A. Mohd Raub, R. Bahru, S.N.A. Mohd Nashruddin, J. Yunas, Advances of nanostructured metal oxide as photoanode in photoelectrochemical (PEC) water splitting application, Heliyon 10 (2024) e39079, https://doi.org/10.1016/J.HELIYON.2024.E39079.
[207] G.H.D. Agbna, S.J. Zaidi, Hydrogel performance in boosting plant resilience to water stress—a review, Gels 11 (2025) 276, https://doi.org/10.3390/GELS11040276.
[208] T. Hibino, H. Ohya, Synthesis of crystalline layered double hydroxides: precipitation by using urea hydrolysis and subsequent hydrothermal reactions in aqueous solutions, Appl. Clay Sci. 45 (2009) 123–132, https://doi.org/10.1016/J.CLAY.2009.04.013.
[209] E. Cianflone, F. Brouillet, D. Grossin, J. Soulié, C. Josse, S. Vig, M.H. Fernandes, C. Tenailleau, B. Duployer, C. Thouron, C. Drouet, Toward smart biomimetic apatite-based bone scaffolds with spatially controlled ion substitutions, Nanomaterials 13 (2023), https://doi.org/10.3390/NANO13030519.
[210] N. Chubar, V. Gerda, O. Megantari, M. Mičušík, M. Omastova, K. Heister, P. Man, J. Fraissard, Applications versus properties of Mg-Al layered double hydroxides provided by their syntheses methods: alkoxide and alkoxide-free sol-gel syntheses and hydrothermal precipitation, Chem. Eng. J. 234 (2013) 284–299, https://doi.org/10.1016/j.cej.2013.08.097.
[211] D.Y. Tian, Y. Wang, S.P. Li, X.D. Li, Synthesis of methotrexatum intercalated layered double hydroxides by different methods: biodegradation process and bioassay explore, Appl. Clay Sci. 118 (2015) 87–98, https://doi.org/10.1016/j.clay.2015.09.007.
[212] C.F. Dai, D.Y. Tian, S.P. Li, X.D. Li, Methotrexate intercalated layered double hydroxides with the mediation of surfactants: mechanism exploration and bioassay study, Mater. Sci. Eng. C 57 (2015) 272–278, https://doi.org/10.1016/j.msec.2015.07.040.
[213] M. Yadollahi, H. Namazi, S. Barkhordari, Preparation and properties of carboxymethyl cellulose/layered double hydroxide bionanocomposite films, Carbohydr. Polym. 108 (2014) 83–90, https://doi.org/10.1016/j.carbpol.2014.03.024.
[214] S. Barkhordari, M. Yadollahi, H. Namazi, PH sensitive nanocomposite hydrogel beads based on carboxymethyl cellulose/layered double hydroxide as drug delivery systems, J. Polym. Res. 21 (2014), https://doi.org/10.1007/S10965-014-0454-Z.
[215] A. Habib, A.H.M. Firdaus, S.M. Sapuan, H. Abral, M.A. Azka, E.S. Zainudin, A. Atiqah, J. Yusuf, Recent advancements in nanocellulose reinforced biopolymer hybrid composites: a review, J. Clean. Prod. 496 (2025) 145115, https://doi.org/10.1016/J.JCLEPRO.2025.145115.
[216] A. Babaei-Ghazvini, R. Patel, B. Vafakish, A.F.A. Yazdi, B. Acharya, Nanocellulose in targeted drug delivery: a review of modifications and synergistic applications, Int. J. Biol. Macromol. 278 (2024) 135200, https://doi.org/10.1016/J.IJBIOMAC.2024.135200.
[217] H.N. Abdelhamid, A.P. Mathew, Cellulose-based materials for water remediation: adsorption, catalysis, and antifouling, Front. Chem. Eng. 3 (2021) 1–23, https://doi.org/10.3389/fceng.2021.790314.
[218] N.S. El-Sayed, S. Dacrory, M. El-Sakhawy, E.B. Hassan, S. Kamel, Fabrication of nanocomposite based on oxidized biochar and oxidized cellulose nanofibers and its potential Cd(II) adsorption, Adsorption 31 (2025), https://doi.org/10.1007/s10450-025-00610-x.
[219] N.H. Anggarini, M. Suhartini, R. Rahmawati, M.A. Ega Putri, M.Y. Yunus, D. Deswita, U. Sugiharto, Synthesis and application of bioadsorbent for Y(III) ions from poly(vinyl amine) grafted onto rayon by radiation-induced grafting, Nucl. Eng. Technol. 57 (2025), https://doi.org/10.1016/j.net.2024.103398.
[220] A. Aguzzi, V. Ambrogi, U. Costantino, F. Marmottini, Intercalation of acrylate anions into the galleries of Zn-Al layered double hydroxide, J. Phys. Chem. Solids 68 (2007) 808–812, https://doi.org/10.1016/j.jpcs.2006.12.031.
[221] D. Basu, A. Das, K.W. Stöckelhuber, U. Wagenknecht, G. Heinrich, Advances in layered double hydroxide (LDH)-based elastomer composites, Prog. Polym. Sci. 39 (2014) 594–626, https://doi.org/10.1016/j.progpolymsci.2013.07.011.
[222] G. Viscusi, F. D'Amico, G. Gorrasi, In situ one-step fabrication of layered double hydroxide deposited on cellulose: effect of modified cellulose on physical properties of polyurethane composites, Polym. Adv. Technol. 33 (2022) 2300–2312, https://doi.org/10.1002/pat.5684.
[223] F.R. Costa, B.K. Satapathy, U. Wagenknecht, R. Weidisch, G. Heinrich, Morphology and fracture behaviour of polyethylene/Mg-Al layered double hydroxide (LDH) nanocomposites, Eur. Polym. J. 42 (2006) 2140–2152, https://doi.org/10.1016/j.eurpolymj.2006.04.005.
[224] P. Ding, B. Qu, Synthesis and characterization of polystyrene/layered double-hydroxide nanocomposites via in situ emulsion and suspension polymerization, J. Appl. Polym. Sci. 101 (2006) 3758–3766, https://doi.org/10.1002/app.23447.
[225] F.A. He, L.M. Zhang, New polyethylene nanocomposites prepared by in-situ polymerization method using nickel a-diimine catalyst supported on organo-modified ZnAl layered double hydroxide, Compos. Sci. Technol. 67 (2007) 3226–3232, https://doi.org/10.1016/j.compscitech.2007.04.002.
[226] M. Kotal, T. Kuila, S.K. Srivastava, A.K. Bhowmick, Synthesis and characterization of polyurethane/Mg-Al layered double hydroxide nanocomposites, J. Appl. Polym. Sci. 114 (2009) 2691–2699, https://doi.org/10.1002/app.30791.
[227] S. Guo, C. Zhang, H. Peng, W. Wang, T. Liu, Structural characterization, thermal and mechanical properties of polyurethane/CoAl layered double hydroxide nanocomposites prepared via in situ polymerization, Compos. Sci. Technol. 71 (2011) 791–796, https://doi.org/10.1016/j.compscitech.2010.12.001.
[228] G. Starukh, V. Budzinska, S.Y. Brychka, Structural characterization, thermal and mechanical properties of polyurethane–MgAl–layered double hydroxide nanocomposites prepared via physical dispersion, Appl. Nanosci. 9 (2019) 987–996, https://doi.org/10.1007/s13204-019-01035-z.
[229] Y. Qian, P. Qiao, L. Li, H. Han, H. Zhang, G. Chang, Hydrothermal synthesis of lanthanum-doped MgAl-layered double hydroxide/graphene oxide hybrid and its application as flame retardant for thermoplastic polyurethane, Adv. Polym. Technol. 2020 (2020) 1–10, https://doi.org/10.1155/2020/1018093.
[230] Y. Yang, L. Xiong, X. Huang, Q. Shi, W. De Zhang, Waterborne polyurethane composites with antibacterial activity by incorporating p-BzOH intercalated MgAl-LDH, Compos. Commun. 13 (2019) 112–118, https://doi.org/10.1016/j.coco.2019.04.003.
[231] L. Xiong, W. De Zhang, Q.S. Shi, A.P. Mai, Waterborne polyurethane/NiAl-LDH/ZnO composites with high antibacterial activity, Polym. Adv. Technol. 26 (2015) 495–501, https://doi.org/10.1002/pat.3478.
[232] H. Xie, Q. Ye, J. Si, W. Yang, H. Lu, Q. Zhang, Synthesis of a carbon nanotubes/ZnAl-layered double hydroxide composite as a novel flame retardant for flexible polyurethane foams, Polym. Adv. Technol. 27 (2016) 651–656, https://doi.org/10.1002/pat.3735.
[233] H. Zhang, J. Zhang, R. Yun, Z. Jiang, H. Liu, D. Yan, Nanohybrids of organo-modified layered double hydroxides and polyurethanes with enhanced mechanical, damping and UV absorption properties, RSC Adv. 6 (2016) 34288–34296, https://doi.org/10.1039/c6ra04398d.
[234] Y. Qian, J. Zheng, L. Li, P. Qiao, Y. Li, Y. Duan, G. Chang, Application of the synergistic flame retardant europium hydrotalcite/graphene oxide hybrid material and zinc borate to thermoplastic polyurethane, RSC Adv. 11 (2021) 21073–21083, https://doi.org/10.1039/d1ra01689j.
[235] S. Satyam, S. Patra, Innovations and challenges in adsorption-based wastewater remediation: a comprehensive review, Heliyon 10 (2024) e29573, https://doi.org/10.1016/J.HELIYON.2024.E29573.
[236] A. Elrafey, A.A. Farghali, W. Kamal, A.A. Allam, Z.E. Eldin, H.A. Rudayni, H. E. Alfassam, A.A.A. Anwar, S. Saeed, R. Mahmoud, Cost-effective eggshell-modified LDH composite for caffeine adsorption, cytotoxicity and antimicrobial activity: exploring the synergy and economic viability in search processes, RSC Adv. 14 (2024) 33281–33300, https://doi.org/10.1039/d4ra04558k.
[237] E. Pérez-Botella, S. Valencia, F. Rey, Zeolites in adsorption processes: state of the art and future prospects, Chem. Rev. 122 (2022) 17647–17695, https://doi.org/10.1021/ACS.CHEMREV.2C00140/ASSET/IMAGES/MEDIUM/CR2C00140_M037.GIF.
[238] R. Ben-Mansour, A.A. El-Maaty, Performance of an adsorption cooling system using MOF-303 adsorbent: mathematical modelling using experimentally measured properties, Res. Eng. Des. 26 (2025) 105308, https://doi.org/10.1016/j.rineng.2025.105308.
[239] M.S. Akhtar, S. Ali, W. Zaman, Innovative adsorbents for pollutant removal: exploring the latest research and applications, Molecules 29 (2024) 4317, https://doi.org/10.3390/MOLECULES29184317.
[240] G.E.S. dos Santos, P.V.S. Lins, L.M.T. de Magalhães, E.O. da Silva, I. Anastopoulos, A. Erto, D.A. Giannakoudakis, A.R.F. de Almeida, J.L.S. Duarte, L. Meili, Layered double hydroxides/biochar composites as adsorbents for water remediation applications: recent trends and perspectives, J. Clean. Prod. 284 (2021), https://doi.org/10.1016/j.jclepro.2020.124755.
[241] S. Ren, S. Yang, H. Chen, L. Wang, M. Liu, G. Wang, C. Xu, A state-of-the-art review on the utilization of biochar as renewable energy for the sustainable steel industry, Appl. Energy 394 (2025) 126188, https://doi.org/10.1016/j.apenergy.2025.126188.
[242] Z.U. Zango, A. Garba, A. Haruna, S.S. Imam, A.U. Katsina, A.F. Ali, A.Z. Abidin, M.U. Zango, Z.N. Garba, A. Hosseini-Bandegharaei, A.U. Yuguda, H. Adamu, A systematic review on applications of biochar and activated carbon derived from biomass as adsorbents for sustainable remediation of antibiotics from pharmaceutical wastewater, J. Water Process Eng. 67 (2024) 106186, https://doi.org/10.1016/j.jwpe.2024.106186.
[243] F. Bahmanzadegan, A. Ghaemi, A comprehensive review on novel zeolite-based adsorbents for environmental pollutant, J. Hazard. Mater. Adv. 17 (2025) 100617, https://doi.org/10.1016/j.hazadv.2025.100617.
[244] A. Kausar, S.T. Zohra, S. Ijaz, M. Iqbal, J. Iqbal, I. Bibi, S. Nouren, N. El Messaoudi, A. Nazir, Cellulose-based materials and their adsorptive removal

efficiency for dyes: a review, Int. J. Biol. Macromol. 224 (2023) 1337–1355, https://doi.org/10.1016/j.ijbiomac.2022.10.220.
[245] S. Hokkanen, A. Bhatnagar, M. Sillanpää, A review on modification methods to cellulose-based adsorbents to improve adsorption capacity, Water Res. 91 (2016) 156–173, https://doi.org/10.1016/j.watres.2016.01.008.
[246] Y. Huang, C. Liu, S. Rad, H. He, L. Qin, A comprehensive review of layered double hydroxide-based carbon composites as an environmental multifunctional material for wastewater treatment, Processes 10 (2022), https://doi.org/10.3390/pr10040617.
[247] Suhas, V.K. Gupta, P.J.M. Carrott, R. Singh, M. Chaudhary, S. Kushwaha, Cellulose: a review as natural, modified and activated carbon adsorbent, Bioresour. Technol. 216 (2016) 1066–1076, https://doi.org/10.1016/j.biortech.2016.05.106.
[248] Y. Sun, W.M. Yin, Y. Wang, N.D. Zhao, X.Y. Wang, J.G. Zhang, Y.R. Guo, S. Li, Q. J. Pan, Fabrication of ultra-thin MgAl layered double oxide by cellulose templating and its immobilization effect toward heavy metal ions: cation-exchange and deposition mechanism, Chem. Eng. J. 427 (2022) 132017, https://doi.org/10.1016/J.CEJ.2021.132017.
[249] M.E. Mahmoud, S.M. El-Bahy, S.M.T. Elweshahy, Decorated Mn-ferrite nanoparticle@Zn–Al layered double hydroxide@cellulose@ activated biochar nanocomposite for efficient remediation of methylene blue and mercury (II), Bioresour. Technol. 342 (2021) 126029, https://doi.org/10.1016/J.BIORTECH.2021.126029.
[250] X. Peng, W. Luo, M. Wang, F. Hu, F. Qiu, H. Dai, Insights into the adsorption mechanism of carbon cellulose fiber loaded globular flowers bimetallic layered double hydroxide for efficiency pollutant removal, J. Mol. Liq. 290 (2019) 111201, https://doi.org/10.1016/j.molliq.2019.111201.
[251] J. Ren, S. Zhang, Y. Wang, H. Shi, C. Zhen, Cr(VI) adsorption by Mg/Al layered double hydroxide-modified sphagnum moss cellulose gel: performance and mechanism, Molecules 30 (2025), https://doi.org/10.3390/molecules30081796.
[252] Y. Pan, L. Li, K. Lu, X. Hong, J. Gao, M. Xia, F. Wang, Synergistic adsorption of real phosphorus-containing domestic wastewater by in-situ growth of MgFe-layered double hydroxides co-doped with dual-functional lignosulfonate and La $(OH)_3$ on wood-derived cellulose aerogel, Chem. Eng. J. 493 (2024) 152725, https://doi.org/10.1016/J.CEJ.2024.152725.
[253] X. Wang, H. Li, X. Li, J. Wu, Z. Pang, Z. Ji, S. Wang, Separation of ethylparaben using cellulose nanocrystals/Mg-Al layered double hydroxides composite films and mechanistic investigation, J. Environ. Chem. Eng. 13 (2025) 115157, https://doi.org/10.1016/J.JECE.2024.115157.
[254] Z. Guo, J. Meng, X. Li, X. Wang, Y. Li, L. Hu, ZIF-8-templated synthesis of hollow porous layered double hydroxide/cellulose aerogel composites for efficient removal of antibiotics from aqueous solution, Sep. Purif. Technol. 363 (2025) 132264, https://doi.org/10.1016/J.SEPPUR.2025.132264.
[255] M. Zubair, H.A. Aziz, I. Ihsanullah, M.A. Ahmad, M.A. Al-Harthi, Engineered biochar supported layered double hydroxide-cellulose nanocrystals composite: synthesis, characterization and azo dye removal performance, Chemosphere 307 (2022) 136054, https://doi.org/10.1016/J.CHEMOSPHERE.2022.136054.
[256] C. Li, F. Wang, X. Xu, Y. Shi, J. Liang, R. Yang, J. Liu, Z. Zhao, A high-capacity malleable cellulose aerogel with layered double hydroxide decorating ZIF-8 for efficient adsorption of ciprofloxacin, Chem. Eng. J. 455 (2023) 140841, https://doi.org/10.1016/J.CEJ.2022.140841.
[257] A.M. Alotaibi, N.H. Elsayed, Adsorption and eliminating of diquat herbicide using layer double hydroxide enclosed in double layer hydrogel beads of carboxymethyl cellulose and alginate: synthesis, characterization, adsorption isotherm, kinetics, thermodynamics and optimization via Box-Behnken design, Int. J. Biol. Macromol. 303 (2025) 140564, https://doi.org/10.1016/J.IJBIOMAC.2025.140564.
[258] M. Aghaziarati, H. Sereshti, A facile in-situ ultrasonic-assisted synthesis of terephthalic acid-layered double hydroxide/bacterial cellulose: application for eco-friendly analysis of multi-residue pesticides in vineyard soils, Microchem. J. 202 (2024) 110761, https://doi.org/10.1016/J.MICROC.2024.110761.
[259] R. Mohadi, Amri, M. Badaruddin, N. Ahmad, A. Lesbani, Adsorption of phenol from aqueous solution using Zn/Al layered double hydroxides-cellulose composite, Sci. Technol. Indones. 8 (2023) 123–128, https://doi.org/10.26554/STI.2023.8.1.123-128.
[260] A. Wijaya, Artha Zahara, Zaqiya, P.M.S.B.N. Siregar, N. Ahmad, A. Amri, N. R. Palapa, R. Mohadi, A. Lesbani, Cellulose-supported Ni/Al layered double hydroxide (LDH) as unique adsorbents for malachite green dye removal in aqueous solutions, Iran. J. Chem. Chem. Eng. 43 (2024) 1566–1578, https://doi.org/10.30492/ijcce.2024.1983141.5779.
[261] H. Kye, J. Kim, S. Ju, J. Lee, C. Lim, Y. Yoon, Microplastics in water systems: a review of their impacts on the environment and their potential hazards, Heliyon 9 (2023) e14359, https://doi.org/10.1016/J.HELIYON.2023.E14359.
[262] S.S. Nemati, G. Dehghan, A. Khataee, L. Alidokht, N. Kudaibergenov, Layered double hydroxides as versatile materials for detoxification of hexavalent chromium: mechanism, kinetics, and environmental factors, J. Environ. Chem. Eng. 12 (2024) 114742, https://doi.org/10.1016/J.JECE.2024.114742.
[263] A. El Mahdaoui, S. Radi, A. Elidrissi, M.A.F. Faustino, M.G.P.M.S. Neves, N.M. M. Moura, Progress in the modification of cellulose-based adsorbents for the removal of toxic heavy metal ions, J. Environ. Chem. Eng. 12 (2024) 113870, https://doi.org/10.1016/J.JECE.2024.113870.
[264] N.W. Sabry, I. Naeem, S.A. Hassanien, O. Abuzalat, A. Baraka, Alkali-treatment of lupine peels for valorizing adsorption of organic cationic pollutants from wastewater: kinetics, isotherm, thermodynamic, regeneration, and mechanism, Next Mater. 8 (2025) 100568, https://doi.org/10.1016/J.NXMATE.2025.100568.
[265] G. Roviello, A. Occhicone, E. De Gregorio, L. Ricciotti, R. Cioffi, C. Ferone, O. Tarallo, Geopolymer-based composite and hybrid materials: the synergistic interaction between components, Sustain. Mater. Technol. 44 (2025) e01404, https://doi.org/10.1016/J.SUSMAT.2025.E01404.
[266] Z. Sun, X. Wang, H. An, S. Liang, N. Li, A review on intelligence of cellulose based materials, Carbohydr. Polym. 338 (2024) 122219, https://doi.org/10.1016/J.CARBPOL.2024.122219.
[267] B.G. Fouda-Mbanga, O.P. Onotu, Z. Tywabi-Ngeva, Advantages of the reuse of spent adsorbents and potential applications in environmental remediation: a review, Green Anal. Chem. 11 (2024) 100156, https://doi.org/10.1016/J.GREEAC.2024.100156.
[268] D. Pattappan, S. Kapoor, S.S. Islam, Y.T. Lai, Layered double hydroxides for regulating phosphate in water to achieve long-term nutritional management, ACS Omega 8 (2023) 24727–24749, https://doi.org/10.1021/ACSOMEGA.3C02576.
[269] K. Wieszczycka, K. Staszak, M.J. Woźniak-Budych, J. Litowczenko, B. M. Maciejewska, S. Jurga, Surface functionalization — the way for advanced applications of smart materials, Coord. Chem. Rev. 436 (2021) 213846, https://doi.org/10.1016/J.CCR.2021.213846.
[270] C. Yang, J. Yuan, Y. Guo, X. Luo, In situ nano-assembly of Mg/Al LDH embedded on phosphorylated cellulose microspheres for tetracycline hydrochloride removal, Cellulose 28 (2021) 301–316, https://doi.org/10.1007/s10570-020-03533-8.
[271] Q. Chen, J. Zheng, L. Wen, C. Yang, L. Zhang, A multi-functional-group modified cellulose for enhanced heavy metal cadmium adsorption: performance and quantum chemical mechanism, Chemosphere 224 (2019) 509–518, https://doi.org/10.1016/j.chemosphere.2019.02.138.
[272] M.A. Abduarahman, M.M. Vuksanović, M. Milošević, A. Egelja, A. Savić, Z. Veličković, A. Marinković, Mn-Fe layered double hydroxide modified cellulose-based membrane for sustainable anionic pollutant removal, J. Polym. Environ. 32 (2024) 3776–3794, https://doi.org/10.1007/s10924-024-03192-x.
[273] D. Ning, Z. Lu, C. Tian, N. Yan, L. Hua, Hierarchical and superwettable cellulose acetate nanofibrous membranes decorated via 3D flower-like layered double hydroxides for efficient oil/water separation, Sep. Purif. Technol. 342 (2024) 127052, https://doi.org/10.1016/j.seppur.2024.127052.
[274] K. Samal, S. Mahapatra, M. Hibzur Ali, Pharmaceutical wastewater as emerging contaminants (EC): treatment technologies, impact on environment and human health, Energy Nexus 6 (2022) 100076, https://doi.org/10.1016/J.NEXUS.2022.100076.
[275] M. Hossein Beyki, M. Mohammadirad, F. Shemirani, A.A. Saboury, Magnetic cellulose ionomer/layered double hydroxide: an efficient anion exchange platform with enhanced diclofenac adsorption property, Carbohydr. Polym. 157 (2017) 438–446, https://doi.org/10.1016/j.carbpol.2016.10.017.
[276] M.D. Raicopol, C. Andronescu, S.I. Voicu, E. Vasile, A.M. Pandele, Cellulose acetate/layered double hydroxide adsorptive membranes for efficient removal of pharmaceutical environmental contaminants, Carbohydr. Polym. 214 (2019) 204–212, https://doi.org/10.1016/J.CARBPOL.2019.03.042.
[277] S.S.L. Sobhana, D.R. Bogati, M. Reza, J. Gustafsson, P. Fardim, Cellulose biotemplates for layered double hydroxides networks, Microporous Mesoporous Mater. 225 (2016) 66–73, https://doi.org/10.1016/j.micromeso.2015.12.009.
[278] S. Razani, A. Dadkhah Tehrani, Development of new organic-inorganic, hybrid bionanocomposite from cellulose nanowhisker and Mg/Al-CO_3-LDH for enhanced dye removal, Int. J. Biol. Macromol. 133 (2019) 892–901, https://doi.org/10.1016/J.IJBIOMAC.2019.04.149.
[279] R.N. Manalu, Z.A. Zahara, R. Mohadi, Ni-Cr layered double hydroxide/microcrystalline cellulose composite as adsorbents for malachite green dye, Indones. J. Mater. Res. 1 (2023) 51–60, https://doi.org/10.26554/ijmr.2023128.
[280] Gustavo Franco de Castro, Jader Alves Ferreira, Denise Eulálio, Allan Robledo Fialho e Moraes, Vera Regina Leopoldo Constantino, Frederico Garcia Pinto, Roberto Ferreira Novais, Jairo Tronto, Organic-inorganic hybrid materials: layered double hydroxides and cellulose acetate films as phosphate recovery, J. Agric. Sci. Technol. B 8 (2018), https://doi.org/10.17265/2161-6264/2018.06.003.
[281] D. Brahma, M.P. Barman, D. Basak, H. Saikia, Prospects of layered double hydroxide (LDH)-based adsorbents for the remediation of environmental inorganic pollutants from wastewater: a critical review, Environ. Sci. Water Res. Technol. 11 (2025) 830–875, https://doi.org/10.1039/d4ew01039f.
[282] X. Yue, T. Zhang, D. Yang, F. Qiu, Z. Li, Y. Zhu, H. Yu, Oil removal from oily water by a low-cost and durable flexible membrane made of layered double hydroxide nanosheet on cellulose support, J. Clean. Prod. 180 (2018) 307–315, https://doi.org/10.1016/j.jclepro.2018.01.160.
[283] M. Zeeshan, T. Javed, C. Kumari, A. Thumma, M. Wasim, M.B. Taj, I. Sharma, M. N. Haider, M. Batool, Investigating the interactions between dyes and porous/composite materials: a comprehensive study, Sustain. Chem. Environ. 9 (2025) 100217, https://doi.org/10.1016/J.SCENV.2025.100217.
[284] G. Darmograi, B. Prelot, A. Geneste, A. Martin-Gassin, F. Salles, J. Zajac, How does competition between anionic pollutants affect adsorption onto Mg-Al layered double hydroxide? Three competition schemes, J. Phys. Chem. C 120 (2016) 10410–10418, https://doi.org/10.1021/acs.jpcc.6b01888.
[285] İ. Akanyeti, J. Abdullahi, Competitive adsorption of anionic dyes from aqueous single and binary solutions with CoAl layered double hydroxide, Int. J. Environ. Geoinformatics 10 (2023) 65–76, https://doi.org/10.30897/ijegeo.1167267.
[286] N. Normah, M. Oktriyanti, A.F. Badri, Effectiveness of modified ZnAl-LDH developed with POM for competitive adsorption of heavy metals in purification systems, indones, J. Mater. Res. 2 (2024) 93–100, https://doi.org/10.26554/ijmr.20242347.
[287] J.Y. Lee, G.H. Gwak, H.M. Kim, T. Il Kim, G.J. Lee, J.M. Oh, Synthesis of hydrotalcite type layered double hydroxide with various Mg/Al ratio and surface

charge under controlled reaction condition, Appl. Clay Sci. 134 (2016) 44–49, https://doi.org/10.1016/J.CLAY.2016.03.029.
[288] L. Tang, X. Xie, C. Li, Y. Xu, W. Zhu, L. Wang, Regulation of structure and anion-exchange performance of layered double hydroxide: function of the metal cation composition of a brucite-like layer, Materials 15 (2022) 7983, https://doi.org/10.3390/MA15227983.
[289] X. Dong, Y. Chu, Z. Tong, M. Sun, D. Meng, X. Yi, T. Gao, M. Wang, J. Duan, Mechanisms of adsorption and functionalization of biochar for pesticides: a review, Ecotoxicol. Environ. Saf. 272 (2024) 116019, https://doi.org/10.1016/J.ECOENV.2024.116019.
[290] B. Qiu, Q. Shao, J. Shi, C. Yang, H. Chu, Application of biochar for the adsorption of organic pollutants from wastewater: modification strategies, mechanisms and challenges, Sep. Purif. Technol. 300 (2022) 121925, https://doi.org/10.1016/J.SEPPUR.2022.121925.
[291] N. Chaukura Nhamochaukura, W.A. Munzeiwa, P. Tsekoa, L.D. Rochell Kammies, K. Chelechele, A.E. Oluwalana-Sanusi, N. Chaukura, Influence of biomass baseline potential on biochar properties and performance for targeted applications, Discov. Water 51 (5) (2025) 1–48, https://doi.org/10.1007/S43832-025-00254-6.
[292] L. Swaren, S. Safari, K.O. Konhauser, D.S. Alessi, Pyrolyzed biomass-derived nanoparticles: a review of surface chemistry, contaminant mobility, and future research avenues to fill the gaps, Biochar 41 (4) (2022) 1–17, https://doi.org/10.1007/S42773-022-00152-3.
[293] F. Zohra Zeggai, Z. Ait-Touchente, K. Bachari, A. Elaissari, Investigation of metal-organic frameworks (MOFs): synthesis, properties, and applications — an in-depth review, Chem. Phys. Impact 10 (2025) 100864, https://doi.org/10.1016/J.CHPHI.2025.100864.
[294] K. Jayaramulu, S. Mukherjee, D.M. Morales, D.P. Dubal, A.K. Nanjundan, A. Schneemann, J. Masa, S. Kment, W. Schuhmann, M. Otyepka, R. Zboril, R. A. Fischer, Graphene-based metal-organic framework hybrids for applications in catalysis, environmental, and energy technologies, Chem. Rev. 122 (2022) 17241–17338, https://doi.org/10.1021/ACS.CHEMREV.2C00270/ASSET/IMAGES/LARGE/CR2C00270_0046.JPEG.
[295] N. Mushahary, A. Sarkar, F. Basumatary, S. Brahma, B. Das, S. Basumatary, Recent developments on graphene oxide and its composite materials: from fundamentals to applications in biodiesel synthesis, adsorption, photocatalysis, supercapacitors, sensors and antimicrobial activity, Results Surf. Interfaces 15 (2024) 100225, https://doi.org/10.1016/J.RSURFI.2024.100225.
[296] T.M. Magne, T. de Oliveira Vieira, L.M.R. Alencar, F.F.M. Junior, S. Gemini-Piperni, S.V. Carneiro, L.M.U.D. Fechine, R.M. Freire, K. Golokhvast, P. Metrangolo, P.B.A. Fechine, R. Santos-Oliveira, Graphene and its derivatives: understanding the main chemical and medicinal chemistry roles for biomedical applications, J. Nanostruct. Chem. 125 (12) (2021) 693–727, https://doi.org/10.1007/S40097-021-00444-3.
[297] O. Okobiah, R.F. Reidy, Surface interactions: functionalization of graphene oxide and wetting of graphene oxide and graphene, Curr. Org. Chem. 20 (2015) 674–681, https://doi.org/10.2174/1385272819666150730220741.
[298] S. Behzadi Nia, M. Pooresmaeil, H. Namazi, Carboxymethylcellulose/layered double hydroxides bio-nanocomposite hydrogel: a controlled amoxicillin nanocarrier for colonic bacterial infections treatment, Int. J. Biol. Macromol. 155 (2020) 1401–1409, https://doi.org/10.1016/j.ijbiomac.2019.11.115.
[299] Y. Xuan, X. Feng, S. Liu, X. Liu, Layered double hydroxide-based membranes for advanced water treatment: structural engineering and multifunctional applications, Chem. Eng. J. 511 (2025), https://doi.org/10.1016/j.cej.2025.161746.
[300] E.M. Abd El-Monaem, H.M. Elshishini, S.S. Bakr, H.G. El-Aqapa, M. Hosny, G. Andaluri, G.M. El-Subruiti, A.M. Omer, A.S. Eltaweil, A comprehensive review on LDH-based catalysts to activate persulfates for the degradation of organic pollutants, Npj Clean Water 6 (2023), https://doi.org/10.1038/s41545-023-00245-x.
[301] E. Jasiukaityte-Grojzdek, M. Kunaver, I. Poljanšek, Influence of cellulose polymerization degree and crystallinity on kinetics of cellulose degradation, BioResources 7 (2012) 3008–3027, https://doi.org/10.15376/biores.7.3.3008-3027.
[302] N. Yadav, M. Hakkarainen, Degradable or not? Cellulose acetate as a model for complicated interplay between structure, environment and degradation, Chemosphere 265 (2021) 128731, https://doi.org/10.1016/j.chemosphere.2020.128731.
[303] S.S. Rumi, S. Liyanage, N. Abidi, Soil burial-induced degradation of cellulose films in a moisture-controlled environment, Sci. Rep. 14 (2024) 1–14, https://doi.org/10.1038/s41598-024-57436-w.
[304] Z.H. Hu, H.Q. Yu, R.F. Zhu, Influence of particle size and pH on anaerobic degradation of cellulose by ruminal microbes, Int. Biodeterior. Biodegrad. 55 (2005) 233–238, https://doi.org/10.1016/j.ibiod.2005.02.002.
[305] M.J. Mochane, S.I. Magagula, J.S. Sefadi, E.R. Sadiku, T.C. Mokhena, Morphology, thermal stability, and flammability properties of polymer-layered double hydroxide (Ldh) nanocomposites: a review, Crystals 10 (2020) 1–26, https://doi.org/10.3390/cryst10070612.
[306] P. Pulyala, M. Jing, W. Young, K. Michels, W. Gao, X. Cheng, Biodegradation of cellulose-based water-soluble polymers through interactions with wastewater bacteria, Polym. Degrad. Stab. 239 (2025) 111378, https://doi.org/10.1016/j.polymdegradstab. 2025.111378.
[307] L. Tan, H. Li, M. Liu, Characterization of CMC-LDH beads and their application in the removal of Cr(VI) from aqueous solution, RSC Adv. 8 (2018) 12870–12878, https://doi.org/10.1039/c8ra00633d.
[308] L.S. Sobhanadhas, L. Kesavan, M. Lastusaari, P. Fardim, Layered double hydroxide-cellulose hybrid beads: a novel catalyst for topochemical grafting of pulp fibers, ACS Omega 4 (2019) 320–330, https://doi.org/10.1021/acsomega.8b03061.
[309] T.P. Tumolva, D.S. Enguero, T.J.C. Laus, B.A. Requejo, Green composites using lignocellulosic waste and cellulosic fibers from corn husks, MATEC Web Conf. 62 (2016) 1–5, https://doi.org/10.1051/matecconf/20166201003.
[310] Khairunnisá, N.J. Wistara, W. Fatriasari, The role of microcrystalline cellulose (MCC) in improving paper strength from rice straw pulp, Int. J. Biol. Macromol. 318 (2025) 144868, https://doi.org/10.1016/j.ijbiomac.2025.144868.
[311] H.R. Hasan, S.M. Hasoon, Novel method for extraction of cellulose from agricultural and industrial wastes, Nature 177 (2014) 861–862, https://doi.org/10.1038/177861a0.
[312] H.A. Rasheed, A.A. Adeleke, P. Nzerem, A.I. Olosho, T.S. Ogedengbe, S. Jesuloluwa, Isolation, characterization and response surface method optimization of cellulose from hybridized agricultural wastes, Sci. Rep. 14 (2024) 1–15, https://doi.org/10.1038/s41598-024-65229-4.
[313] S.M. Lohmousavi, H. Heidari, S. Abad, G. Noormohammadi, B. Delkhosh, Synthesis and characterization of a novel controlled release nitrogen-phosphorus fertilizer hybrid nanocomposite based on banana peel cellulose and layered double hydroxides nanosheets, Arab. J. Chem. 13 (2020) 6977–6985, https://doi.org/10.1016/j.arabjc.2020.06.042.
[314] F. Zhang, J. Li, Y. Chen, S. Zhao, Y. Zhang, R. Wang, Y. He, P. Song, Combination of recycled cellulose with nano-thick flower layered double hydroxides: biomass water retention slow-release fertilizer for sustainable agriculture, Colloids Surf. A Physicochem. Eng. Asp. 702 (2024) 135144, https://doi.org/10.1016/j.colsurfa.2024.135144.
[315] N. Sikri, S. Kumar, B. Behera, J. Mehta, Graphene oxide/layered double hydroxide composite as highly efficient and recyclable adsorbent for removal of ciprofloxacin from aqueous phase, Front. Nanotechnol. 7 (2025) 1–13, https://doi.org/10.3389/fnano.2025.1578620.
[316] K. Bisaria, C.S. Seth, R. Singh, Life cycle assessment of chitosan modified Ni-Fe layered double hydroxide for arsenic(III) sequestration in aqueous medium: comparison of the impacts of adsorbent recycling, instrument use and source of energy, Environ. Sci. Adv. 3 (2024) 1153–1162, https://doi.org/10.1039/d3va00312d.
[317] L. Li, I. Soyhan, E. Warszawik, P. van Rijn, Layered double hydroxides: recent progress and promising perspectives toward biomedical applications, Adv. Sci. 11 (2024) 2306035, https://doi.org/10.1002/ADVS.202306035.
[318] G. Ramezani, I. Stiharu, T.G.M. van de Ven, V. Nerguizian, Advancements in hybrid cellulose-based films: innovations and applications in 2D nano-delivery systems, J. Funct. Biomater. 15 (2024) 93, https://doi.org/10.3390/JFB15040093.
[319] V.R.L. Constantino, M.P. Figueiredo, V.R. Magri, D. Eulálio, V.R.R. Cunha, A.C. S. Alcântara, G.F. Perotti, Biomaterials based on organic polymers and layered double hydroxides nanocomposites: drug delivery and tissue engineering, Pharmaceutics 15 (2023) 413, https://doi.org/10.3390/PHARMACEUTICS15020413.
[320] Y.G. Wibowo, D. Anwar, H. Safitri, A. Rohman, A. Rinovian, B.S. Ramadan, I. Surya, Sudibyo, A.T. Yuliansyah, H.T. Bayu Murti Petrus, Biochar-layered double hydroxide vs biochar-layered double oxide: a critical review on their applications in water pollution control, Water-Energy Nexus (2025), https://doi.org/10.1016/J.WEN.2025.07.007.
[321] A.M.S. Ahmed, A.M. Radalla, S.M. Mahgoub, S.A.A. Elsuccary, M.A. Korany, A. E. Allah, F. Mohamed, A.A. Allam, H.E. Alfassam, R. Mahmoud, Advanced electrochemical detection of clindamycin from aqueous solutions using zinc aluminium layered double hydroxide: green chemistry approaches and cytotoxicity evaluation, Chin. J. Anal. Chem. 53 (2025) 100553, https://doi.org/10.1016/j.cjac.2025.100553.